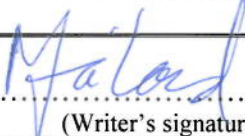




University of
Stavanger

Faculty of Science and Technology

MASTER'S THESIS

Study program/ Specialization: Offshore Technology – Marine and Subsea Technology	Spring semester, 2015 Restricted access
Writer: Magnus Hebnes Håland	 (Writer's signature)
Faculty supervisor: Sverre Haver External supervisor(s): Joel Ireland	
Thesis title: Planning of a Marine Operation with Focus on Discussing Limiting Wave Conditions	
Credits (ECTS): 30 SP	
Key words: Hindcast Data Simulated Operation Duration Wave Spectra Total Sea Wind Wave and Swell Vessel Motion	Pages: 110 + enclosure: 12 Stavanger, 12/06-2015 Date/year

ABSTRACT

The planning of a specific marine operation done by Ocean Installer is carried out in this thesis with regards to weather conditions on the Norwegian Continental Shelf. This is done by looking into the wave statistics from hindcast data at four different locations close to Ekofisk, Statfjord, Heidrun and Snøhvit.

Metocean data is established for all fields for the purpose of understanding the impact from wind waves and swells, summer and winter, at the different locations.

The author has developed a script in the mathematical software MATLAB for simulating the operation with various criteria. The output from the script gives the mean, P-10, P-50 and P-90 durations, with the assumption that the operation starts waiting for weather the 1st each month. The simulations are based on weather criteria provided by Ocean Installer and vessel motions calculated from probability models.

The weather criteria provided by Ocean Installer is used to simulate the basis operation durations, and assuming vessel motion limitations. The basis simulated operation duration is further referred to as the weather criteria simulation. The weather criteria simulation is done by using total sea from one direction. These simulated operation durations are compared to simulations using vessel motion limitation. The vessel motions are calculated with impact from both wind waves and swells from different directions using RAOs for the vessel Normand Vision provided by Ocean Installer. The simulated operation durations show how the impact from waves with two different directions (wind waves and swells) vary from the same vessel motion criteria with waves from one direction (weather criteria simulation).

The results from the simulated operation durations shows that limiting the whole operation to heave motion gives far longer duration than seen from the weather criteria simulation. Limiting the vessel roll motion gives more comparable durations to the weather criteria simulation, which is also the basis for Ocean Installers weather criteria.

The Ekofisk field is operable almost all year long. Statfjord and Heidrun are very similar and are operable in the summer months of May to August. Snøhvit has the same operable months as Statfjord and Heidrun but less risk of waiting for weather during the rest of the year.

PREFACE

My studies are now about to end with the delivery of this thesis. These 5 years of studies at Bergen University Collage (Bachelor in Marine Technology) and The University of Stavanger (Masters in Offshore Technology – Marine and Subsea Technology) has been exciting, challenging and enlightening. During these years I have gained more knowledge about the marine and subsea structures, physics and operations that I ever could imagine before I started my studies. There have been a lot of struggles towards this degree, which at that moment were terrifying. Looking back at the struggles now, these have been the most memorable moments with regards to my learning curve. The master thesis has been no exception. I have gained a lot of new knowledge to the field of wave statistics, which I at first thought was odd. As the knowledge of wave statistics grew I got more interested, and now finishing the master thesis I really hope that I can use this at work and grow my knowledge within the field of wave statistics even more. I look forward to start working and the years as student has given me a whole lot of new experiences academically and socially outside of school, which I will bring with me.

ACKNOWLEDGEMENT

First of all I would like to express my gratitude to my supervisor Sverre Haver for his help during this thesis. As an expert within the field of wave statistics he has made this thesis fun and exciting. I also would like to thank him for useful comments, input, discussions and guiding.

Furthermore, I would like to thank Ocean Installer AS for giving me the opportunity of writing the thesis in co-operation with them. They gave me a warm welcome and provided me with information and expertise that has been necessary to develop this thesis. I would also like to thank my external supervisor Joel Ireland who has been of great help with the understanding of the marine operation, planning the work of the master thesis and guidance. I would also like to thank Abdilahi Qayre for good discussions and guidance.

-Thank you all!

Stavanger, June 12th 2015

-Magnus Hebnes Håland

TABLE OF CONTENTS

ABSTRACT	I
PREFACE	II
ACKNOWLEDGEMENT	II
TABLE OF CONTENTS	III
LIST OF FIGURES	VI
LIST OF TABLES	X
ABBREVIATION LIST	XII
LIST OF SYMBOLS	XIII
1 INTRODUCTION	1
2 BACKGROUND	2
2.1 HINDCAST AND METOCEAN DATA	2
2.1.1 CORRECTING THE HINDCAST DATA PERIOD	3
2.1.2 DISCUSSION ON THE HINDCAST SWELL AND WIND WAVES DATA	5
2.1.2.1 How wind waves are generated	6
2.1.2.2 Summer and Winter Storm/Wind	9
2.1.2.3 Verification of the Metocean calculation	11
2.1.2.4 Wind Waves on the Norwegian Continental Shelf	11
2.1.2.5 Impact from Swell on the Norwegian Continental Shelf	15
2.1.2.6 Swells from the North Atlantic Ocean coming to Ekofisk	20
2.1.2.7 Comparing Direction of Wind, Swell and Wind Wave	21
2.2 DESCRIPTION OF FIELDS	23
2.2.1 HEIDRUN	23
2.2.2 EKOFISK	24
2.2.3 STATFJORD	24

2.2.4	SNØHVIT	25
2.3	NORMAND VISION – THE OPERATING VESSEL	26
2.3.1	VERTICAL LAY SYSTEM (VLS)	27
2.4	INSTALLATION OF FLEXIBLE PIPE	28
2.4.1	SUBSEA END INITIATION TO VISUND PULL IN WINCH WIRE (PIW)	29
2.4.2	LAY AWAY	29
2.4.3	VISUND TEMPORARY LAYDOWN OF SUBSEA ETH	31
2.4.4	CATENARY FLIP AND LAY DYNAMIC SECTION TOWARDS PLATFORM	31
2.4.5	TOPSIDE END HANDSHAKE TO VISUND PIW	32
2.4.6	CONTINGENCY LAYDOWN OF DYNAMIC SECTION	33
3	ANALYSIS AND RESULTS	35
3.1	TOTAL SEA SIMULATION USING JONSWAP SPECTRA	35
3.1.1	METHOD USED FOR CALCULATION OF RESPONSE MOTION	35
3.1.1.1	General Probability Models for Vessel Response	37
3.1.1	VERIFICATION THAT THE JONSWAP SPECTRA IS CORRECT	40
3.1.2	LAY AWAY (LANDING CLUMP WEIGHT)	41
3.1.2.1	Results	42
3.1.2.2	Analyzing the results	44
3.1.3	WEATHER CRITERIA AND DURATIONS	48
3.1.3.1	Duration of the operation using hindcast data	48
3.2	TOTAL SEA SIMULATION USING TORSETHAUGEN SPECTRA	54
3.2.1	VERIFICATION THAT THE TORSETHAUGEN SPECTRA IS CORRECT	57
3.2.2	LAY AWAY WEATHER CRITERIA	57
3.2.3	CONVERTING CRITERIA FROM JONSWAP TO TORSETHAUGEN	58
3.2.4	WEATHER CRITERIA AND DURATIONS	61
3.2.4.1	Duration of the operation using hindcast data	62

3.3	WIND WAVES AND SWELLS SIMULATION USING JONSWAP SPECTRA	64
3.3.1	RESULTANT HEAVE MOTION SIMULATION	65
3.3.1.1	Weather Criteria	68
3.3.1.2	Simulation	68
3.3.2	ROLL ANGLE SIMULATION	70
3.3.2.1	Pitch Motion Contribution to Damage Pipe	72
3.3.2.2	Linear Roll Angle Calculations	73
3.3.2.3	Roll criteria and operation simulation	74
3.3.3	ROLL ANGLE AND HEAVE COMBINED IN ONE SIMULATION	79
4	COMPARING SIMULATIONS FOR DIFFERENT FIELDS	82
4.1	TOTAL SEA USING JONSWAP SPECTRUM	82
4.2	4M RESULTANT HEAVE MOTION FOR THE OPERATION TASKS	84
4.3	3° ROLL LIMITATION FOR THE OPERATION TASKS	86
4.4	3° ROLL WITH 0.6M HEAVE LIMITATION FOR THE LAY AWAY TASK	88
5	DISCUSSING SIMULATED OPERATION DURATION RESULTS	90
5.1	EKOFISK	90
5.2	STATFJORD AND HEIDRUN	90
5.3	SNØHVIT	90
6	CONCLUSION	92
6.1	FURTHER WORK	93
	REFERENCES	94
	APPENDIX A: SIMULATED OPERATION DURATION TABLES	96
	APPENDIX B: MASTER THESIS OBJECTIVES	104

LIST OF FIGURES

Figure 2-1: Observed Hs vs Generated Hs from WAM10 (Reistad, et al., 2009)	2
Figure 2-2: Observed Hs vs Generated Hs from WAM10 (p95 left, p99 right), (Reistad, et al., 2009)	3
Figure 2-3 Spectral peak period before correcting	3
Figure 2-4: Spectral peak period after correcting	4
Figure 2-5: Locations of Hindcast Data and well-known fields close by (Generated with http://www.darrinward.com/lat-long (Ward, 2015))	5
Figure 2-6: Critical Height (left) and Low and High Pressure Generation (right). (Thomson, 1981)	6
Figure 2-7: Criss-Cross Pattern of Waves 80° of Wind Direction (Thomson, 1981)	7
Figure 2-8: Criss-Cross Pattern of Waves 30° of wind direction (Thomson, 1981)	7
Figure 2-9: Fetch and Dispersion (Pinet, 2003)	8
Figure 2-10: Monthly average wind speed and direction 01/2008 (Remote Sensing Systems (RSS), 2009)	9
Figure 2-11: Monthly average wind speed and direction 07/2008 (Remote Sensing Systems (RSS), 2009)	10
Figure 2-12: Comparing Metocean Data from Statoil (right), (Eik, 2012), and Calculated Metocean Data (left)	11
Figure 2-13: Wind Wave Direction Ekofisk January	12
Figure 2-14: Wind Wave Direction Ekofisk July	12
Figure 2-15: Wind Wave Direction Statfjord January	13
Figure 2-16: Wind Wave Direction Statfjord July	13
Figure 2-17: Wind Wave Direction Heidrun January	13
Figure 2-18: Wind Wave Direction Heidrun July	14
Figure 2-19: Wind Wave Direction Snøhvit January	14
Figure 2-20: Wind Wave Direction Snøhvit July	14
Figure 2-21: Swell Direction Ekofisk January	15
Figure 2-22: Swell Direction Ekofisk July	16
Figure 2-23: Swell Direction Statfjord January	16
Figure 2-24: Swell Direction Statfjord July	16
Figure 2-25: Swell Direction Heidrun January	17
Figure 2-26: Swell Direction Heidrun July	17
Figure 2-27: Swell Direction Snøhvit January	17

Figure 2-28: Swell Direction Snøhvit July	18
Figure 2-29: Location of Storm and Dispersion Length	19
Figure 2-30: Comparing Swell Direction at Ekofisk and Staffjord	20
Figure 2-31: Probability of a Swell between 285° and 0° at Ekofisk within the next 12 hours	21
Figure 2-32: Heidrun location (Statoil, 2015)	23
Figure 2-33: Ekofisk location (Statoil, 2015)	24
Figure 2-34: Staffjord location (Statoil, 2015)	24
Figure 2-35: Snøhvit location (Statoil, 2015)	25
Figure 2-36: Normand Vision at sea (Ocean Installer, 2015)	26
Figure 2-37: Vertical Lay System (Ocean Installer, 2015)	27
Figure 2-38: Riser Configuration	28
Figure 2-39: Subsea ETH transfer	29
Figure 2-40: Riser Catenary to Seabed	29
Figure 2-41: Before Landing of Clump Weight	30
Figure 2-42: After Landing of Clump Weight	30
Figure 2-43: Landing of subsea ETH	31
Figure 2-44: Catenary Flip	31
Figure 2-45: Vessel towards Visund FPU	32
Figure 2-46: A&R winch to Crane Transfer	32
Figure 2-47: Crane to Visund PIW wire transfer	33
Figure 2-48: Crane Disconnection	33
Figure 2-49: Contingency position	34
Figure 3-1: JONSWAP Wave Spectrum with Different γ	36
Figure 3-2: Provided RAO for Heave Motion	37
Figure 3-3: Heave Response Spectrum Head Sea (0°)	37
Figure 3-4: Global Response Maxima Rayleigh Distribution (Characteristic Largest Response Amplitude (x) for 3 hour Window Pointed Out)	39
Figure 3-5: The Distribution of the Largest Response Amplitude in a 3-Hour Sea State	40
Figure 3-6: Distribution of Global Response Maxima and Largest 3 hour Maximum	40
Figure 3-7: Waves coming from $0^\circ \pm 15^\circ$ (Head seas $\pm 15^\circ$)	41

Figure 3-8: H_s Resulting in 0.6m Heave Motion	43
Figure 3-9: RAO for 0 and 15 degrees	44
Figure 3-10: H_s Limitations for Different Heave Motion using Z0.95	44
Figure 3-11: JONSWAP spectrum, $\gamma=1.66$ (calculated), $H_s=2.3m$ and $T_p=8s$	46
Figure 3-12: JONSWAP spectrum, $\gamma=7$ (set), $H_s=2.3m$ and $T_p=8s$	46
Figure 3-13: H_s for Heave Motion of 0.6m using Z0.95, and different γ	46
Figure 3-14: Operation Duration Critical Operation $H_s<3m$ for 48 hours, Heidrun.	51
Figure 3-15: Operation Duration Critical Operation $H_s<3m$ for 48 hours, Norne. (Eik, 2012)	51
Figure 3-16: Duration of the operation using JONSWAP, Heidrun	52
Figure 3-17: Wind and swell dominated sea states with $af=6.6$	54
Figure 3-18: JONSWAP spectra $H_s=3.5m$ and $T_p=5s$	60
Figure 3-19: Torsethaugen spectra $H_s=3.5m$ and $T_p=5s$	60
Figure 3-20: JONSWAP spectra $H_s=3.5m$ and $T_p=8s$	60
Figure 3-21: Torsethaugen spectra $H_s=3.5m$ and $T_p=8s$	60
Figure 3-22: JONSWAP spectra $H_s=3.5m$ and $T_p=13s$	61
Figure 3-23: Torsethaugen spectra $H_s=3.5m$ and $T_p=13s$	61
Figure 3-24: Duration of the operation using Torsethaugen, Heidrun	62
Figure 3-25: Hindcast data showing wind- and swell waves	64
Figure 3-26: Vessel with wind- and swell waves	64
Figure 3-27: Normand Vision RAO for heave motion	65
Figure 3-28: JONSWAP Swell spectrum	66
Figure 3-29: JONSWAP Wind Wave spectrum	66
Figure 3-30: Heave response Swell spectrum	67
Figure 3-31: Heave response Wind Wave spectrum	67
Figure 3-32: Total Heave Response Spectrum	67
Figure 3-33: Duration of the Operation Resultant Heave Motion	69
Figure 3-34: Duration of the Operation Total Sea JONSWAP	69
Figure 3-35: Roll angle with horizontal pipe colliding with moonpool	71
Figure 3-36: Roll angle with bending pipe colliding with moonpool	71
Figure 3-37: RAOs for roll Normand Vision	72

Figure 3-38: RAO pitch 0°	72
Figure 3-39: Grouping of limiting Hs to roll of 4° and wave direction of 90°	75
Figure 3-40: Operation Duration 2° roll	76
Figure 3-41: Operation Duration 3° roll	76
Figure 3-42: Operation Duration 4° roll	76
Figure 3-43: Duration of the Operation Total Sea JONSWAP	76
Figure 3-44: Section of RAOs for roll for selected wave directions	79
Figure 3-45: Operation Duration 3° Roll and 0.6m Heave	81
Figure 3-46: Operation Duration 3° Roll	81
Figure 4-1: Simulated Durations for Total Sea using JONSWAP spectra, Different Fields	83
Figure 4-2: Simulated Durations for Resultant Heave Motion	85
Figure 4-3: Simulated Durations for 3° Roll Motion	87
Figure 4-4: Simulated Durations for 3° Roll Motion and 0.6m Heave Motion	89

LIST OF TABLES

Table 1: Comparing Wind Direction with Swell and Wind Wave Direction	22
Table 2: Normand Vision Specifications	26
Table 3: Check of JONSWAP spectra	41
Table 4: H_s Resulting in 0.6m Heave Motion	43
Table 5: H_s Limitations for Different Heave Motion using Z0.95	45
Table 6: H_s for Heave Motion of 0.6m using Z0.95, and different γ	47
Table 7: Weather criteria lay away using JONSWAP	47
Table 8: Weather criteria and duration JONSWAP	48
Table 9: Changes of durations to the MATLAB simulation	49
Table 10: Screen shot of the results of the MATLAB simulation	50
Table 11: Duration of the operation using JONSWAP, Heidrun	52
Table 12: Check of Torsethaugen spectra	57
Table 13: Weather criteria lay away using Torsethaugen	58
Table 14: Conversion of weather criteria to Torsethaugen	59
Table 15: Weather criteria and duration Torsethaugen	61
Table 16: Duration of the operation using Torsethaugen, Heidrun	62
Table 17: Sea state from hindcast data	66
Table 18: Weather Criteria Heave Motion Simulation	68
Table 19: Duration of the Operation Resultant Heave Motion	69
Table 20: Comparing Total Sea and Resultant Heave Motion Durations	70
Table 21: H_s limiting Pitch Motion with Wind Waves head seas (0°)	73
Table 22: Roll angle simulation criteria	74
Table 23: H_s giving roll angle of 3° to corresponding groups of T_p	78
Table 24: Operation Criteria combining resultant heave motion and roll angle	80
Table 25: Wind Wave giving 0.6m Heave Motion	80
Table 26: Durations for 3° Roll Simulation and Combined Heave and Roll Simulation	81
Table 27: Main Findings, Total Sea using JONSWAP spectrum	82
Table 28: Main Findings, 4m Resultant Heave Motion for the Operation Tasks	84

Table 29: Main Findings, 3° Roll Limitation for the Operation Tasks	86
Table 30: Main Findings, 3° Roll with 0.6m Heave Limitation for the Lay Away Task	88

APPENDIX A: SIMULATED OPERATION DURATION TABLES

Table A - 1: Total Sea using JONSWAP spectrum, Heidrun.....	96
Table A - 2: Total Sea using JONSWAP spectrum, Ekofisk	96
Table A - 3: Total Sea using JONSWAP spectrum, Statfjord.....	97
Table A - 4: Total Sea using JONSWAP spectrum, Snøhvit	97
Table A - 5: 2m Resultant Heave Motion for the Operation Tasks, Heidrun.....	98
Table A - 6: 2m Resultant Heave Motion for the Operation Tasks, Ekofisk	98
Table A - 7: 2m Resultant Heave Motion for the Operation Tasks, Statfjord.....	99
Table A - 8: 2m Resultant Heave Motion for the Operation Tasks, Snøhvit	99
Table A - 9: 3° Roll Limitation for the Operation Tasks, Heidrun.....	100
Table A - 10: 3° Roll Limitation for the Operation Tasks, Ekofisk	100
Table A - 11: 3° Roll Limitation for the Operation Tasks, Statfjord.....	101
Table A - 12: 3° Roll Limitation for the Operation Tasks, Snøhvit	101
Table A - 13: 3° Roll with 0.6m Heave Limitation for the Lay Away Task, Heidrun	102
Table A - 14: 3° Roll with 0.6m Heave Limitation for the Lay Away Task, Ekofisk	102
Table A - 15: 3° Roll with 0.6m Heave Limitation for the Lay Away Task, Statfjord	103
Table A - 16: 3° Roll with 0.6m Heave Limitation for the Lay Away Task, Snøhvit	103

ABBREVIATION LIST

Abbreviation:	Full name/description:
A&R	Abandonment and Recovery
AHC	Active Heave Compensation
AUX Winch	Auxiliary Winch
COG	Center of Gravity
DP3	Dynamic Positioning Class 3
FPU	Floating Production Unit
FSU	Floating Storage Unit
H _s	Significant Wave Height
NGL	Natural Gas Liquids
PDCW	Pull Down Clump Weight
PIW	Pull In Winch Wire
RAO	Response Amplitude Operator
Subsea ETH	Subsea End Termination Head
TLP	Tension Leg Platform
T _p	Spectral Peak Period
VLS	Vertical Lay System

LIST OF SYMBOLS

Symbol:	Description:
A_y	Normalizing Factor
E	Wave Energy Density
$F_{x_{3h}}$	Rayleigh Distribution of the Largest Value in a 3-hour Sea State.
F_{x_m}	Rayleigh Distribution of the Global Response Maxima
G_0	The Normalizing Factor Related to be the Pierson-Moskowitz Form
H_S	Significant Wave Height
H_{S1}	Primary Peak H_S
H_{S2}	Secondary Peak H_S
H_{Ssw}	Swell H_S
H_{Sw}	Wind Wave H_S
RAO	Response Amplitude Operator
S	Spectrum
S_J	JONSWAP spectrum
S_{TH}	Torsethaugen Spectrum
S_x	Response Spectrum
T	Period
T_f	Peak Period for Fully Developed Sea
T_p	Spectral Peak Period
T_{p1}	Primary Peak T_p
T_{p2}	Secondary Peak T_p
T_{psw}	Swell T_p

T_{pw}	Wind Wave T_p
a_f	Fetch Length Factor
f	Frequency
f_p	Spectral Peak Frequency
g	Acceleration of Gravity
j	Primary Spectrum=1 or Secondary Spectrum=2
m_k	Spectral Moments
n	Value Number
n_τ	Expected Number of Global Maxima
r_{ps}	Swell Wave Significant Wave Height Ratio
r_{pw}	Wind Wave Significant Wave Height Ratio
tm_{02}	Expected Zero-Up Crossing Period
\tilde{x}	Characteristic Largest Response Maxima
x_α	α -Percentile
Γ_S	Pierson-Moskowitz Form of the Wave Spectrum
γ	Peak Enhancement Factor
γ_F	Peak Enhancement Function
σ	Standard Deviation
σ^2	Variance
ϑ	Spectral Width Parameter

1 INTRODUCTION

This thesis covers various simulations of a marine operation performed by Ocean Installer at Visund at different locations on the Norwegian continental shelf (Heidrun, Ekofisk, Statfjord and Snøhvit). The simulation is done using the mathematical software MATLAB. The author has developed a MATLAB script to simulate the operation duration using hindcast data provided by the Meteorologisk Institutt. The simulated operations present the average, 10-, 50- and 90-percentile durations each month. The development of the simulation script is based on this background knowledge:

- Understand the use and development of hindcast data
- The marine operation
- Development of wave spectra
- Use of probability models for vessel response

Section 2.1 covers the use of hindcast data, how it is developed and metocean data explaining the differences at the four locations. The metocean data is helpful to understand the variation of the simulated operation durations. Section 2.4 covers the description of the marine operation used as input for the operation simulation. This involves identifying the different operation tasks, which throughout the thesis will be separated with corresponding weather criteria and durations. The simulations are mainly done by using JONSWAP spectra, since a comparison of the simulated operation between JONSWAP spectra (section 3.1) and Torsethaugen spectra (section 3.2) showed minor differences (section 3.2.4.1). These two spectrum are developed by observing the wave conditions on the Norwegian continental shelf. Section 3.1.1 covers the theory, with mathematical expressions, used for calculation of vessel response. This theory is necessary to understand when using limiting vessel motions as operational criteria for the operation simulation.

The different operation simulations are gradually presented throughout the thesis with theoretically explanations and discussions using the hindcast data from Heidrun. Section 4 and 5 covers the discussion and results concerning the variation of the simulated operation durations for Heidrun, Ekofisk, Statfjord and Snøhvit.

Appendix B: Master Thesis Objectives, gives the master thesis objectives written in cooperation with professor Sverre Haver.

2 BACKGROUND

2.1 Hindcast and Metocean data

The hindcast data are provided by Meteorologisk Institutt in Bergen. The wave data is generated through numerically models based on observed atmospheric pressure fields. The pressure fields are used to calculate the wind speed at the ocean surface, and then wave parameters are derived from a wave model. The wave model used for the provided hindcast data is the WAM10 model, which has a grid of 10km and a time resolution of 3 hours. There are several models using different grids, and shorter grid gives data that are more accurate. The report “A high-resolution hindcast of wind and waves for The North Sea, The Norwegian Sea and The Barents Sea” (Reistad, et al., 2009) explains the accuracy of the generated significant wave height (H_s) vs observed H_s using the wave model WAM10. What is seen in this report is that there are some spreading comparing the observed and generated H_s (Figure 2-1), but by looking at the higher percentiles of H_s the differences are smaller. Figure 2-2 compares respectively the 95-percentile and 99-percentile of the observed and generated H_s using WAM10.

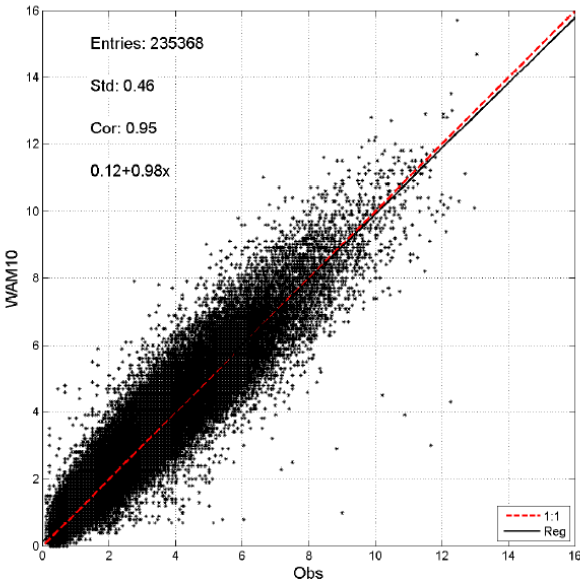


Figure 2-1: Observed H_s vs Generated H_s from WAM10 (Reistad, et al., 2009)

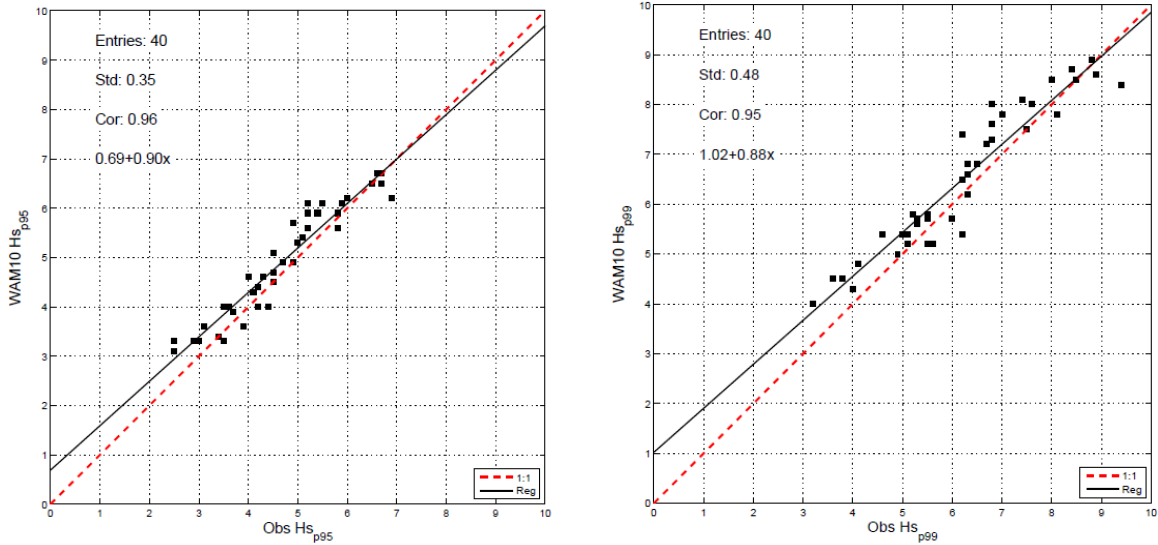


Figure 2-2: Observed Hs vs Generated Hs from WAM10 (p95 left, p99 right), (Reistad, et al., 2009)

2.1.1 Correcting the Hindcast Data Period

The provided hindcast data has a spectral peak period (T_p) with discrete logarithmic spacing, shown in Figure 2-3. A solution to this problem is described in (Andersen, 2009).

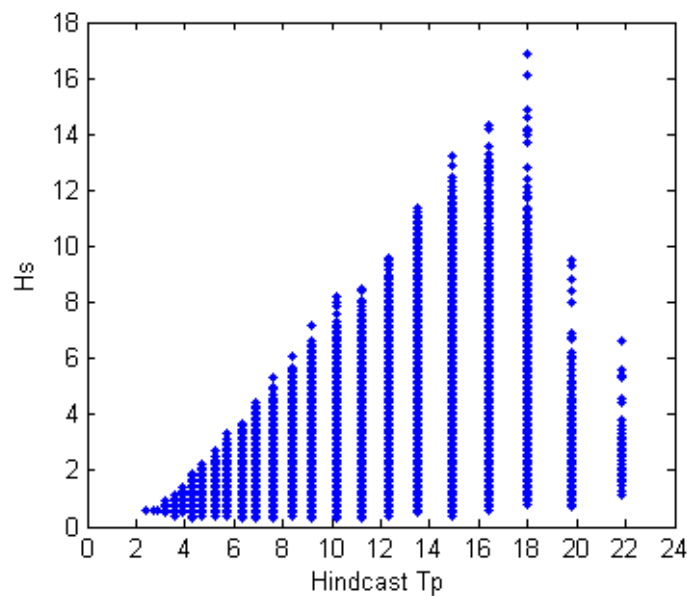


Figure 2-3 Spectral peak period before correcting

The solution is to create an associated random period around the period value from the archive. Andersen's solution is as follows

$$T_p = 3.244 \cdot \exp(0.09525 \cdot (i - 0.5 - rnd)) \quad 2-(1)$$

Where rnd is uniformly distributed in the range of 0-1, and

$$i = ROUND \left[1 + \frac{\ln \left(\frac{T_p^*}{3.244} \right)}{0.09525} \right] \quad 2-(2)$$

Where T_p^* is the peak period from the archive. The round function rounds the number x to closest 0 digit. Figure 2-4 shows the result of correcting the spectral peak period for the hindcast data at Heidrun.

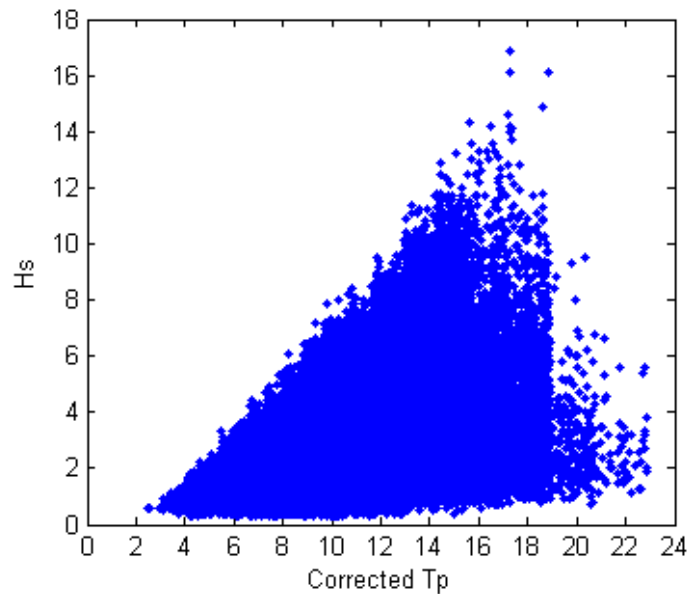


Figure 2-4: Spectral peak period after correcting

2.1.2 Discussion on the Hindcast Swell and Wind Waves Data

To get a better understanding of the results, the generation of swells and wind waves, and how they impact the various areas of the Norwegian continental shelf needs to be covered. The hindcast data locations and well-known field close by is shown in the figure below.



Figure 2-5: Locations of Hindcast Data and well-known fields close by
(Generated with <http://www.darrinward.com/lat-long> (Ward, 2015))

2.1.2.1 How wind waves are generated

Many scientists have tried to explain how wind waves are generated; this is quite complicated and still not very well understood. The last well-known and most accepted theory is called the Miles-Phillips theory. This theory was put up by O.M. Phillips and further developed by J.W. Miles. The theory is based on the fact that air moves faster and faster the further away from the water until (height of 10m) it reaches the speed meteorologists call the *wind speed*. At some height below this, the air and the wave are moving at the same speed, usually less than a few centimeters above the water surface, which is known as the critical height. Below the critical height, the air is moving more slowly than the wave. According to Miles, at the critical height the wind flow deforms over the existing waves so that it produces a low pressure on the leeward face of the wave and a high pressure on the windward face. This is what is needed to add energy to the waves, which will make the waves grow with wind duration and fetch. Fetch is the area of contact between the wind and the water and is where the wind wave generation begins.

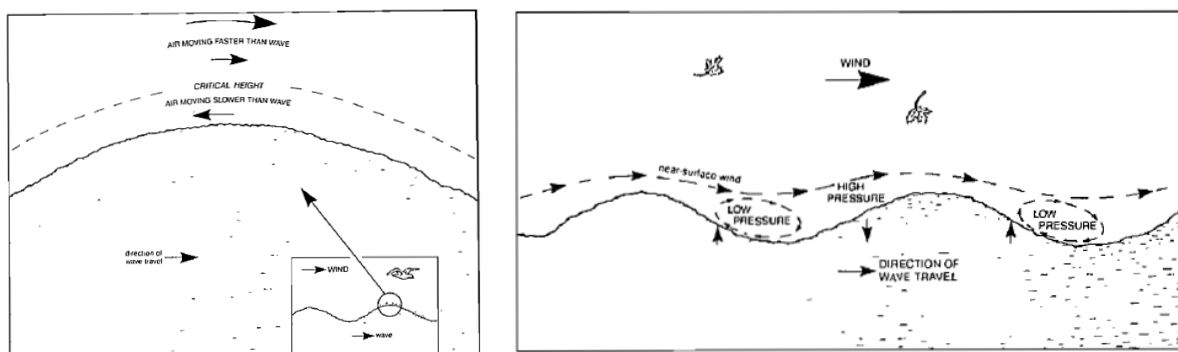


Figure 2-6: Critical Height (left) and Low and High Pressure Generation (right).
(Thomson, 1981)

Ripples develop on a calm water surface when the wind reaches a certain threshold velocity. Capillary waves controlled by the combined forces of gravity and surface tension are always the first ripples to appear on calm water once the wind begins to blow. These waves have minimum possible speed of 0.23 m/s and form a crisscross pattern of two sets of wave crest, each set moving at an angle 70-80° to the wind direction (Figure 2-7). The spacing between the individual crest is 0.018 m and have periods of 0.0073 s. The large angle between the wind direction and the direction of the wave-crest is due to the fact that the slow propagation speed of the capillary waves makes it impossible for them to travel at the downwind speed of the pressure fluctuations. Instead, the waves head off in the direction where their speed matches the speed of one of the wind's velocity components.

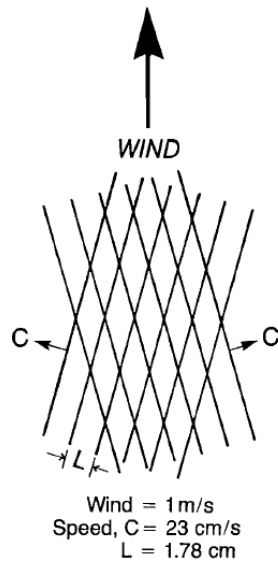


Figure 2-7: Criss-Cross Pattern of Waves 80° of Wind Direction (Thomson, 1981)

If the wind dies the ripples disappear, but if it strengthens, the length, height, and periods of the ripples increase and there is a resulting increase in their speed of propagation. If the wind strengthens the angle of the travel direction of the waves with respect to wind direction will decrease which last for winds until 2-3 m/s where the travel direction of the waves are 30° to the wind. The reason is that the component of the wind velocity, which now matches the propagation speed of the waves, lies even closer to the true wind direction. At this stage the intersecting region with wrinkles, of the internal criss-cross pattern of the waves, is travelling in the direction of the wind (Figure 2-8). The airflow is still unaffected by the waves and the surface is *hydrodynamically smooth*.

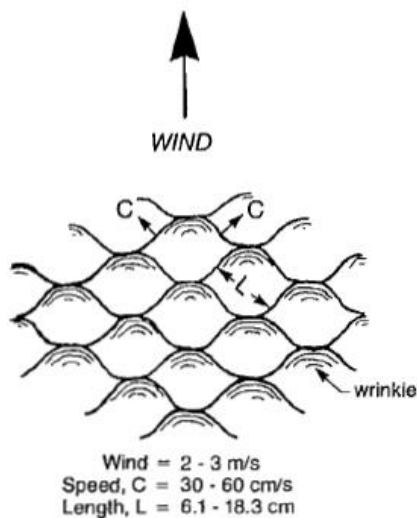


Figure 2-8: Criss-Cross Pattern of Waves 30° of wind direction (Thomson, 1981)

For wind speeds above 3 m/s, the growing waves are independent of the surface tension and their heights become large enough to affect the airflow. The surface is now *hydrodynamically rough*. This induces turbulent pressure fluctuations in the wind, which increases the amount of energy fed into the waves, and accelerate their length and height. The energy transmitted from the wind to the waves favors the wave which direction is nearly the same direction as the wind. With increased wind speed above 3 m/s, the wave field becomes irregular with different heights, lengths, speed and periods. In the generation region a wave-wave interaction now starts, transferring energy from shorter to longer waves and the dominant wavelength increases. It is no longer possible to distinguish between individual wave groups. Instead, an ensemble of waves moves within approximately 50° to the left and right of the wind direction, which is only meaningful in a statistical sense. Instead of a collection of identifiable groups of waves there is now a continuous spectrum of waves where height, periods, etc., range from the smallest capillaries to the largest waves. (Thomson, 1981)

Wind waves and swells are both wind-generated waves. The difference is that wind waves are locally generated while swells are generated at a different location and is not affected by the local winds. Swells often have a long wavelength and contain a lot of energy, but this varies with the weather system (wind speed) that generated the swells. A consequence of storms in the ocean is generation of swells, and the energy that the swell waves can transmit to offshore structures, vessels, etc., depends on the fetch and dispersion length. Dispersion is a gradual separation of wave types based on their relative wavelengths and speeds.

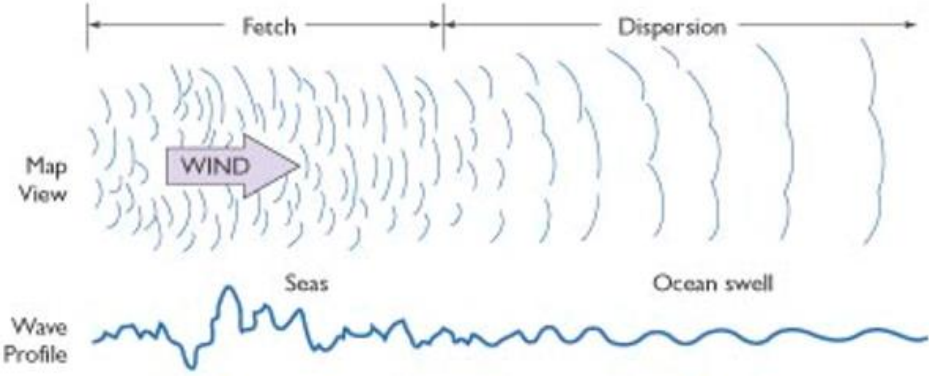


Figure 2-9: Fetch and Dispersion (Pinet, 2003)

2.1.2.2 Summer and Winter Storm/Wind

The simulated operation duration (section 3) shows that the summer months has a much better weather than the winter months. To explain this a statistical monthly average wind speed figure for January 2008 and July 2008 (Figure 2-10 and Figure 2-11) is gathered from Remote Sensing Systems.

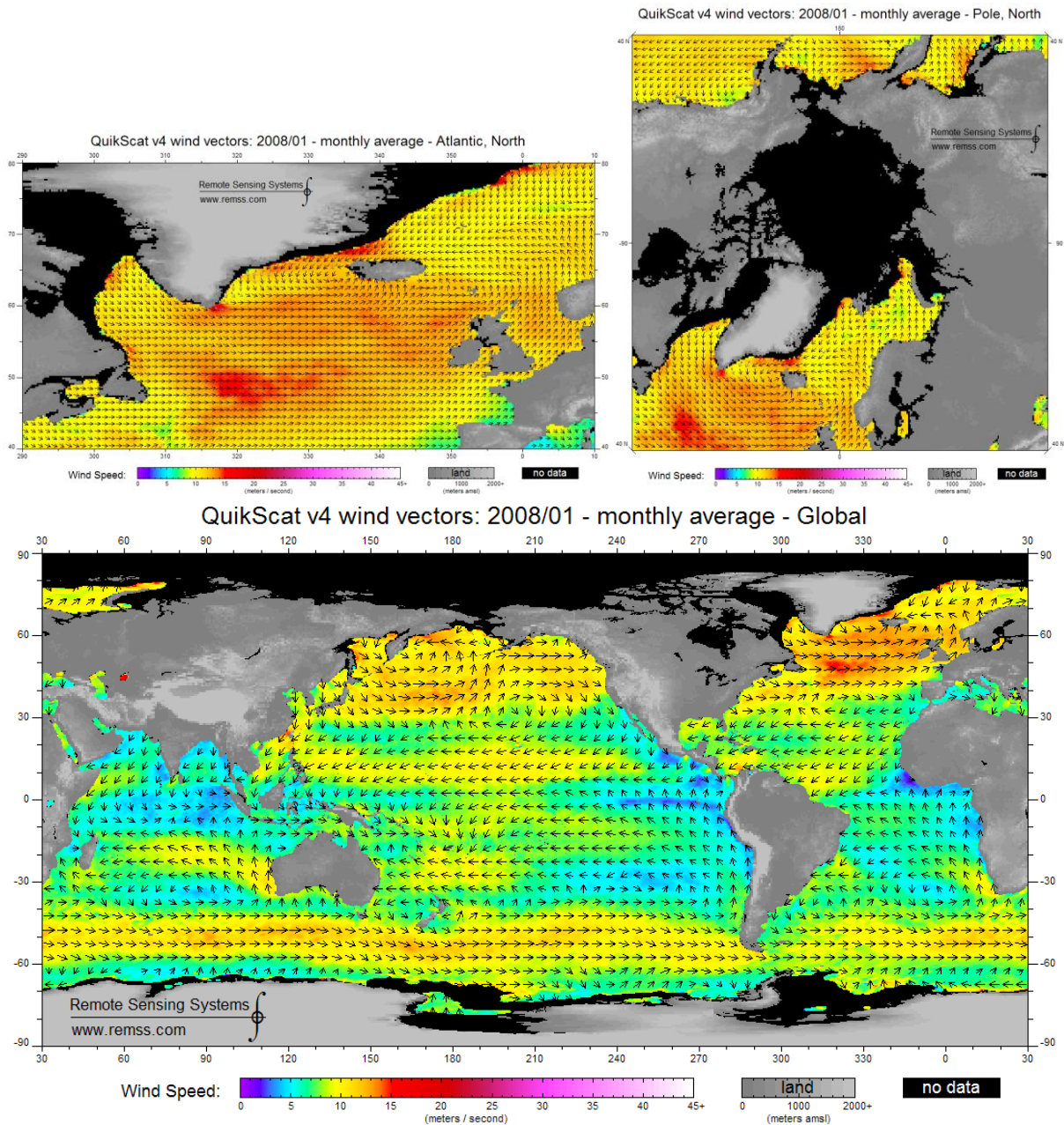


Figure 2-10: Monthly average wind speed and direction 01/2008 (Remote Sensing Systems (RSS), 2009)

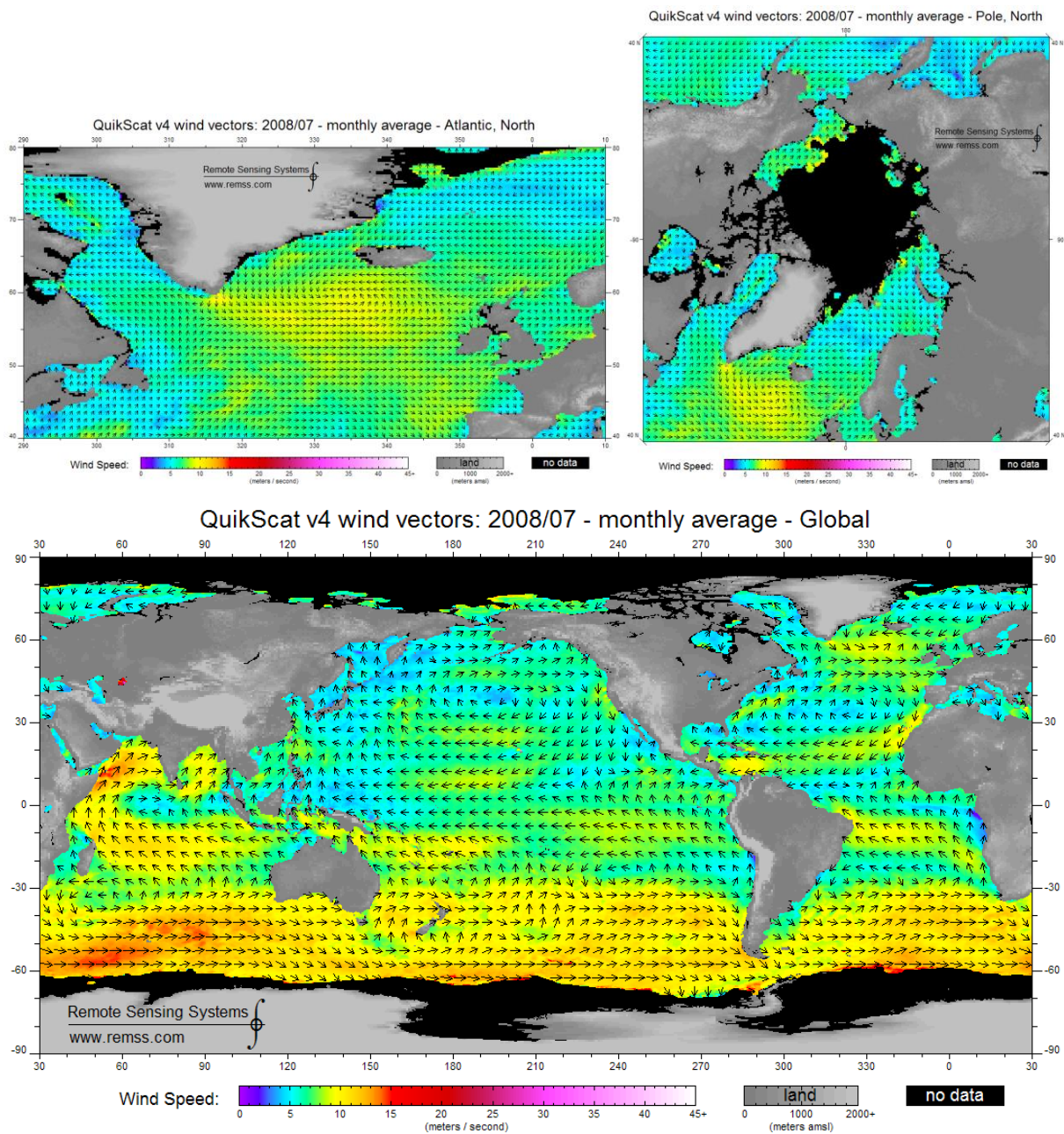


Figure 2-11: Monthly average wind speed and direction 07/2008
(Remote Sensing Systems (RSS), 2009)

As seen in Figure 2-10 and Figure 2-11 the wind speeds in January are faster than in July for the area close to Norway, which means that the wave height and periods are larger in the winter season than in the summer season. Locally larger wind waves are therefore generated, and more and larger swells are generated from for example the North Atlantic Sea where there is a huge difference between average wind speed in January and July.

2.1.2.3 Verification of the Metocean calculation

To get a better understanding of wave's impact on the Norwegian continental shelf the wave direction needs to be known. For this purpose metocean data is established. To verify that the metocean calculations are correct Ocean Installer has provided yearly metocean data for the Norne field established by Statoil (Eik, 2012). The Norne field is close to Heidrun and should have similar weather conditions. The metocean data for Norne is for the total sea using the mean direction. The total sea are a combination of the wind waves and swells, and is used for one directional calculations in the thesis. The total sea metocean data comparison only gives an indication on whether the metocean calculations are correct and these are not used further in the thesis. The direction are 0° when waves are coming from north, 90° when waves are coming from east, 180° when waves are coming from south and 270° when waves are coming from west.

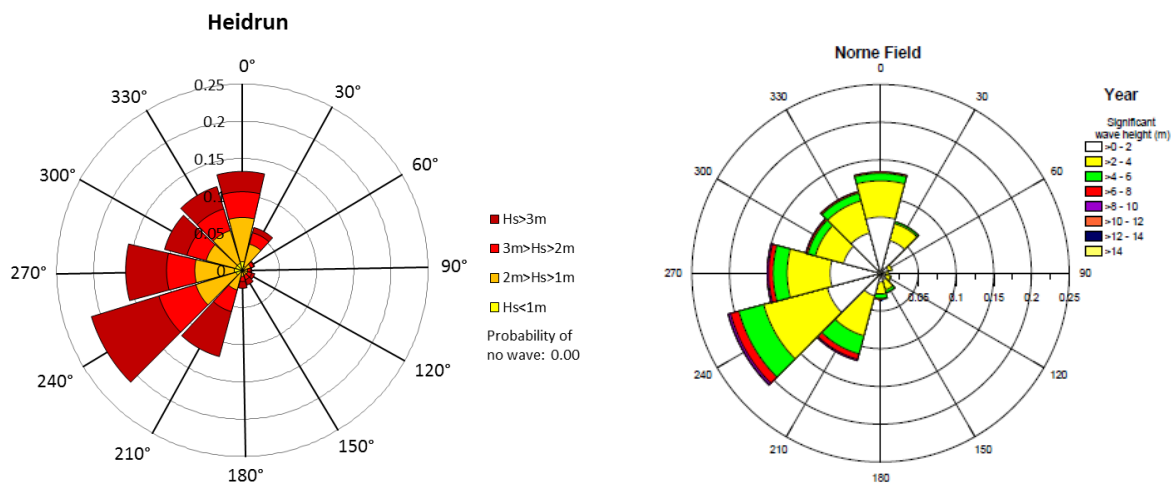


Figure 2-12: Comparing Metocean Data from Statoil (right), (Eik, 2012), and Calculated Metocean Data (left)

Figure 2-12 shows that there are nearly none differences in the calculated metocean data and the metocean data developed by Statoil. This verifies that the metocean calculations are correct.

2.1.2.4 Wind Waves on the Norwegian Continental Shelf

Wind waves vary with direction and energy from summer and winter. Figure 2-13 to Figure 2-20 shows the variation between January and July for the different fields. The hindcast database contains a lot of data where the wind wave T_p is 0s and H_s is 0.1m. Wind waves with $T_p=0s$ and $H_s=0.1m$ are assumed to be still water and no waves. These data are set to be the same direction in the hindcast data base and would give a wrong impression of the wind wave

direction, presented in Figure 2-13 to Figure 2-20, and are displayed as probability of no waves in the figures.

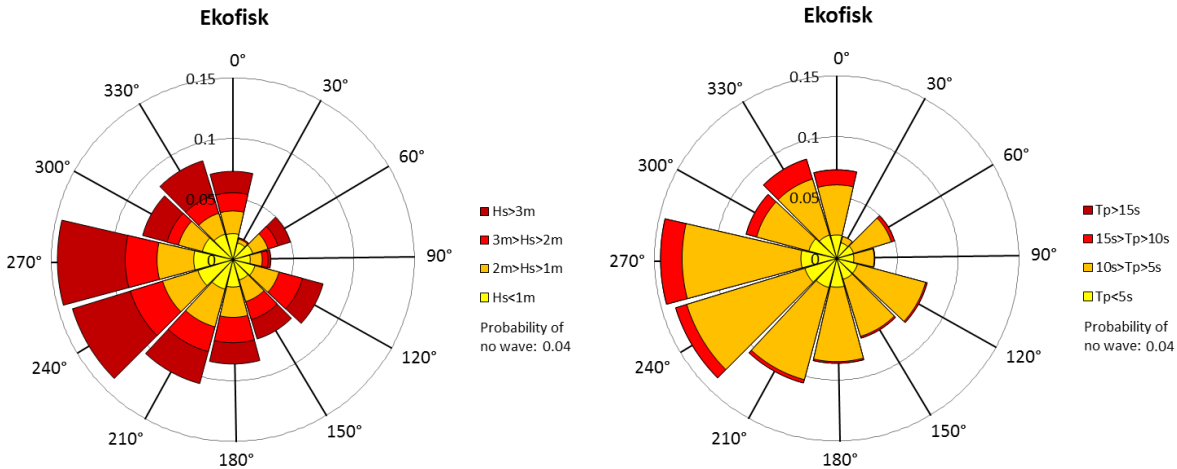


Figure 2-13: Wind Wave Direction Ekofisk January

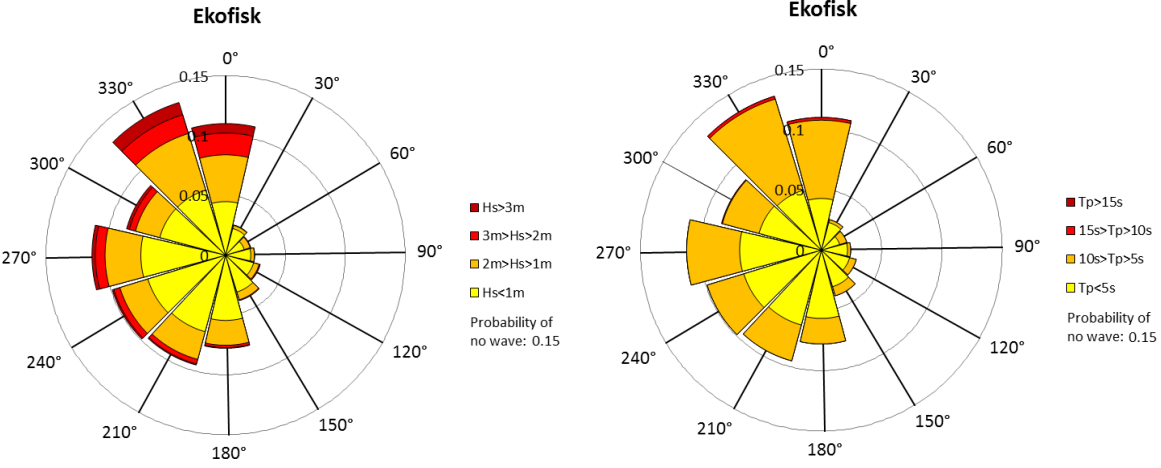


Figure 2-14: Wind Wave Direction Ekofisk July

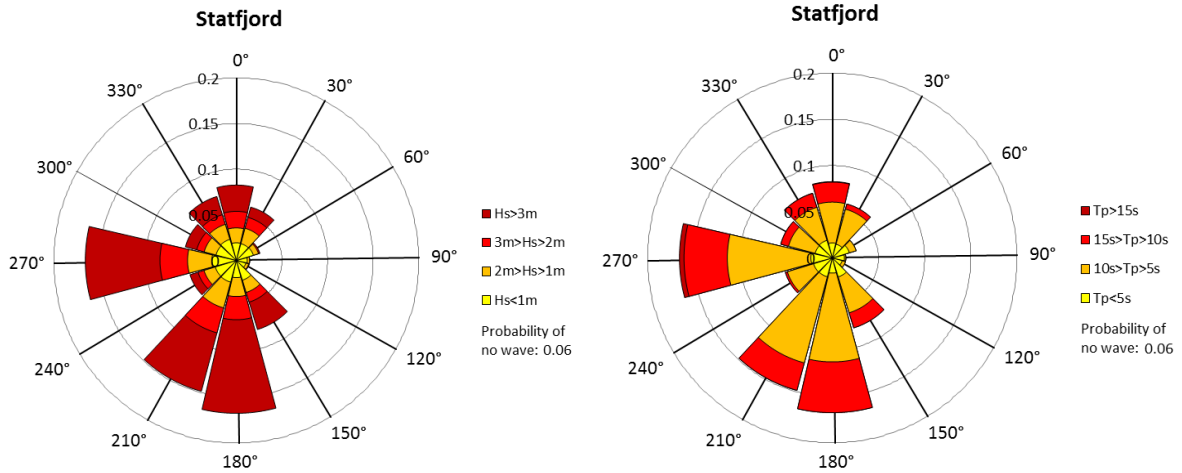


Figure 2-15: Wind Wave Direction Statfjord January

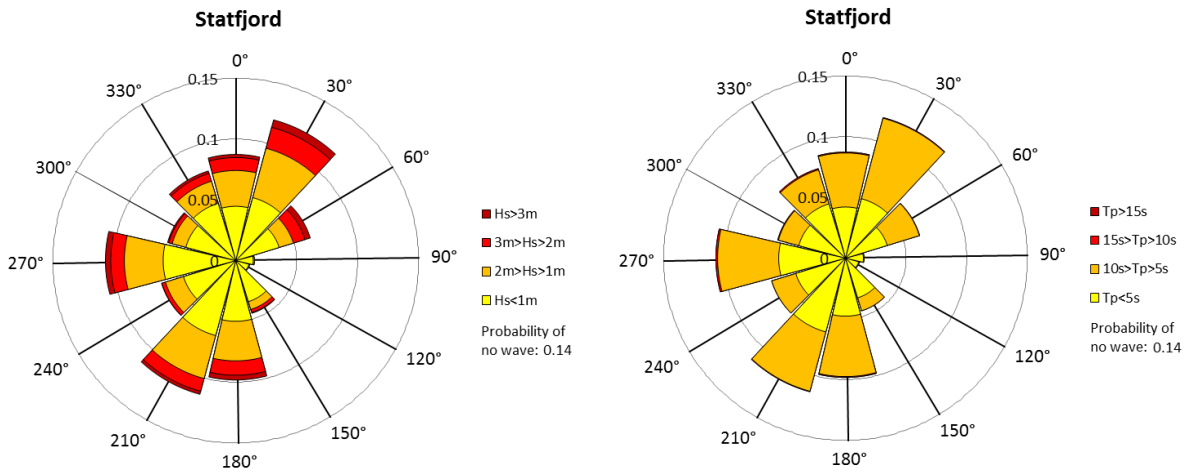


Figure 2-16: Wind Wave Direction Statfjord July

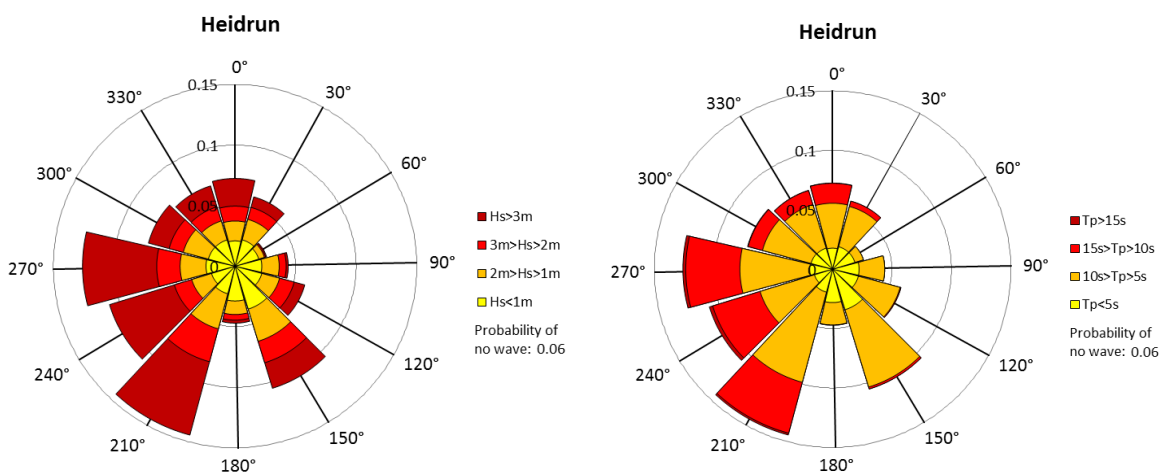


Figure 2-17: Wind Wave Direction Heidrun January

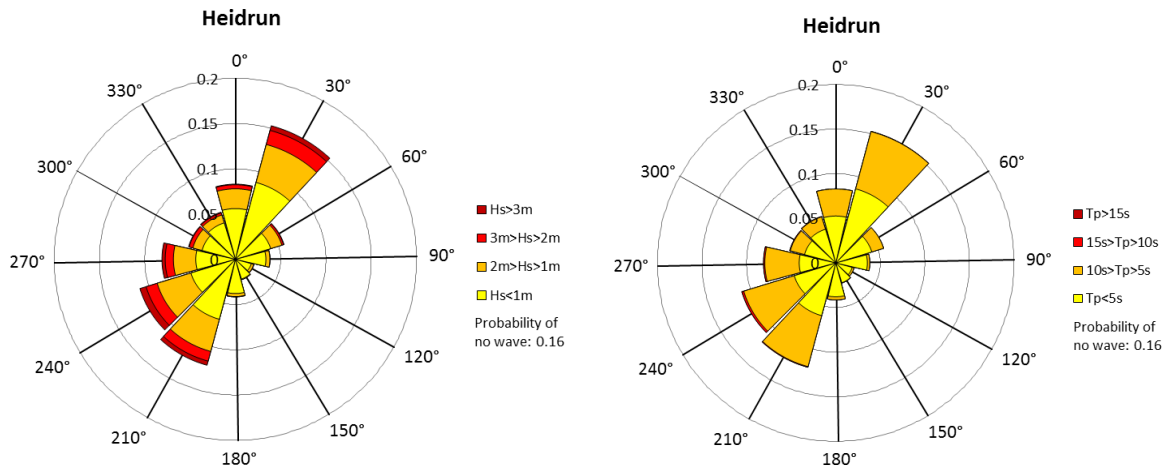


Figure 2-18: Wind Wave Direction Heidrun July

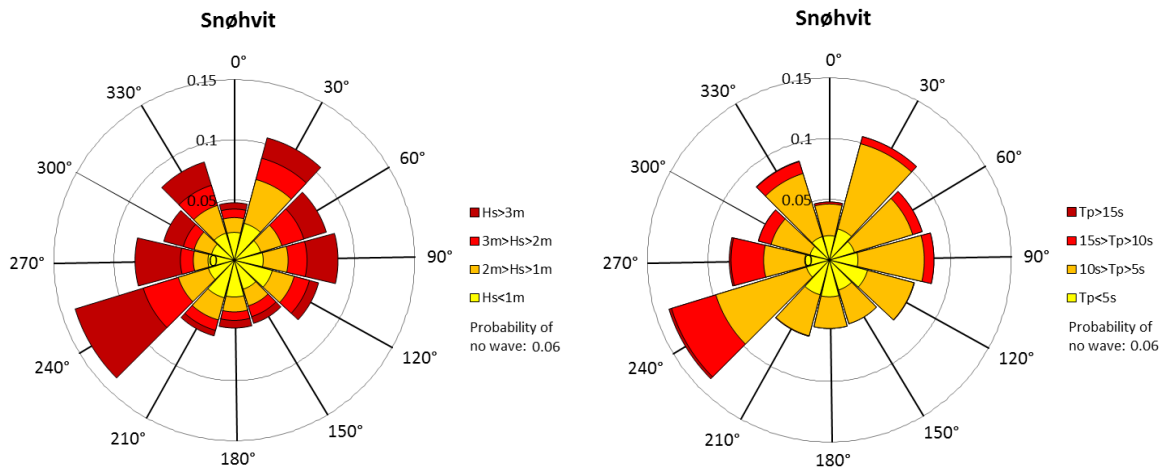


Figure 2-19: Wind Wave Direction Snøhvit January

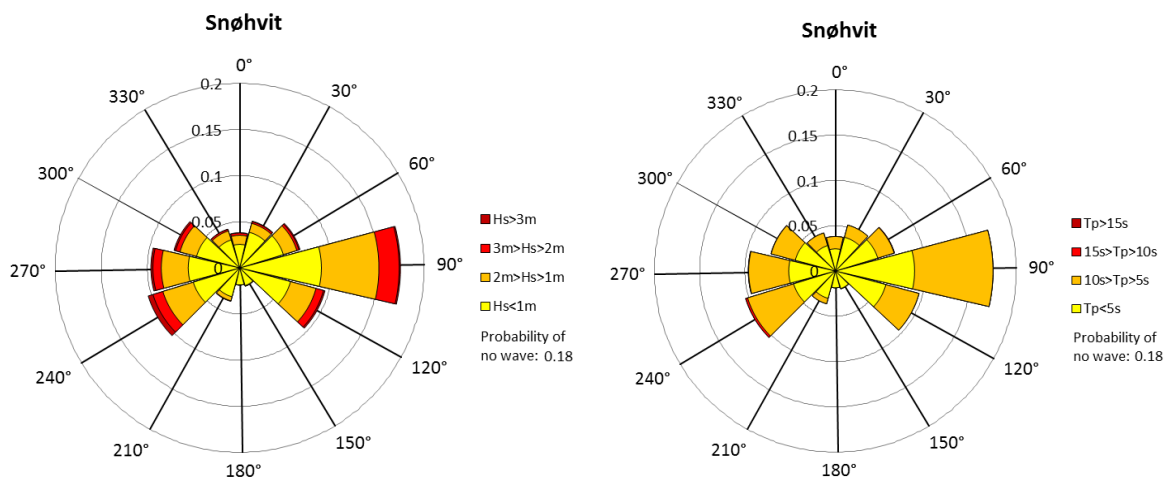


Figure 2-20: Wind Wave Direction Snøhvit July

Figure 2-13 to Figure 2-20 show that the energy of the waves is a lot less for July than January. Comparing this to the map of average wind speed of January and July 2008 (Figure 2-10 and Figure 2-11) the wind wave energy difference between January and July seems reasonable. This is one of the reasons why the simulated operation durations in the winter months are a lot longer than for the summer months.

2.1.2.5 Impact from Swell on the Norwegian Continental Shelf

By knowing the swell direction it is possible to find the swells origin (the storm that created the swells). If the swells have the same origin for the various hindcast data points it is possible to compare the simulated operation durations with the dispersion length or if countries such as the United Kingdom and Ireland are blocking the swells. If the dispersion length is long the operation duration should be shorter since the swell energy is transferred to a wider area. For this purpose the probability of the direction of the swells, January and July, were calculated for each hindcast data points and compared. Figure 2-21 to Figure 2-28 shows a rose diagram separating the directions of swells for the different fields of January and July, and separating into categories of T_p and H_s .

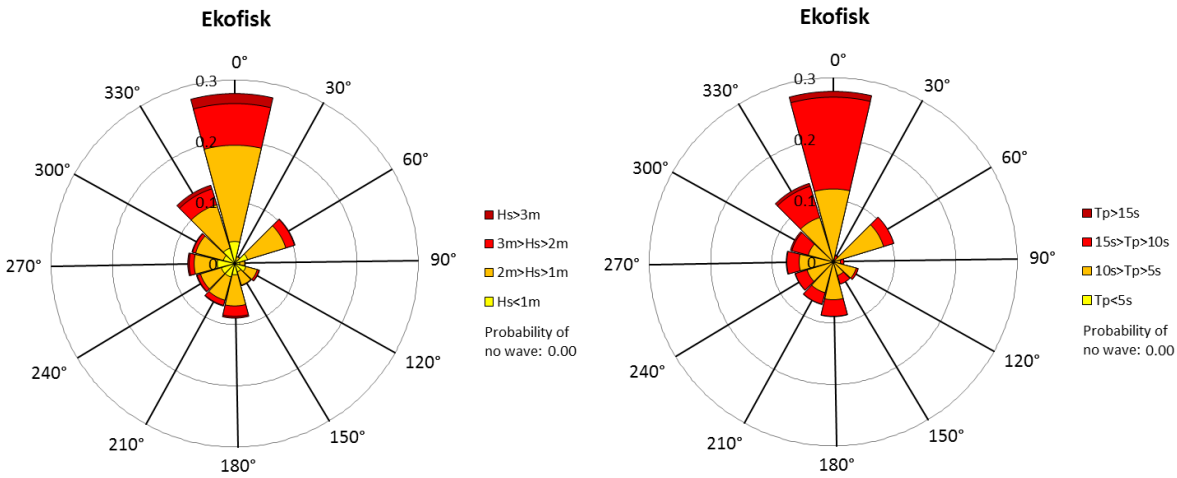


Figure 2-21: Swell Direction Ekofisk January

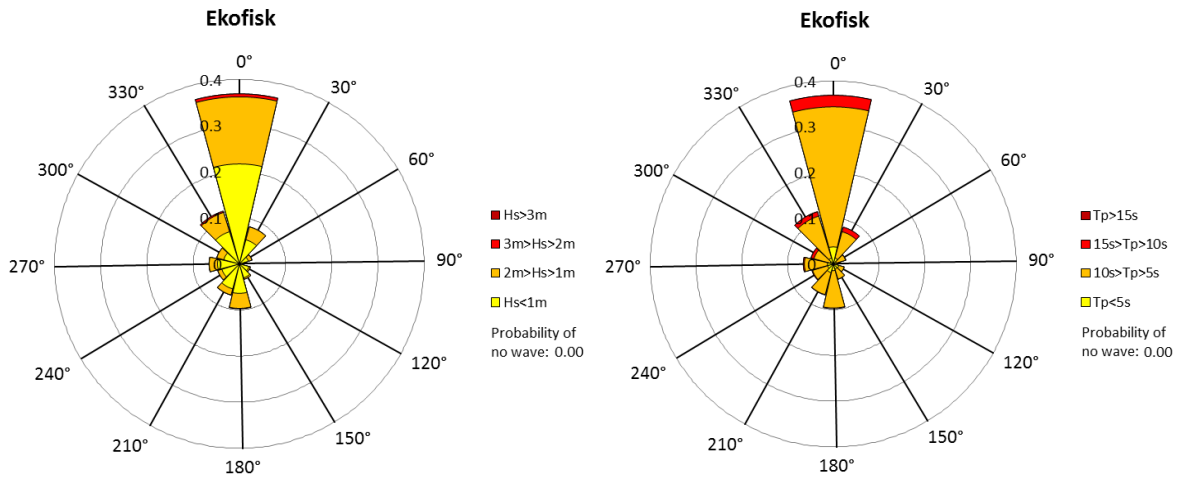


Figure 2-22: Swell Direction Ekofisk July

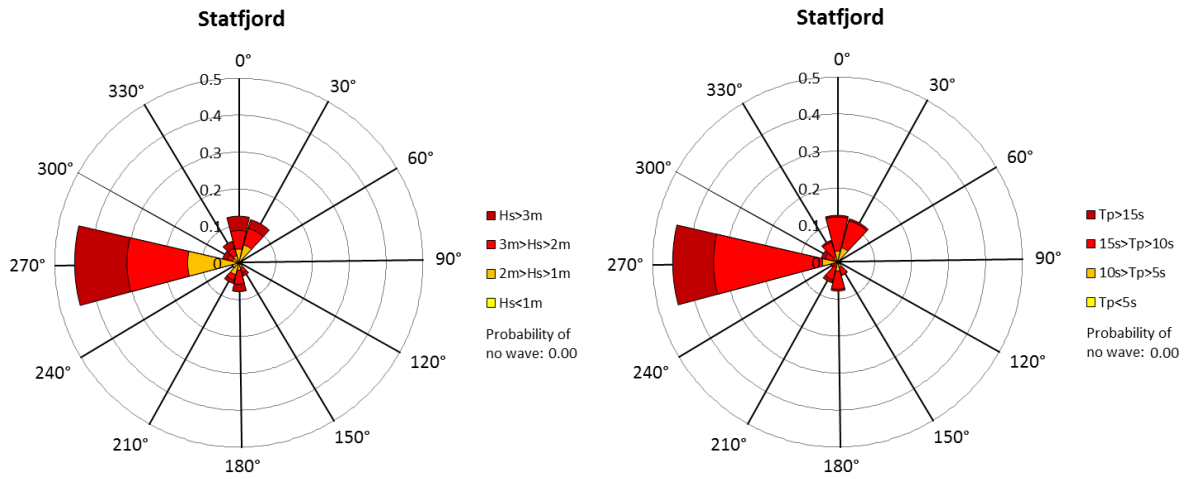


Figure 2-23: Swell Direction Statfjord January

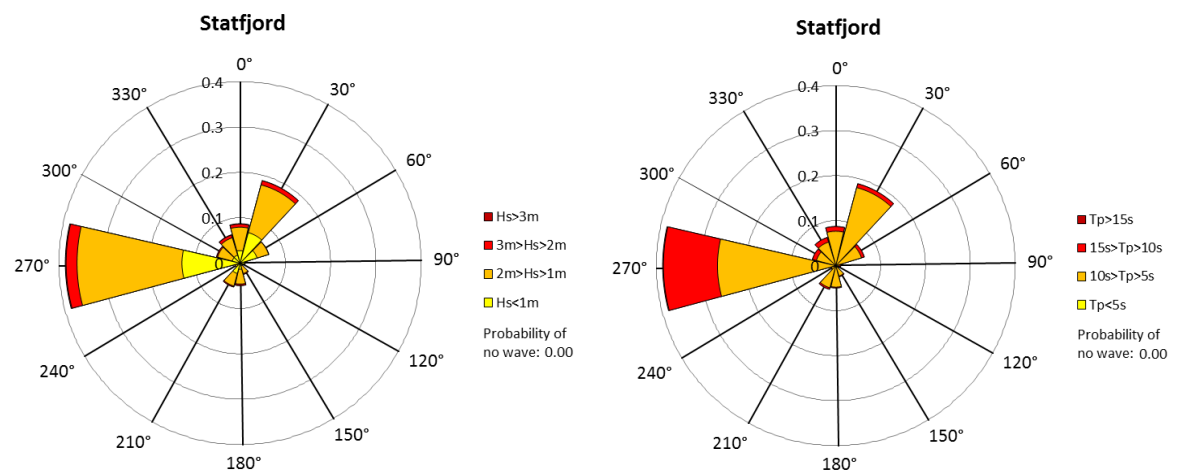


Figure 2-24: Swell Direction Statfjord July

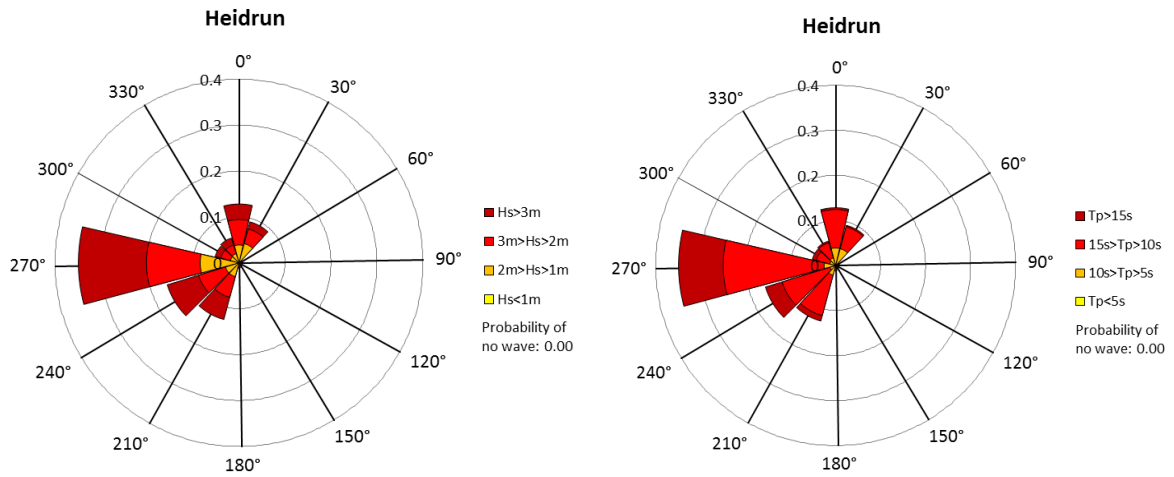


Figure 2-25: Swell Direction Heidrun January

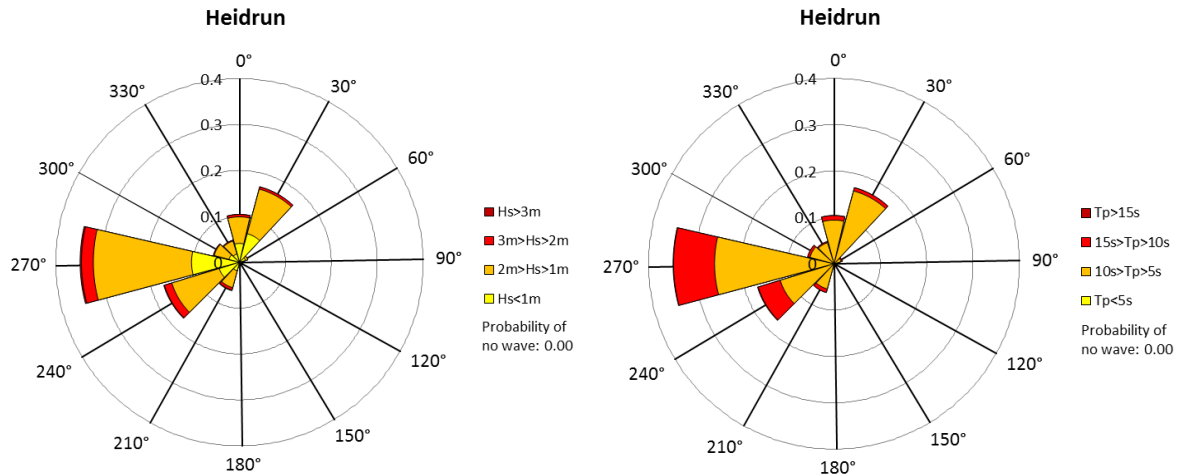


Figure 2-26: Swell Direction Heidrun July

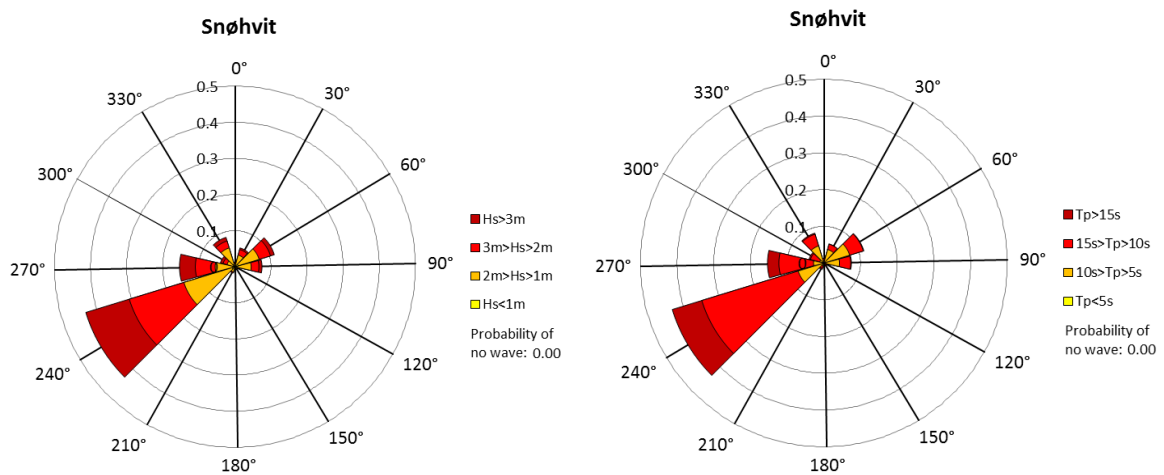


Figure 2-27: Swell Direction Snøhvit January

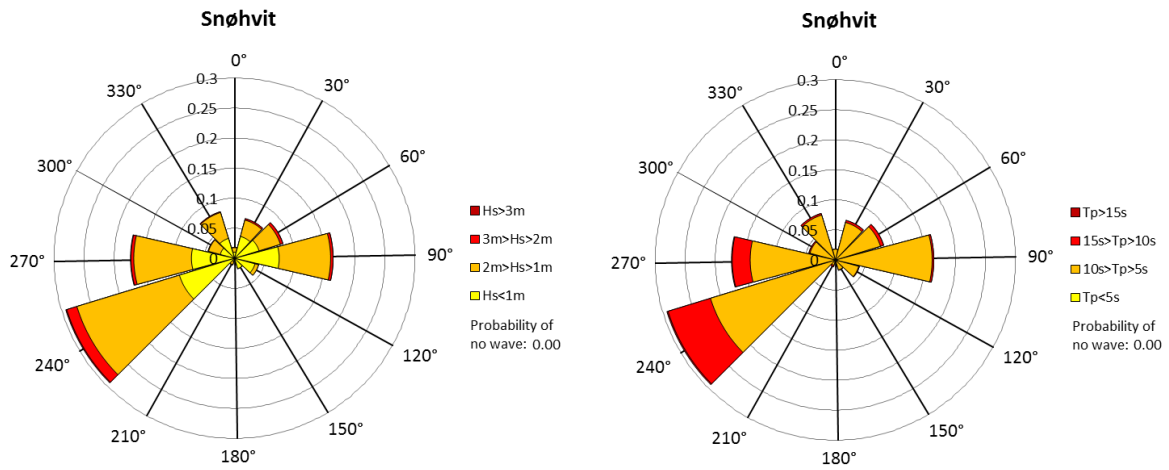


Figure 2-28: Swell Direction Snøhvit July

Figure 2-21 to Figure 2-28 shows that for all locations the swell direction is from the west, except Ekofisk. This means that there are probably storms in the North Atlantic Ocean generating the swells.

Now getting into the dispersion length and blocking of swells from the United Kingdom and Ireland. Figure 2-29 shows how the dispersion length varies for Statfjord, Heidrun and Snøhvit, and how the swell energy is blocked for Ekofisk.

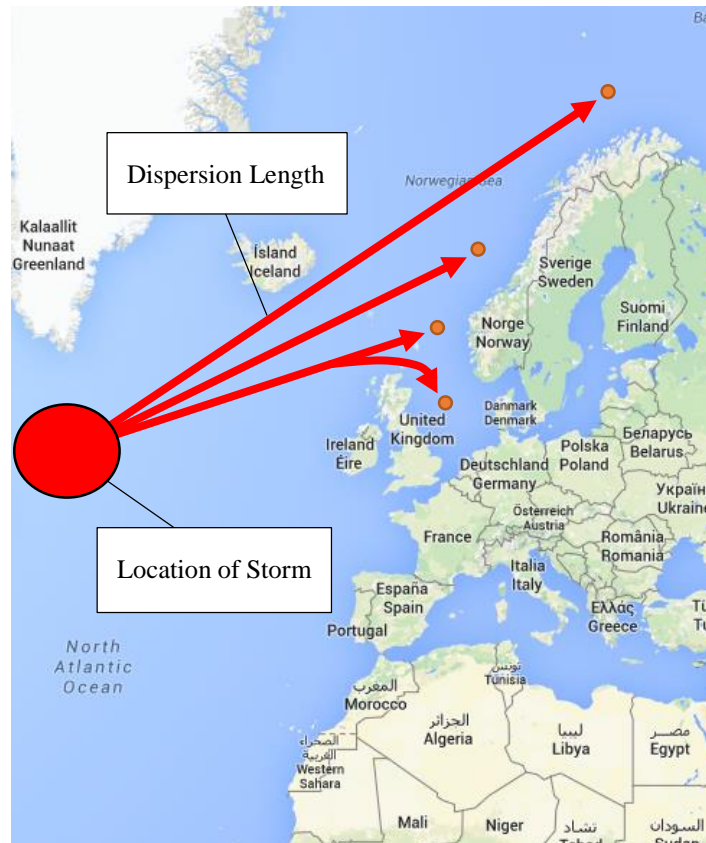


Figure 2-29: Location of Storm and Dispersion Length

Statfjord and Heidrun have a lot of swells coming from west, and by being close to each other the dispersion length is relatively close. Both Statfjord and Heidrun are blocked by the United Kingdom and Ireland from southwest swells, which can also be seen in Figure 2-21 to Figure 2-28. This should result in very close simulated operation durations since both swell and local wind waves can be set to be almost equal for the two areas (section 4). Snøhvit have a lot of swells from the southwest, and it is probably a lot of the same swells as Heidrun and Statfjord, but the dispersion length is a lot longer for swells generated in the North Atlantic Ocean. This should result in swells with less energy and simulated operation duration less than Heidrun and Statfjord (section 4). When it comes to Ekofisk the swell direction is mostly from north. This is because Ekofisk is sheltered from swells in all direction except north. These swells is probably the same swells which hits Heidrun, Statfjord and Snøhvit, but the big swells coming from the North Atlantic Ocean are now bent around the United Kingdom and has lost a lot of their potential energy. The simulated operation duration should be a lot less for this area (section 4).

2.1.2.6 Swells from the North Atlantic Ocean coming to Ekofisk

An assumption made in section 2.1.2.5, that swells from the North Atlantic Ocean are bent around the United Kingdom and end up in Ekofisk needs to be further investigated. The first reason for the assumption is the differences in the directions of swells at Statfjord and Ekofisk (Figure 2-30).

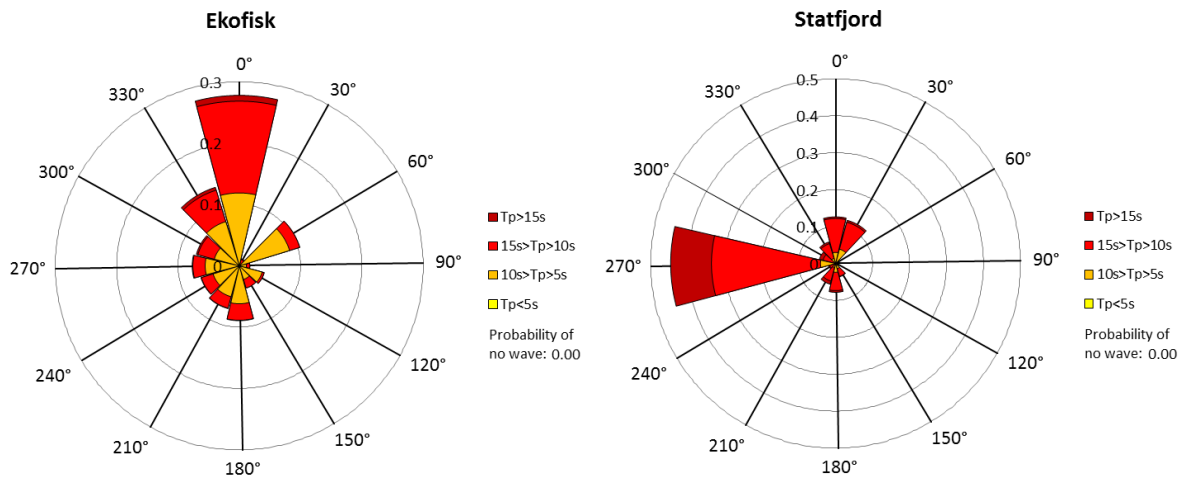


Figure 2-30: Comparing Swell Direction at Ekofisk and Statfjord

Ekofisk has a lot of swells coming from north, these swells should pass Statfjord as well. But Statfjord does not have that much swells coming from north, instead there are a lot of swells coming from west (the North Atlantic Ocean). The portion of swells coming from west at Statfjord is close to the portion of swells coming from north and northwest at Ekofisk. This is the reason why these swells are believed to be the same swells.

Further investigations is done by looking at the swell direction at a specific time for Statfjord, and then see whether the swell direction at Ekofisk is between 285° and 0° within the next 12 hours. Figure 2-31 gives the probability of at least one swell direction between 285° and 0° at Ekofisk within the next 12 hours after passing through Statfjord with a specific direction.

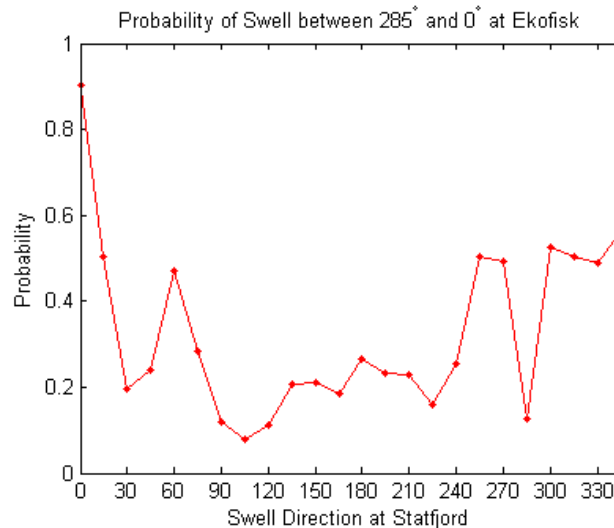


Figure 2-31: Probability of a Swell between 285° and 0° at Ekofisk within the next 12 hours

Figure 2-31 shows that when a swell passing through Statfjord at 0°, the probability of a swell between 285° and 0° at Ekofisk within the next 12 hours is close to 0.9 which makes the calculations reasonable. For the swells passing through Statfjord from south, the probability of a swell between 285° and 0° at Ekofisk within the next 12 hours is low. This is also reasonable. Looking at swells passing through Statfjord from west to north (270°-345°) the probability of a swell between 285° and 0° at Ekofisk within the next 12 hours is close to 0.5 except 285°. This indicates that some waves from west are bent around the United Kingdom. This need to be further investigated by looking at specific time series from the hindcast data at Statfjord and then see if it is possible to find the same time series at a reasonable time after passing through Ekofisk. This is not investigated in this thesis but is a possibility for further work.

2.1.2.7 Comparing Direction of Wind, Swell and Wind Wave

Some of the swells in the hindcast database might be local wind waves that the hindcast database believes to be swells. This can be investigated by comparing wind direction with swell and wind wave direction. To do a simple analysis, the number of events in the hindcast data where the wind direction are $\pm 30^\circ$ compared to swell and wind wave direction is done for different locations.

Table 1 shows that most of the wind wave and wind direction are in the same direction. Most of the swells are in a different direction than the wind, which tells that the swells are not affected by the local winds. This validates that the calculation of the swell and wind wave direction in the hindcast database is reasonable.

Table 1: Comparing Wind Direction with Swell and Wind Wave Direction

Field	Probability of swell and wind direction $\pm 30^\circ$ in the hindcast data	Probability of wind wave and wind direction $\pm 30^\circ$ in the hindcast data
Ekofisk	0.19	0.88
Statfjord	0.21	0.85
Heidrun	0.22	0.85
Snøhvit	0.21	0.85

2.2 Description of Fields

The hindcast data used in this thesis is from locations close to the fields described in this section (Norwegian Petroleum Directorate, 2015). The thesis will use the Heidrun field for the explanations of the analysis in section 3. Section 4 covers comparison between of the different fields.

2.2.1 Heidrun

The Heidrun oil and gas field consists of two blocks, 6507/7 and 6507/8. The operator of the Heidrun field is Statoil with 13.04% interest. The other licensees are divided between Petoro (57.79%), ConocoPhillips (23.99%) and Eni (5.18%).

The Heidrun field was discovered in 1985 and started producing in 1995. The recoverable reserves at the field were originally 183.3 million cubic meters of oil, 47.3 billion cubic meters of gas, and 2.2 million tons of natural gas liquids (NGL). The depth of the reservoir is up to 2,300m beneath the seabed. The water depth is about 350m.

The field has been developed with a TENSION LEG PLATFORM (TLP) which is installed over a subsea template consisting of 56 well slots. The oil is loaded with a buoy loading system and transported mainly via shuttle tankers. By 2015 the existing buoy loading system will be replaced by a FLOATING STORAGE UNIT (FSU) which will be permanently connected to a buoy. The gas output is transported via pipelines.



Figure 2-32: Heidrun location (Statoil, 2015)

2.2.2 Ekofisk

The Ekofisk oil and gas field is located in block 2/4. The operator of the Ekofisk field is ConocoPhillips with 35.11% interest. The other licensees are divided between Total E&P Norge (39.90%), Eni Norge (12.39%), Statoil Petroleum (7.60%) and Petoro (5.00%).

The Ekofisk field was discovered in 1969 and started producing in 1971. The recoverable reserves at the field were originally 553.9 million cubic meters of oil, 162.2 billion cubic meters of gas, and 14.4 million tons of natural gas liquids (NGL). The depth of the reservoir is up to 3,250m below mean sea level. The water depth is about 70-75m. The field has been developed with several platforms (production, wellhead and processing). The oil and gas are routed to export pipelines via the processing facility at Ekofisk J.



Figure 2-33: Ekofisk location (Statoil, 2015)

2.2.3 Statfjord

The Statfjord oil and gas field is located in block 7120/5, 7120/6, 7120/7, 7120/8, 7120/9, 7121/4, 7121/5 and 7121/7. The operator of the Statfjord field is Statoil Petroleum with 44.34% interest. The other licensees are divided between ExxonMobil Exploration & Production Norway (21.37%), Centrica Resources Norge (19.76%), and Centrica Resources Limited (14.53%)

The Statfjord field was discovered in 1974 and started producing in 1979. The recoverable reserves at the field were originally 573.7 million cubic meters of oil, 80.3 billion cubic meters of gas, and 22.6 million tons of natural gas liquids (NGL). The depth of the reservoir is up to 3,000m. The water depth is about 150m. The field has been developed with three fully integrated facilities. Stabilized oil is stored in storage cells at each facility and loaded onto tankers. Gas is exported through pipelines.



Figure 2-34: Statfjord location (Statoil, 2015)

2.2.4 Snøhvit

The Snøhvit gas field is located in block 33/9 and 33/12. The operator of the Statfjord field is Statoil Petroleum with 36.79% interest. The other licensees are divided between Petoro (30.00%), Total E&P Norge (18.40%), GDF SUEZ E&P Norge (12,00%) and DEA Norge (2.81%)

The Snøhvit field was discovered in 1984 and started producing in 2007. The recoverable reserves at the field were originally 218.70 billion cubic meters of gas, and 7.50 million tons of natural gas liquids (NGL). The depth of the reservoir is approximately 2,300m. The water depth is about 310-340m. The field has been developed with subsea templates for 19 production wells and one injection well for CO₂. Gas is transported through pipelines to Melkøya in Hammerfest for processing and export.



Figure 2-35: Snøhvit location
(Statoil, 2015)

2.3 Normand Vision – The operating vessel

RESPONSE AMPLITUDE OPERATORS (RAOs) and analysis throughout the thesis will be based on Ocean Installer’s operating vessel Normand Vision. Normand Vision is a large DYNAMIC POSITIONING CLASS 3 (DP3) vessel of VARD 3 06 L design and was built by VARD, Norway. VARD’s previous experience and feedback of delivering 8 versions of the OSCV 06 L design gave the basis for improving the design, and ensure that Normand Vision is the class leading asset which will be the new benchmark for large construction vessels in the North Sea and beyond.



Figure 2-36: Normand Vision at sea (Ocean Installer, 2015)

Normand Vision has a main crane with a capacity of 400Te. The main crane winch and the 20Te AUXILIARY (AUX) winch are ACTIVE HEAVE COMPENSATED (AHC) with 3000m of wire. Normand Vision’s offshore crane has a capacity of 70Te with a main winch with capacity of 100Te (double fall) for harbor and deck lifting and 70Te (single fall) with 3000m wire for subsea lifting. The 70Te offshore crane also has a 10Te AUX winch with AHC of 400m.

Table 2: Normand Vision Specifications

Length overall	156.7 m
Breadth	27.0 m
Max draught	8.5 m
Transit speed up to	16.8 knots
Total free deck space	2100 m ²
Dynamic Position class	DP3

2.3.1 Vertical Lay System (VLS)

The 150Te VERTICAL LAY SYSTEM (VLS) is positioned over the moonpool of Normand Vision. It is placed in an optimal position vs flotation center/CENTER OF GRAVITY (COG) which offers maximum safety and access as well as minimizing heave motion due to pitch and roll. The VLS is able to install and recover flexible products ranging from 50mm to 600mm in diameter. The two 75Te tensioners with 4 track tensioner system holds the product and can be operated in both 4 track and 2 track mode. The VLS crane is equipped with an 185Te ABANDONMENT AND RECOVERY (A&R) winch for safely lowering or deploying end of product to seabed.

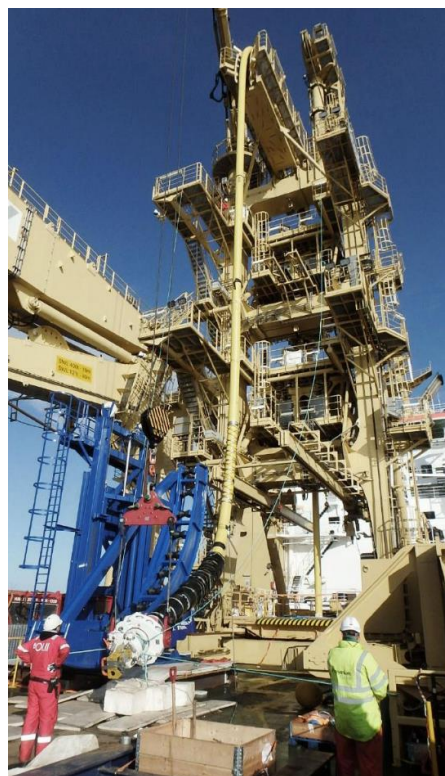
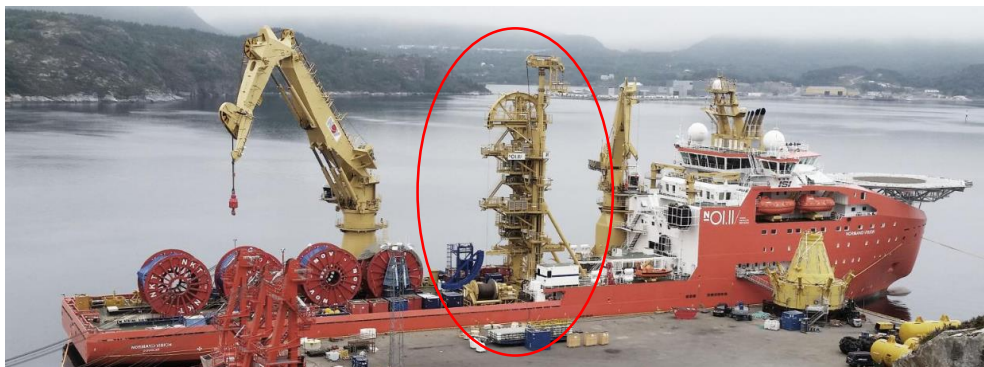


Figure 2-37: Vertical Lay System (Ocean Installer, 2015)

2.4 Installation of flexible pipe

The installation procedure used in this master thesis will be based on Ocean Installers installation analysis report for the Visund A21 riser (Ocean Installer, 2015). The flexible pipe/riser will be installed by the vessel Normand Vision. Since the meaning of the thesis is analysis of wave statistics, and not procedure analysis, the Visund procedure is chosen as a basis because of its good overview. The A21 riser will be connected to a tie-in point, then stretching to a hold-down anchor, from there creating a dynamic riser configuration (S-shaped part of the riser) using buoyancy modules and then connected to the Visund FLOATING PRODUCTION UNIT (FPU). It should be noted that the method for A21 installation presented here is using the SIMOPRO method (Simultaneous Marine Operation and PROduction) whereby the FPU continues to produce whilst marine operations for riser replacements are performed. This requires the vessel to stay at least 200m away from the FPU at all times. This is different to normal riser operations and imposes some additional limitations on operations (e.g. side loading on vessel due to crane loads during topside end handshake operations, see Figure 2-47).

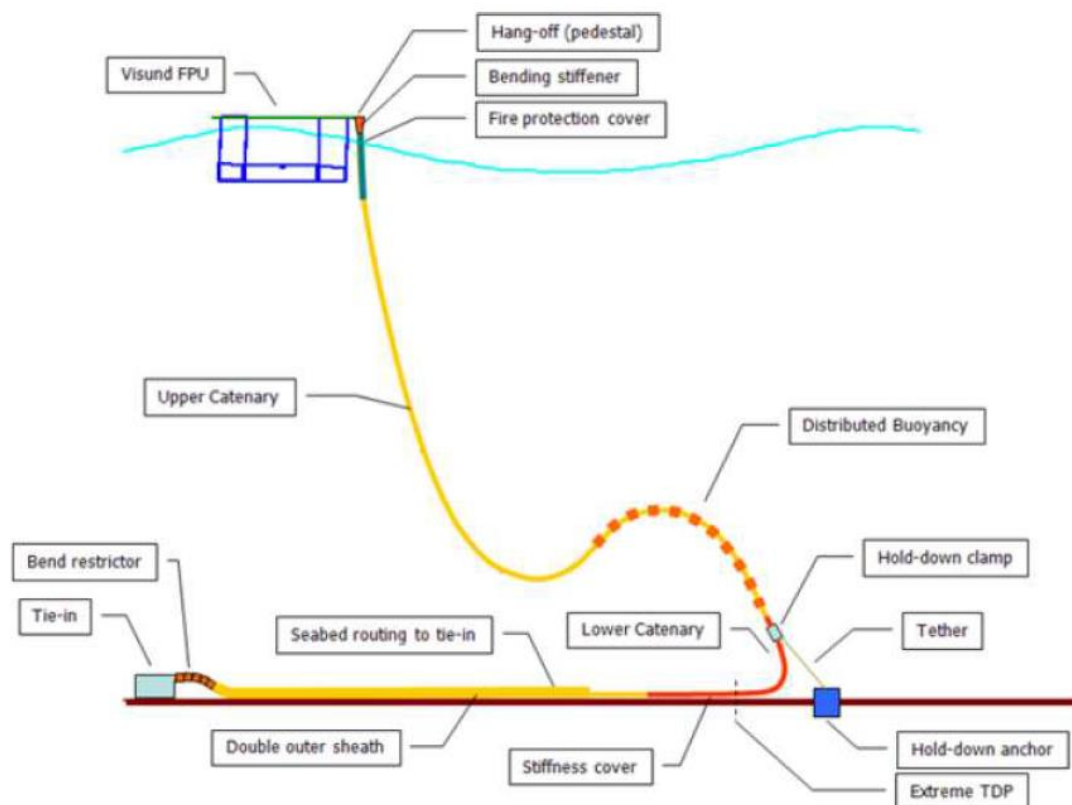


Figure 2-38: Riser Configuration

2.4.1 Subsea end Initiation to Visund Pull In Winch Wire (PIW)

The first part of this task is transferring the subsea END TERMINATION HEAD (ETH), which will be connected to the tie-in point, from Normand Vision to the Visund FPU. This means that the Visund FPU is taking some of the riser weight. For a better understanding the sequence is shown below. The red circle marks the spot of the subsea ETH at the different parts of the subsea ETH transfer. Throughout section 2.4 the sequence figures display several operation parts. Marked with grey are sequences of the operation that has been done before the actual sequence (with color).

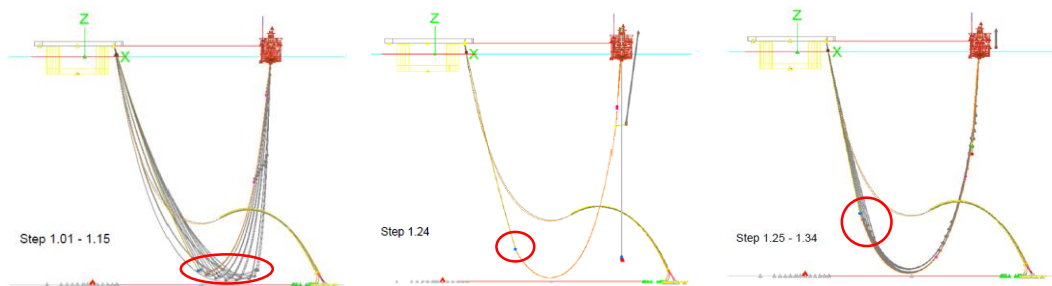


Figure 2-39: Subsea ETH transfer

The Second part of this task is landing the riser catenary safely on the seabed. The riser catenary is landed safe once the riser is landed on the seabed and sufficient length of riser is on seabed to be in a stable configuration/position. This is done by paying out the riser. The meaning of “paying out” is letting go slowly of the riser from VLS on top the vessel towards the seabed. The figure below shows sequences of the landing the riser catenary.

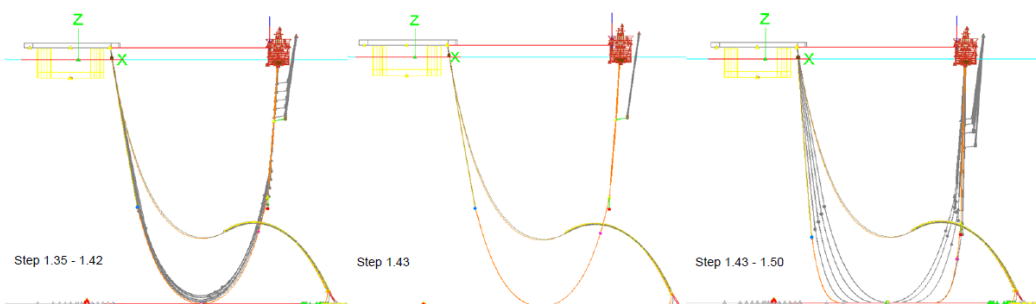


Figure 2-40: Riser Catenary to Seabed

2.4.2 Lay away

After the riser catenary is landed safely, the next step is to lay the rest of the static section of the riser on the seabed and then start landing the PULL DOWN CLUMP WEIGHT (PDCW). The PDCW pulls the riser towards the seabed at the same time as the vessel is holding the riser, this creates tension in the riser and is necessary to pull the buoyant section of riser and tether clamp

to seabed. The buoyant section consists of several buoyancy modules which creates the dynamic section shown in Figure 2-38 marked with Distributed Buoyancy. The tether clamp is shown in Figure 2-41 marked with a red circle.

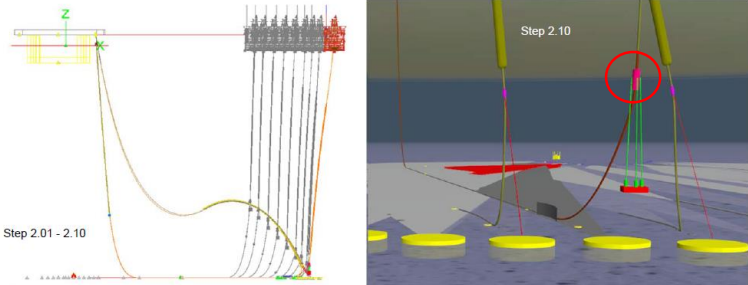


Figure 2-41: Before Landing of Clump Weight

Before the PDCW is landed the riser and the PDCW moves together with the heave motion of the vessel, but once the PDCW is landed the riser alone has to compensate for the heave motion of the vessel. The result is that the riser starts bending and there is a possibility of tension and compression over the risers' tolerances. This is why there are strict weather criteria for particularly the landing of the PDCW and a short time after. An assumption of a heave motion limited to 0.6m (double amplitude) for this task, in the thesis, is made based on previous operations and experience. Although the period of motion which has an influence on the acceleration and velocity of heave is important. Section 3.1.2 and 3.2.2 will cover the analysis of setting weather criteria for the lay away task, respectively using JONSWAP and Torsethaugen spectra.

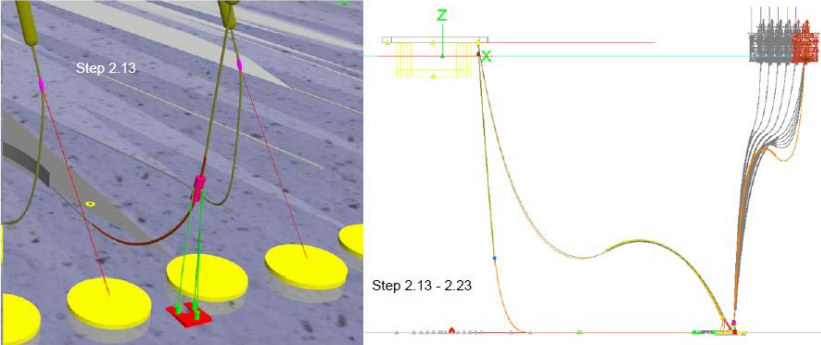


Figure 2-42: After Landing of Clump Weight

After landing the PDCW safely on the seabed, the vessel moves further away from the Visund FPU and at the same time pays out more of the riser. In this configuration the problem regarding too much tension and compression in the riser because of the PDCW is gone since more of the riser is paid out and can take the motions caused by the vessel heave motion.

2.4.3 Visund temporary laydown of Subsea ETH

After creating a configuration that allows more vessel heave motion, the procedure of laying down the subsea ETH on seabed starts. This is done by using the platform PULL IN WINCH WIRE (PIW) which slowly lowers the subsea ETH towards the seabed and at the same time the platform moves towards the tie-in point (away from the vessel). This is where the subsea ETH later will be connected. When the subsea ETH is landed safely on the seabed the PIW disconnects from the subsea ETH. The red circles in the figure below shows the location of the subsea ETH from start to finish for this part of the procedure.

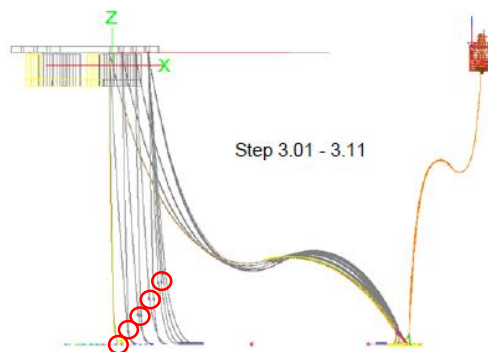


Figure 2-43: Landing of subsea ETH

2.4.4 Catenary flip and lay dynamic section towards platform

The next step is to move the vessel towards the platform keeping the same riser configuration and at the same time moving the vessel towards the platform, by moving the vessel in a half circle around the PDCW placed on the seabed. This is called the catenary flip.

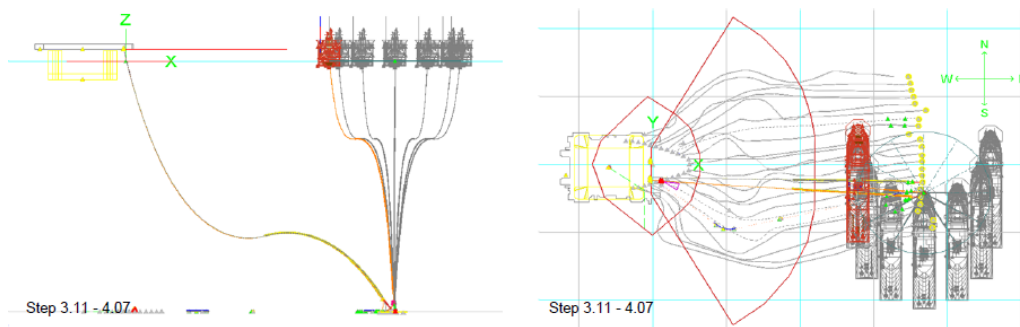


Figure 2-44: Catenary Flip

Once the catenary flip is done the vessel moves towards the platform in line with the riser path, and at the same time paying out and start to create the dynamic riser section. The dynamic section will become the dynamic section of the pliant wave riser configuration. This part of the

installation procedure stops when the vessel is just outside the 200m exclusion zone, which is the safe distance from the platform.

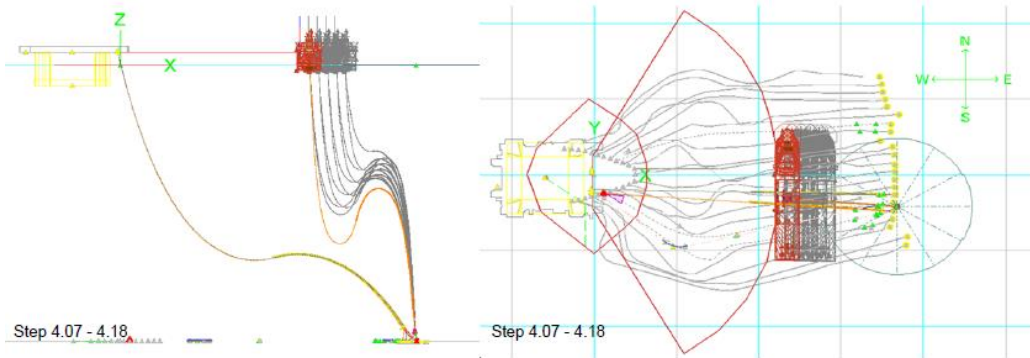


Figure 2-45: Vessel towards Visund FPU

2.4.5 Topside end handshake to Visund PIW

The topside end handshake to Visund PIW part of the installation procedure is done in 2 main steps. The first step is to lower the topside end into the sea through the moonpool. Then the weight of the riser will have to be transferred from the A&R winch (holding the riser at the moonpool) to the 70Te crane which is placed on the vessel side. The transfer from the A&R winch to crane is called a handshake, and is done by connecting to riser and pulling in on the crane and at the same time paying out on the A&R winch. This will slowly transfer all the weight from A&R winch to crane, and then the winch wire disconnects.

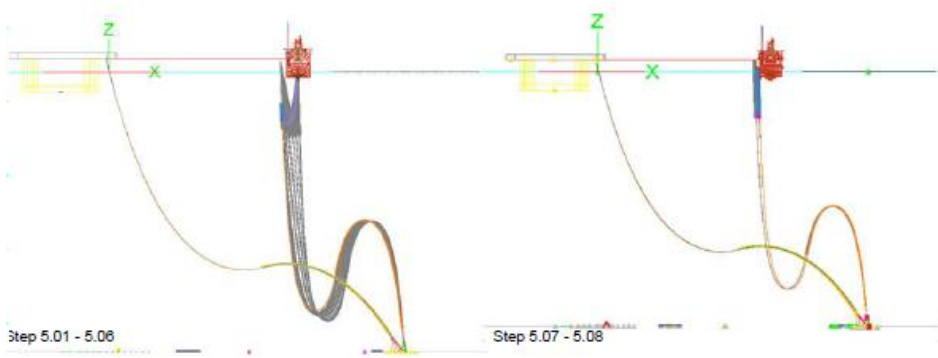


Figure 2-46: A&R winch to Crane Transfer

The second step is to do a handshake from the vessel 70Te crane to the Visund PIW wire, disconnect the vessel from the riser and pull the riser up to Visund FPU, connect the topside end to Visund FPU, and at last place Visund back to its original position.

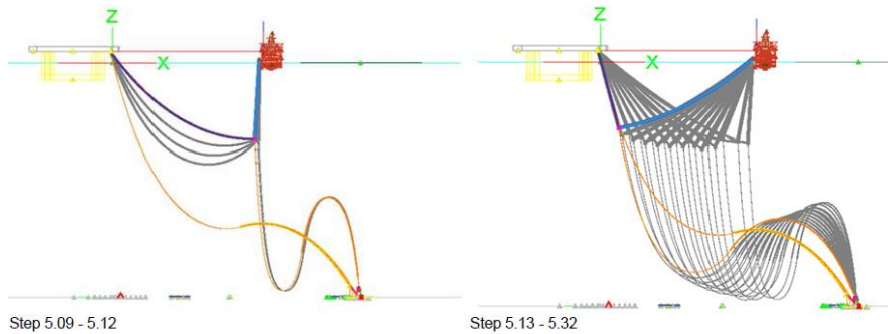


Figure 2-47: Crane to Visund PIW wire transfer

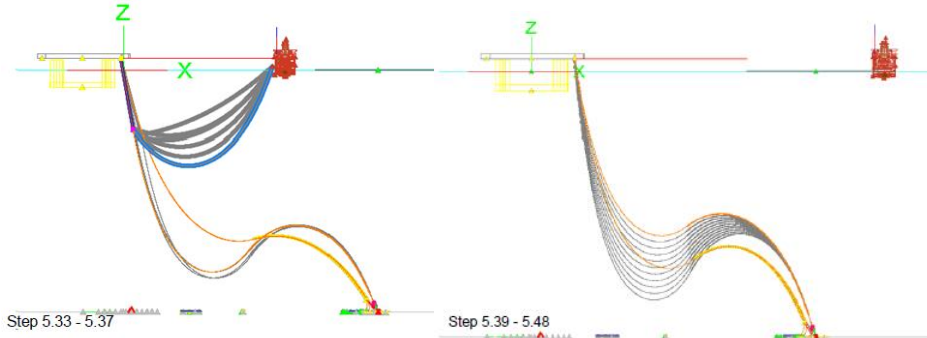


Figure 2-48: Crane Disconnection

2.4.6 Contingency laydown of dynamic section

This section will cover the contingency plan for the installation procedure, which is a safe condition in case of changes in weather conditions. For the whole installation procedure there is only one contingency plan, which is laying down the riser on the seabed. The contingency laydown has the same start position as the catenary flip. The plan is to move away from the platform and paying out on the riser laying it safely on the seabed. There are two configurations for safe conditions in this contingency plan, the first is when the topside end is underneath the moonpool. This allows for some worse weather since the riser cannot hit the moonpool. In the case where the weather is even worse than what is allowed when the topside end is underneath the moonpool, the topside end needs to be laid down on the seabed. This part of laying the topside end on seabed is not considered in the simulated operations.

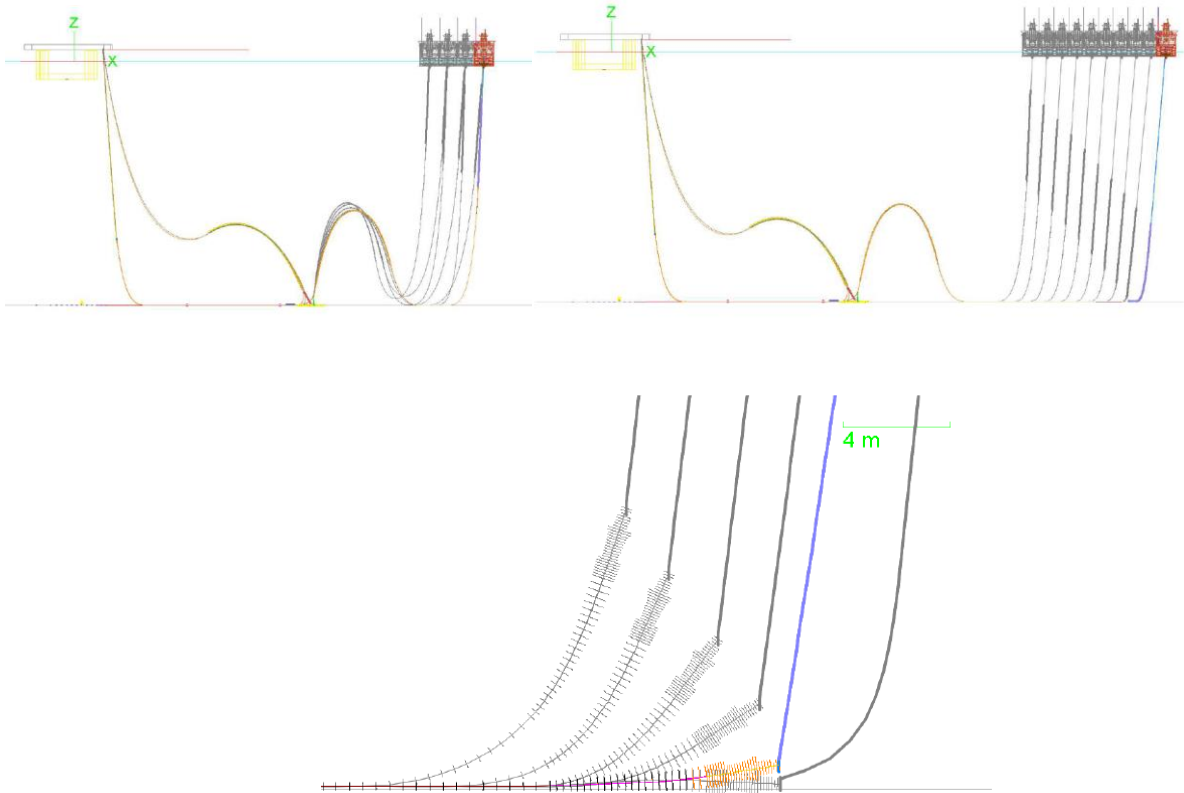


Figure 2-49: Contingency position

3 ANALYSIS AND RESULTS

This chapter will cover analysis for different situations of the operation described in section 2.4. The results in this chapter are based on the hindcast data from Heidrun, as this was the first hindcast data provided. For comparing of operation simulations for different fields see section 4.

3.1 Total Sea Simulation using JONSWAP spectra

3.1.1 Method used for calculation of response motion

For the calculations the software MATLAB is used, which allows quick calculations of several datasets. To give a figurative and better understanding of what is being calculated a JONSWAP spectrum of the total sea with $H_s=3.4\text{m}$ and $T_p=9.2\text{s}$ is used. The period (T) is converted in to frequency by using:

$$f = \frac{1}{T} \quad 3-(1)$$

Following will be the systematic procedure for calculating the response. Formulas from (Haver, 2013)

The most common way of giving the JONSWAP spectrum is:

$$S_j(f) = 0.3125 \cdot H_s^2 \cdot T_p \cdot \frac{f^{-5}}{f_p} \cdot \exp\left(-1.25 \cdot \left(\frac{f}{f_p}\right)^4\right) \cdot (1 - (0.287 \cdot \ln \gamma)) \cdot \gamma^{\exp\left(-0.5 \cdot \left(\frac{f-f_p}{f_p \cdot \vartheta}\right)^2\right)} \quad 3-(2)$$

where $f_p = t_p^{-1}$ and the spectral width parameter reads:

$$\vartheta = \begin{cases} 0.07, & f \leq f_p \\ 0.09, & f > f_p \end{cases} \quad 3-(3)$$

The peak enhancement factor can be computed from:

$$\gamma = 42.2 \left(\frac{2\pi h_s}{g t_p^2} \right)^{\frac{6}{7}} \quad 3-(4)$$

$g = 9.81 \text{ m/s}^{-2}$ is the acceleration of gravity.

For the calculations done in the thesis, γ above 5.0 is set to be 5.0 to prevent nonrealistic narrow wave spectra.

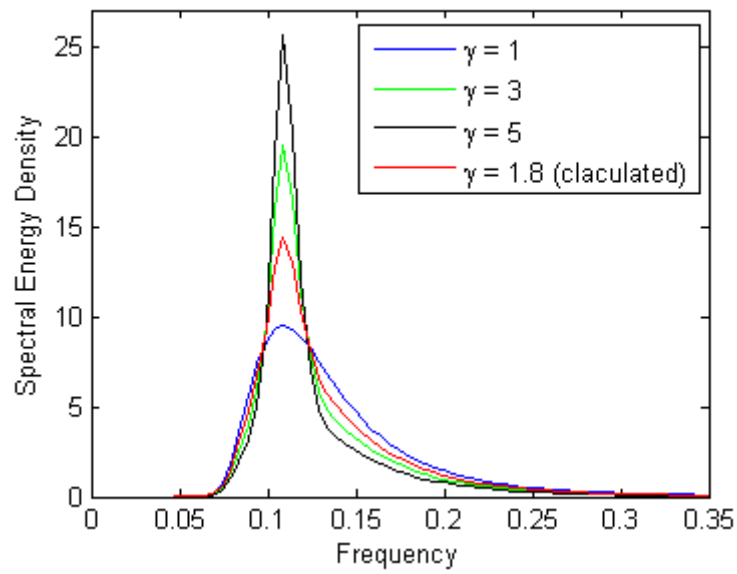


Figure 3-1: JONSWAP Wave Spectrum with Different γ

3.1.1.1 General Probability Models for Vessel Response

Knowing the transfer function (in this case, the provided RESPONSE AMPLITUDE OPERATOR (RAO) tables) the response spectrum is given by (in this case the JONSWAP spectrum is used as wave spectrum):

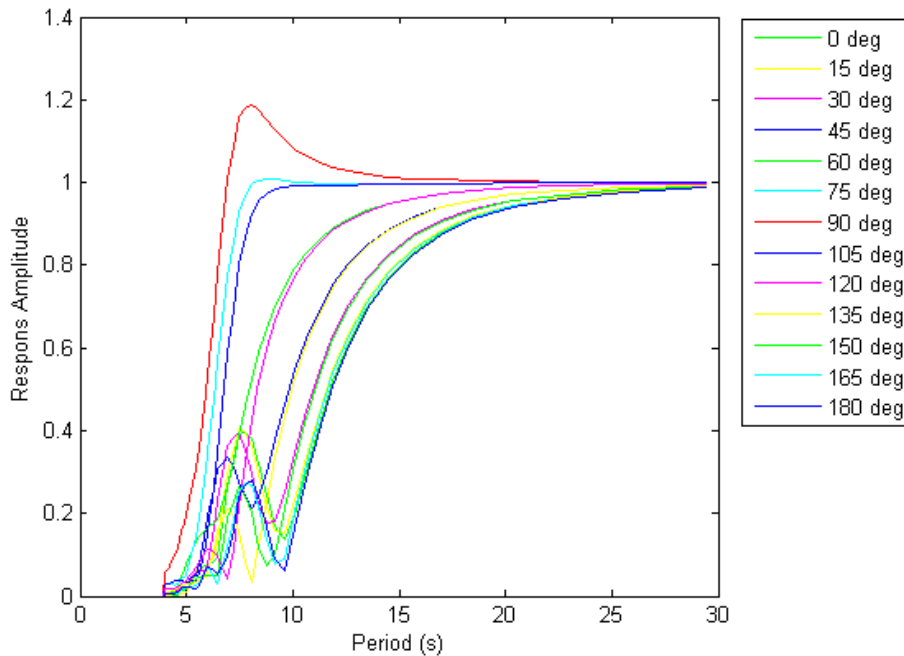


Figure 3-2: Provided RAO for Heave Motion

$$S_x(f_i) = |RAO(f_i)|^2 \cdot S_J(f_i) \quad 3-(5)$$

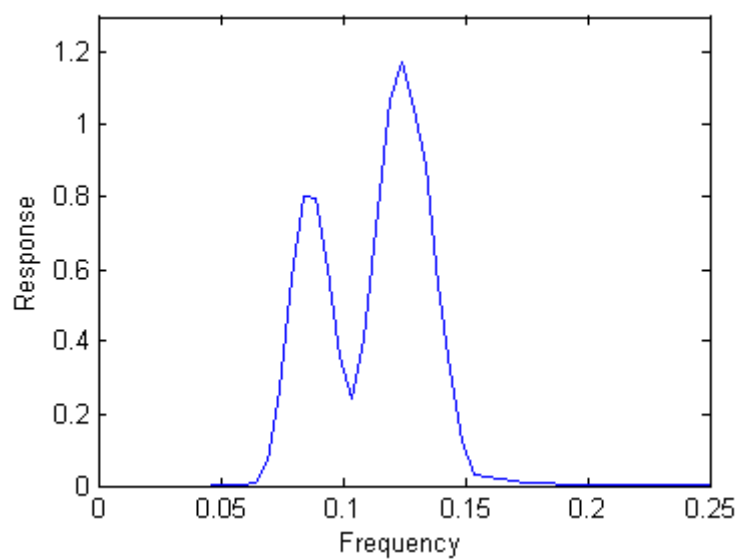


Figure 3-3: Heave Response Spectrum Head Sea (0°)

Figure 3-3 shows how the response spectrum is following the RAO with the same trough at approximately 10s (frequency of 0.1).

The spectral moments are defined by:

$$m_k = \sum f_i^k \cdot S_x(f_i) \cdot \Delta f_i \quad 3-(6)$$

The variance is:

$$\sigma^2 = m_0 \quad 3-(7)$$

The standard deviation is:

$$\sigma = \sqrt{\sigma^2} \quad 3-(8)$$

Expected zero-up crossing period is defined by:

$$tm_{02} = \sqrt{\frac{m_0}{m_2}} \quad 3-(9)$$

Assuming that the system is linear or lightly damped or close to linear, the global response maxima is assumed to have a Rayleigh distribution written as:

$$F_{x_m}(x) = 1 - \exp\left(-\frac{1}{2}\left(\frac{x}{\sigma}\right)^2\right) \quad 3-(10)$$

For a specific duration, τ , of the sea state, the characteristic largest response amplitude, \tilde{x} , is given by:

$$1 - F_{x_m}(x) = \frac{1}{n_\tau} \Rightarrow \tilde{x} = \sigma\sqrt{2 \ln n_\tau} \quad 3-(11)$$

where n_τ is the expected number of global maxima in the sea state. In this case the duration, τ , of the windows are 3 hours.

$$n_\tau = \frac{3600 \cdot \tau}{tm_{02}} \Rightarrow n_{3h} = \frac{3600 \cdot 3}{tm_{02}} \quad 3-(12)$$

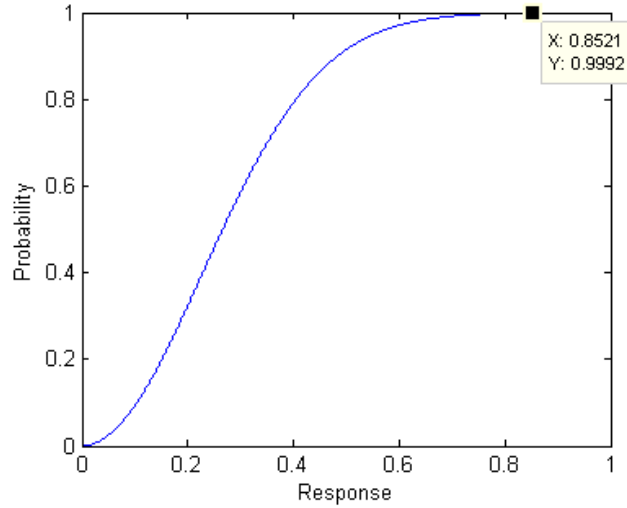


Figure 3-4: Global Response Maxima Rayleigh Distribution
(Characteristic Largest Response Amplitude (\tilde{x}) for 3 hour Window Pointed Out)

By assuming that all global response crest during the sea state are independent and identically distributed, the distribution of the largest value in a 3 hour sea state is given by:

$$F_{x_{3h}}(z) = F_{x_m}(z)^{n_{3h}} = \left(1 - \exp\left(-\frac{1}{2}\left(\frac{z}{\sigma}\right)^2\right)\right)^{n_{3h}} \quad 3-(13)$$

For this thesis, an interesting estimate is the value which is exceeded with a probability of $1 - \alpha$ during the sea state. By doing this it is possible to be sure of not exceeding a specific response motion with a high probability (α) within a sea state. It has here been chosen to use $\alpha = 0.9$ and $\alpha = 0.95$. The estimate is found by solving $F_{Z_{3h}}(x) = \alpha$ for the specific response motion value, this is further referred to as the α -percentile:

$$x_\alpha = \sigma \sqrt{-2 \ln\left(1 - \alpha^{\frac{1}{n_{3h}}}\right)} \quad 3-(14)$$

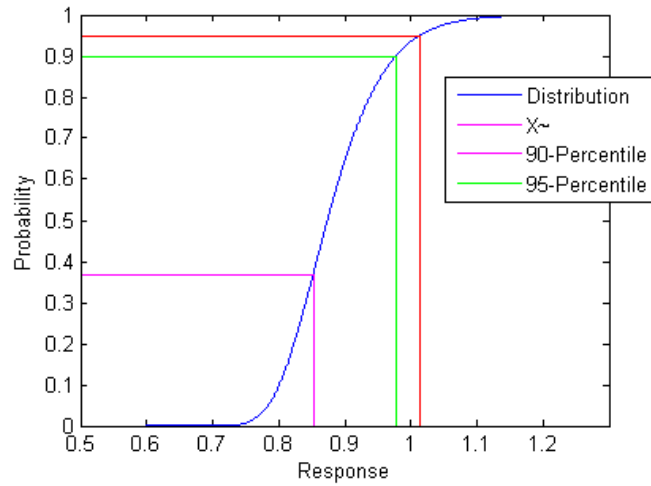


Figure 3-5: The Distribution of the Largest Response Amplitude in a 3-Hour Sea State

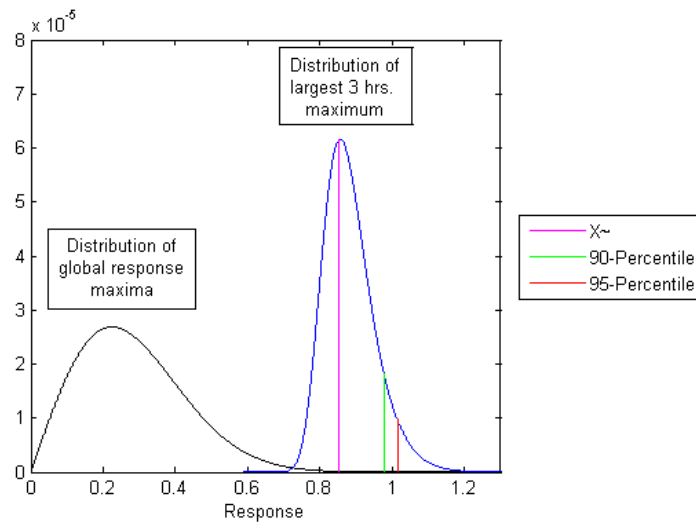


Figure 3-6: Distribution of Global Response Maxima and Largest 3 hour Maximum

3.1.1 Verification that the JONSWAP spectra is correct

To check if the JONSWAP spectrum is done correct in the MATLAB calculations the following formula should match

$$H_S = 4\sigma \tag{3-15}$$

$$\sigma^2 = \sum S_j(f_i) \cdot \Delta f_i \tag{3-16}$$

where S_j is the JONSWAP spectrum.

H_S is defined as 4 times the standard deviation and therefore this check was done numerous of times to be sure that the calculations give the correct JONSWAP spectra.

Table 3: Check of JONSWAP spectra

H_S (m)	T_P (s)	σ^2	σ	$H_S = 4\sigma$
3	5	0.5598	0.7482	2.9927
5	8	1.5613	1.2495	4.9982
7	6	3.0554	1.7480	6.9918
9	13	5.0620	2.2499	8.9995
13	10	10.5593	3.2495	12.9980

There extremely small differences in the selected H_S and the calculated H_S which makes it safe to present data using this JONSWAP spectrum further in the thesis.

3.1.2 Lay away (landing clump weight)

As explained in section 2.4.2, an assumption of heave motion limitation of 0.6 meters for the lay away task is considered relevant based on previous operations. Using formulas 3-(1) to 3-(14) and RAOs provided by Ocean Installer for the vessel Normand Vision, the H_S limiting the heave motion to 0.6m for different groups of T_P is calculated. Throughout this thesis, the heave motion will be referred to as the double amplitude. This is a conservative approach as the waves do not have the same distance from the crests and trough to the waterline. The H_S limiting the heave motion to 0.6m will later be set to the weather criteria for the lay away task. For this calculation, the vessel motions are head seas with a safety factor of 15 degrees, meaning that the worst-case heave motion of 0 and 15 degree wave direction is used as result.

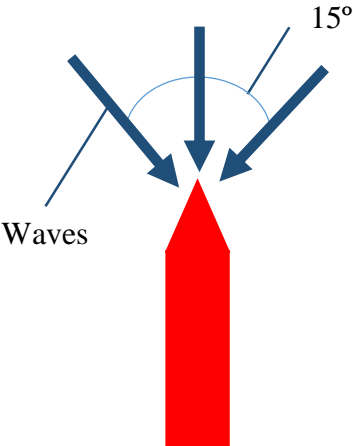


Figure 3-7: Waves coming form $0^\circ \pm 15^\circ$ (Head seas $\pm 15^\circ$)

The three different values of H_S limiting the heave motion to 0.6m represents as follows:

- \tilde{Z} : Calculated from formula 3-(11), and represents the most probable heave motion amplitude based on the distribution of the largest response amplitude and that the waves are Rayleigh distributed. The response spectrum is generated from the RAO and wave spectrum (formula 3-(5)).
- $Z_{0.90}$: Calculated form formula 3-(14), and represents the 90-percentile of the distribution of the largest heave motion amplitude, which is the heave motion with a probability of 90% not exceeding. This probability is also based on the response spectrum and the assumption that the waves are Rayleigh distributed.
- $Z_{0.95}$: Also calculated form formula 3-(14), and represents the 95-percentile of the distribution of the largest heave motion amplitude, which is the heave motion with a probability of 95% not exceeding. This probability is also based on the response spectrum and the assumption that the waves are Rayleigh distributed.

It should be noted that the referred formulas are for single amplitude calculations. To calculate a heave motion of 0.6m (double amplitude) single amplitude heave motion of 0.3m is used.

3.1.2.1 Results

By changing the H_S for different T_p (steps of 0.1s from 0s to 13s) to the point where \tilde{Z} , $Z_{0.90}$ and $Z_{0.95}$ is less or equal to 0.3m (which gives the double amplitude of 0.6m), it is possible to find the H_S limiting the heave motion to 0.6m. The calculations are done in MATLAB and the results are shown in Figure 3-8 and Table 4 where the lowest value of H_S for T_p with steps of 0.5s. The results do not show H_S for T_p below 5s. These values are much larger than the maximum recorded H_S for these T_p in the hindcast data.

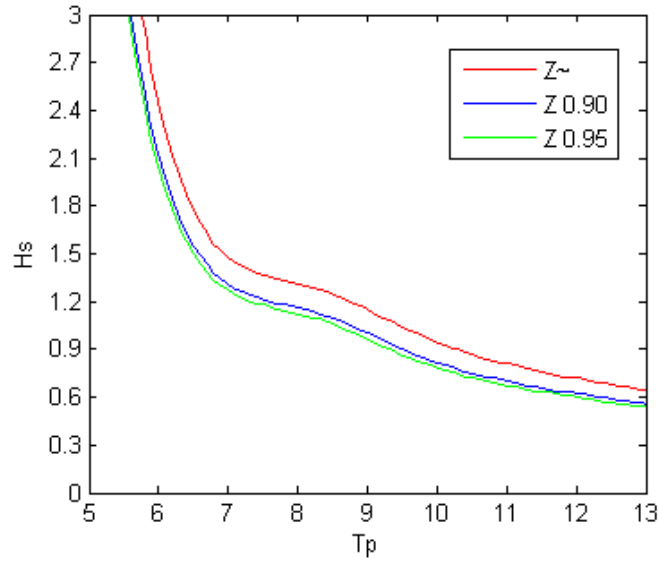


Figure 3-8: H_s Resulting in 0.6m Heave Motion

Table 4: H_s Resulting in 0.6m Heave Motion

T_p	H_s for \tilde{z}	H_s for $z_{0.90}$	H_s for $z_{0.95}$
$5 \leq T_p < 5.5$	4.26	3.72	3.58
$5.5 \leq T_p < 6$	2.66	2.3	2.21
$6 \leq T_p < 6.5$	1.87	1.64	1.58
$6.5 \leq T_p < 7$	1.52	1.34	1.3
$7 \leq T_p < 7.5$	1.38	1.23	1.19
$7.5 \leq T_p < 8$	1.32	1.17	1.13
$8 \leq T_p < 8.5$	1.26	1.11	1.07
$8.5 \leq T_p < 9$	1.17	1.02	0.98
$9 \leq T_p < 9.5$	1.06	0.92	0.88
$9.5 \leq T_p < 10$	0.96	0.83	0.8
$10 \leq T_p < 10.5$	0.88	0.76	0.73
$10.5 \leq T_p < 11$	0.82	0.71	0.68
$11 \leq T_p < 11.5$	0.77	0.67	0.64
$11.5 \leq T_p < 12$	0.73	0.63	0.61
$12 \leq T_p < 12.5$	0.69	0.6	0.57
$12.5 \leq T_p \leq 13$	0.65	0.56	0.54

3.1.2.2 Analyzing the results

The first thing which comes to mind when looking at the results of the H_s calculated for a heave motion limited to 0.6m, is that the results does not match the vessel RAO (Figure 3-9). For the periods from 8s to 10s there should be an increase in the H_s . Instead it just flattens out for the area of 7s to 9s and then starting decrease from 9s and out. This is because a spectrum consists of a spectrum of wave periods and the resultant outcome is a combination of wave energies and does not typically show the extreme responses seen in regular waves.

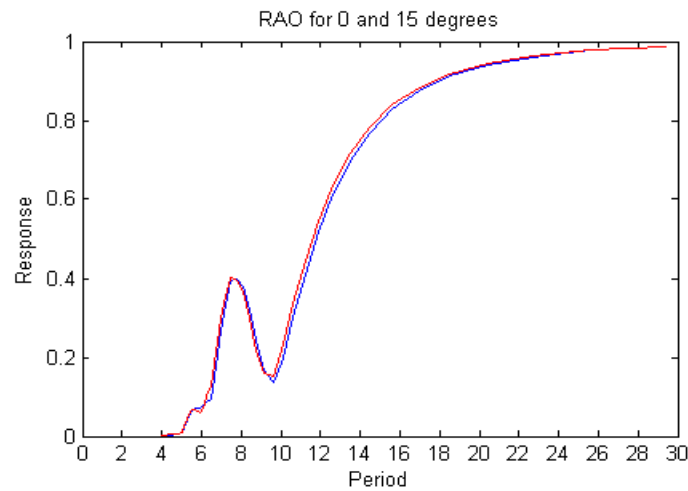


Figure 3-9: RAO for 0 and 15 degrees

This is an expected result for irregular waves. To check whether the calculations are correct, the limitations to the heave motion were changed to motions larger than 0.6m (double amplitude). It does not matter whether using \tilde{Z} , $Z_{0.90}$ or $Z_{0.95}$, and therefor $Z_{0.95}$ is used to show the calculations done.

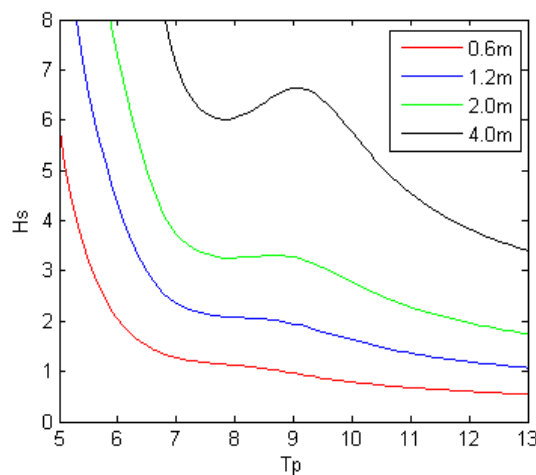


Figure 3-10: H_s Limitations for Different Heave Motion using $Z_{0.95}$

Table 5: H_S Limitations for Different Heave Motion using $Z_{0.95}$

T_p	H_S for $Z_{0.95}$, with heave motion restricted to			
	0.6 m.	1.2 m.	2.0 m.	4.0 m.
$5 \leq T_p < 5.5$	3.58	7.19	11.98	23.96
$5.5 \leq T_p < 6$	2.21	4.73	7.88	15.76
$6 \leq T_p < 6.5$	1.58	3.18	5.38	10.75
$6.5 \leq T_p < 7$	1.3	2.44	3.9	7.53
$7 \leq T_p < 7.5$	1.19	2.16	3.38	6.23
$7.5 \leq T_p < 8$	1.13	2.08	3.26	6.02
$8 \leq T_p < 8.5$	1.07	2.05	3.26	6.05
$8.5 \leq T_p < 9$	0.98	1.97	3.29	6.35
$9 \leq T_p < 9.5$	0.88	1.82	3.11	6.5
$9.5 \leq T_p < 10$	0.8	1.65	2.83	5.9
$10 \leq T_p < 10.5$	0.73	1.5	2.55	5.21
$10.5 \leq T_p < 11$	0.68	1.38	2.32	4.64
$11 \leq T_p < 11.5$	0.64	1.28	2.13	4.22
$11.5 \leq T_p < 12$	0.61	1.2	1.99	3.89
$12 \leq T_p < 12.5$	0.57	1.14	1.87	3.63
$12.5 \leq T_p \leq 13$	0.54	1.06	1.75	3.39

What Figure 3-10 and Table 5 shows is that the larger the limitation the more the limiting H_S follows the vessel RAO. The reason behind the results is the increase in γ (formula 3-(4)) when calculating the wave spectra. Larger H_S gives a larger γ which will make the spectrum narrower around spectral peak period. The increase in γ for a specific spectral peak period is shown in Figure 3-11 and Figure 3-12.

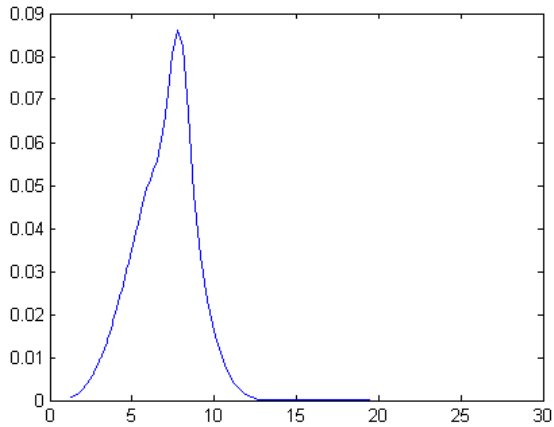


Figure 3-11: JONSWAP spectrum, $\gamma=1.66$ (calculated), $H_s=2.3m$ and $T_p=8s$

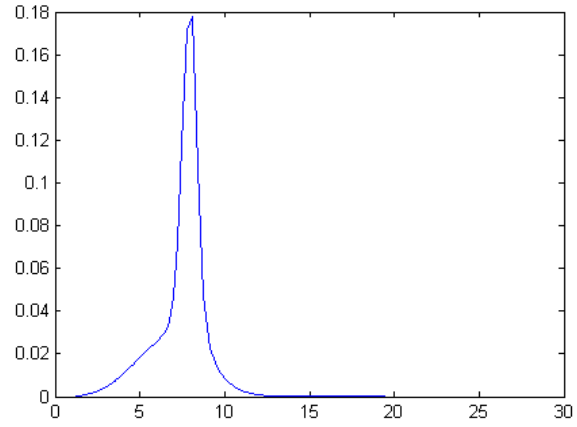


Figure 3-12: JONSWAP spectrum, $\gamma=7$ (set), $H_s=2.3m$ and $T_p=8s$

Whether it is the spectral width (decided by γ) which makes the limiting H_s flattening out around the area where the RAO has a top (7s to 10s) is further checked. The calculations of limiting H_s for heave motion of 0.6m (double amplitude) is done once more, but now by changing γ instead of calculating. In addition, this time $Z_{0.95}$ is used.

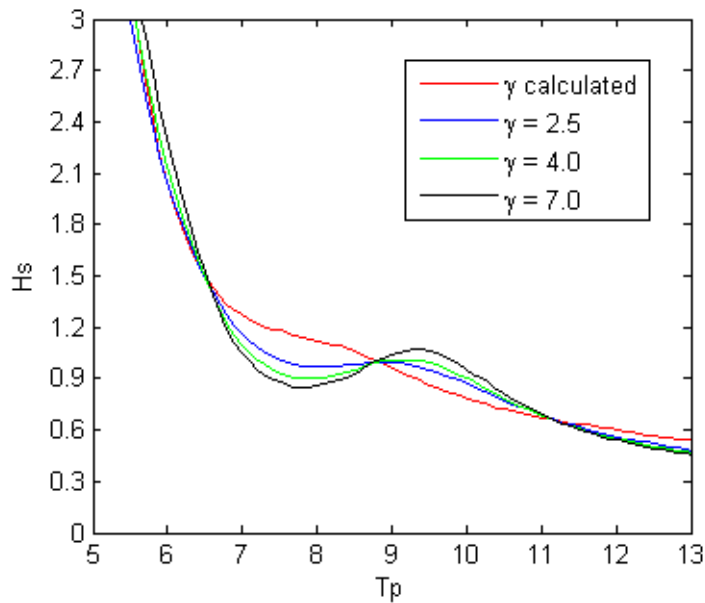


Figure 3-13: H_s for Heave Motion of 0.6m using $Z_{0.95}$, and different γ

Table 6: H_S for Heave Motion of 0.6m using $Z_{0.95}$, and different γ

T_p	H_S for $Z_{0.95}$, with			
	calculated γ	$\gamma = 2.5$	$\gamma = 4$	$\gamma = 7$
$5 \leq T_p < 5.5$	3.58	3.32	3.5	3.78
$5.5 \leq T_p < 6$	2.21	2.2	2.31	2.49
$6 \leq T_p < 6.5$	1.58	1.58	1.6	1.65
$6.5 \leq T_p < 7$	1.3	1.21	1.15	1.11
$7 \leq T_p < 7.5$	1.19	1.03	0.95	0.89
$7.5 \leq T_p < 8$	1.13	0.97	0.9	0.85
$8 \leq T_p < 8.5$	1.07	0.97	0.91	0.86
$8.5 \leq T_p < 9$	0.98	0.98	0.95	0.93
$9 \leq T_p < 9.5$	0.88	0.96	1.00	1.04
$9.5 \leq T_p < 10$	0.8	0.89	0.92	0.98
$10 \leq T_p < 10.5$	0.73	0.79	0.81	0.84
$10.5 \leq T_p < 11$	0.68	0.7	0.7	0.71
$11 \leq T_p < 11.5$	0.64	0.63	0.62	0.62
$11.5 \leq T_p < 12$	0.61	0.57	0.56	0.55
$12 \leq T_p < 12.5$	0.57	0.53	0.51	0.5
$12.5 \leq T_p \leq 13$	0.54	0.48	0.47	0.46

The reason behind the changes in the H_S limiting the heave motion to 0.6m with changes of γ (Figure 3-13 and Table 6) can be explained by using Figure 3-11 and Figure 3-12. Since spectrum in Figure 3-12 is much narrower, the probability of a wave to stay within the periods 7s to 10s is much higher than the spectrum in Figure 3-11. The conclusion of the calculations shown in Figure 3-10 and Figure 3-13 is that results showing the limiting H_S flattening out in the area of 7-9s are correct. It has been chosen to use the 95-percentile for further calculations in the thesis. Thereby weather criteria for the lay away task are:

Table 7: Weather criteria lay away using JONSWAP

T_p (s)	H_S (m)
$0 \leq T_p < 5$	All
$5 \leq T_p < 7$	1.3
$7 \leq T_p < 10$	0.8
$10 \leq T_p < 13$	0.5

3.1.3 Weather criteria and durations

The table below shows the weather criteria as well as the expected durations for the different parts of the installation procedure described in section 2.4. The parts are numbered by task number shown in the table. For this simulation, the limiting wave condition is the total sea from the hindcast data. The total sea is a sum of both wind waves and swells, which is set to one direction.

Table 8: Weather criteria and duration JONSWAP

Operation	Weather Criteria (Hs)				Duration
	$0 \leq T_p < 5$	$5 \leq T_p < 10$	$10 \leq T_p < 13$		
Task 1 - Subsea end initiation to Visund PIW.	All	3.5 m	3.5 m		49 hrs.
	$0 \leq T_p < 5$	$5 \leq T_p < 7$	$7 \leq T_p < 10$	$10 \leq T_p < 13$	
Task 2 - Lay away. (see section 3.1.1)	All	1.3 m	0.8 m	0.5 m	3 hrs.
	$0 \leq T_p < 5$	$5 \leq T_p < 10$	$10 \leq T_p < 13$		
Task 3 - Visund temporary laydown of subsea ETH.	All	3.5 m	3.5 m		11 hrs.
	$0 \leq T_p < 5$	$5 \leq T_p < 10$	$10 \leq T_p < 13$		
Contingency laydown of dynamic section.	All	5.0 m	5.0 m		
	$0 \leq T_p < 5$	$5 \leq T_p < 10$	$10 \leq T_p < 13$		
Task 4 - Catenary flip and lay dynamic section towards platform.	All	3.5 m	3.5 m		16 hrs.
	$0 \leq T_p < 5$	$5 \leq T_p < 10$	$10 \leq T_p < 13$		
Task 5 - Topside end handshake to Visund PIW.	All	3.5 m	3.5 m		34 hrs.

3.1.3.1 Duration of the operation using hindcast data

To check the duration of the operation starting waiting for weather the 1st of each month, a simulation of an operation was made in MATLAB using Table 8. Some changes to the duration were needed since the hindcast data only gives 3-hour windows.

Table 9: Changes of durations to the MATLAB simulation

Operation	Original Duration	MATLAB Duration
Task 1 - Subsea end initiation to Visund PIW.	49 hrs.	51 hrs.
Task 2 - Lay away.	3 hrs.	3 hrs.
Task 3 - Visund temporary laydown of subsea ETH.	11 hrs.	9 hrs.
Task 4 - Catenary flip and lay dynamic section towards platform.	16 hrs.	18 hrs.
Task 5 - Topside end handshake to Visund PIW.	34 hrs.	33 hrs.
Total	113 hrs.	114 hrs.

The MATLAB simulation looks through the hindcast data to find the first possible option of finishing the operation. The criterion of finishing the operation is as follow in steps:

1. Finding a window matching the duration and weather criteria for the first two steps of the operation.
2. Finding a window matching the duration and weather criteria for the last three steps of the operation.
3. If the window does not match the duration and weather criteria for the last three steps, the simulation goes to the contingency plan.
4. Once the MATLAB simulation goes to the contingency plan, the simulation stays here until finding a window matching the duration and weather criteria for the last three steps. This is as long as the weather criteria for the contingency plan are not exceeded.
5. If the weather criteria for the contingency plan is exceeded the simulation goes to the first step, searching for the next possible window.

The output of the MATLAB simulation is:

- Waiting time to start the operation from the 1st of each month, giving the start date of the operation.
- Time spent in contingency position.
- Total duration of the operation starting with waiting for weather the 1st each month, giving the date when the operation ends.

Table 10: Screen shot of the results of the MATLAB simulation

Start waiting for weather	Duration of waiting to start operation	Start of operation	Duration of contingency	Duration of the operation	End of operation	Total duration
01.06.1993	258	11.06.1993	3	117	16.06.1993	375
01.07.1993	237	10.07.1993	0	114	15.07.1993	351
01.08.1993	3	01.08.1993	0	114	05.08.1993	117
01.09.1993	39	02.09.1993	0	114	07.09.1993	153
01.10.1993	156	07.10.1993	0	114	12.10.1993	270
01.11.1993	4155	23.04.1994	90	204	01.05.1994	4359
01.12.1993	3435	23.04.1994	90	204	01.05.1994	3639
01.01.1994	2691	23.04.1994	90	204	01.05.1994	2895
01.02.1994	1947	23.04.1994	90	204	01.05.1994	2151
01.03.1994	1275	23.04.1994	90	204	01.05.1994	1479
01.04.1994	531	23.04.1994	90	204	01.05.1994	735
01.05.1994	375	16.05.1994	3	117	21.05.1994	492
01.06.1994	387	17.06.1994	0	114	21.06.1994	501
01.07.1994	24	02.07.1994	0	114	06.07.1994	138
01.08.1994	0	01.08.1994	0	114	05.08.1994	114
01.09.1994	225	10.09.1994	0	114	15.09.1994	339
01.10.1994	666	28.10.1994	21	135	03.11.1994	801
01.11.1994	4089	20.04.1995	3	117	25.04.1995	4206
01.12.1994	3369	20.04.1995	0	114	25.04.1995	3483

Using the statistics achieved from the MATLAB simulation the average duration of the operation starting with waiting for weather 1st each month is plotted. The 10-, 50- and 90-percentile (shown as P10, P50 and P90) is calculated as follow

X-percentile

$$ROUND\left(\frac{X}{100}N\right) \quad 3-(17)$$

where N is the number of observed operations for the specific month (1957-2014).

The X-percentile shows the value where X percent of the values are below.

This gives a good understanding of which months the operation should be done without spending too much time with the vessel waiting for acceptable windows. It is an extremely beneficial tool to use by contractor and operators when assessing commercial risk for waiting on weather. The difference in mean and X-percentiles duration describes the risk of operating in the different months. If the 50-percentile duration is lower than the mean duration, there are has been some bad years that have much longer durations than the 50 percent lowest duration. If the mean is lower than the 50-percentile it has been some years where the duration is much shorter than the 50-percentile. The 90-percentile gives an estimate on the probable worst-case scenario, and the 10-percentile best-case scenario. As Contractors compete against other contractors they want to give the client the best possible offer, and at the same time have a manageable risk. Clients tend to have several marine operation contracts and are often flexible of taking the risk if it is profitable in the end, and if the risk of loss of human life is acceptable.

Clients also often have more money than the contractors and can afford more expensive operations than contractors due to under estimated costs.

To verify that the simulated operation durations are correct, a critical operation of 48 hours with $H_s < 3m$ at Heidrun is compared to a similar simulated operation at Norne done by Statoil (Eik, 2012). These two fields are close to each other and have similar climate, thereby the simulated operation duration should be similar but not identical.

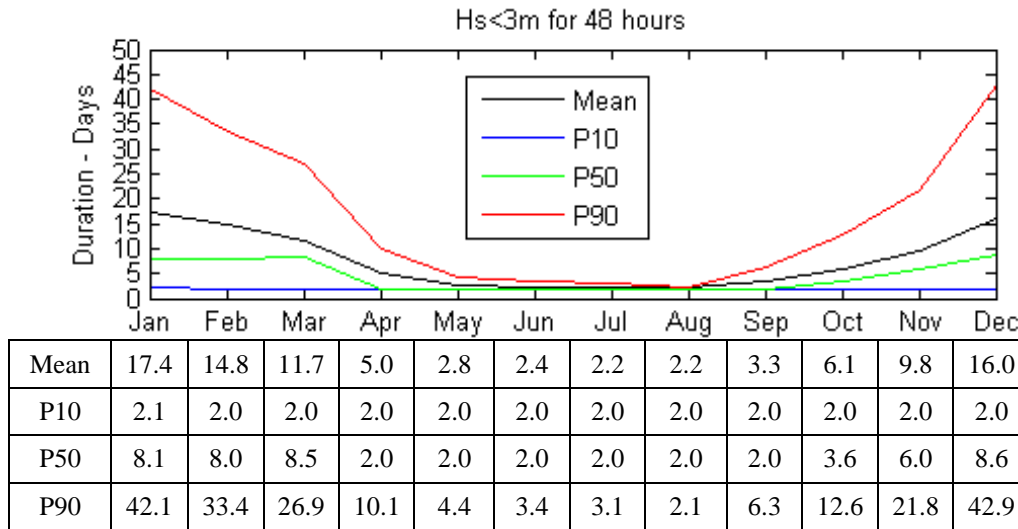


Figure 3-14: Operation Duration Critical Operation $H_s < 3m$ for 48 hours, Heidrun.

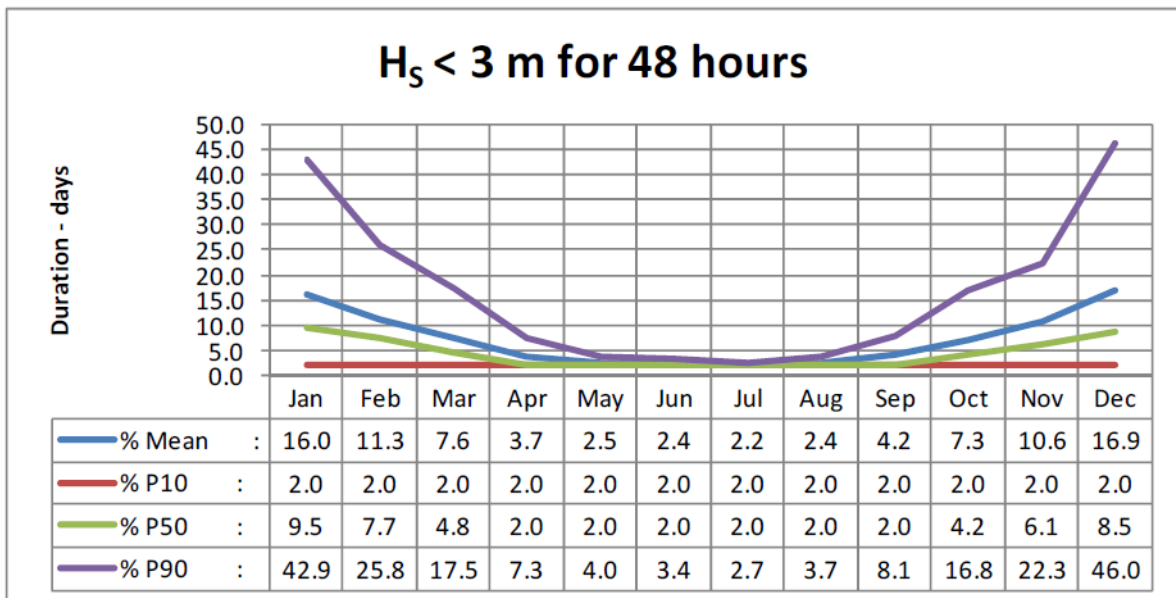


Figure 3-15: Operation Duration Critical Operation $H_s < 3m$ for 48 hours, Norne. (Eik, 2012)

Figure 3-14 and Figure 3-15 are similar enough to confirm that the simulating MATLAB script gives reasonable durations. The operation simulation for the specified marine operation at the Heidrun field is shown below.

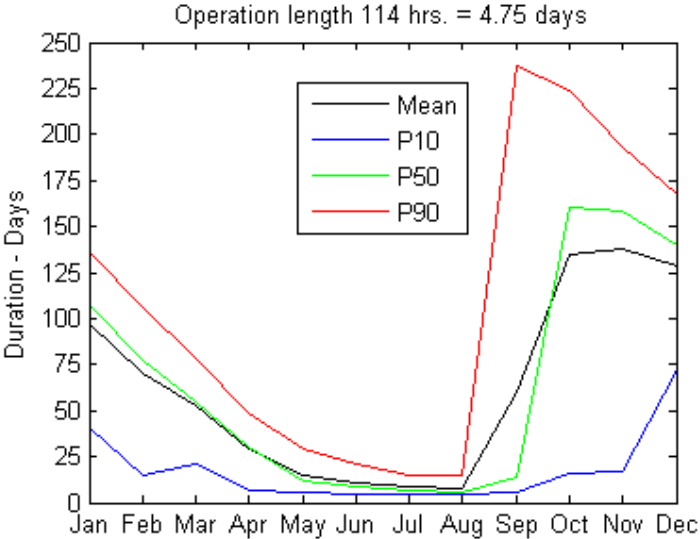


Figure 3-16: Duration of the operation using JONSWAP, Heidrun

Table 11: Duration of the operation using JONSWAP, Heidrun

Operation length 114 hrs. = 4,75 days				
Month	Mean Duration JONSWAP (days)	P10 Duration JONSWAP (days)	P50 Duration JONSWAP (days)	P90 Duration JONSWAP (days)
January	96.94	40.75	108.13	136.63
February	70.42	14.75	77.13	105.63
March	52.38	20.63	55.13	78.25
April	29.46	6.25	30.63	49
May	14.92	5.25	12.13	29.63
June	10.78	4.75	9	21
July	9.1	4.75	7.13	14.63
August	7.75	4.75	6.13	14.88
September	60.29	5.25	14.13	237.13
October	134.96	15.63	160.75	223.63
November	137.97	17.13	158.38	193
December	128.23	71.75	139.63	167.63

By looking at the average durations the months from May to August stands out by far as the best months of doing the operation. Within these months, July and August, is definitely the best months, and should be considered first when trying to fit the operation into the vessels schedule. First choice of month should be July since if something unpredictable happens, a delay into the month of August will not make a big difference. Having a delay in August going into the month of September could, by looking at the statistics, result in duration of the operation much longer than what was originally planned. Typically, operators in the North Sea try to aim for challenging and time consuming subsea operations in the summer months.

3.2 Total Sea Simulation using Torsethaugen spectra

The formulas and description of the Torsethaugen spectrum are collected from DNV-RP-C205, Appendix A.

The Torsethaugen spectrum is a double peak spectral model (wind- and swell waves) developed based on measured spectra for Norwegian waters (Haltenbanken and Staffjord) (Torsethaugen & Haver, 2004) and (Torsethaugen, 1996). Each sea system is defined by five parameters H_s , T_p , γ , N and M , which are parameterized in terms of the sea state significant wave height (unit meters) and spectral peak period (unit seconds).

The distinction between wind dominated and swell dominated sea states is defined by the fully developed sea for the location where peak period is given by

$$T_f = a_f H_s^{1/3} \quad 3-(18)$$

Then $T_p < T_f$ is the wind dominated range, and $T_p > T_f$ is the swell dominated range. The factor a_f depend on the fetch length, viz. $a_f = 6.6 \text{ (sm}^{-1/3}\text{)}$ for a fetch length of 370 km, and $a_f = 5.3 \text{ (sm}^{-1/3}\text{)}$ for a fetch length of 100 km.

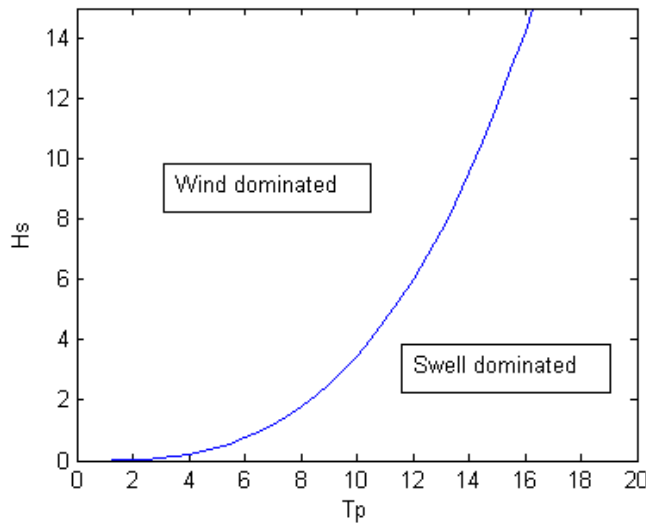


Figure 3-17: Wind and swell dominated sea states with $a_f=6.6$

The spectrum is defined as a sum of wind sea and swell:

$$S_{TH}(f) = \sum_{j=1}^2 E_j S_{nj}(f_{nj}) \quad 3-(19)$$

$j = 1$ is for the primary sea system, and $j = 2$ for the secondary sea system. Here

$$f_{nj} = f \cdot T_{Pj} \quad 3-(20)$$

$$E_j = \frac{1}{16} H_{Sj}^2 T_{Pj} \quad 3-(21)$$

$$S_{nj}(f) = G_0 A_{\gamma j} \Gamma_{Sj} \gamma_{Fj} \quad 3-(22)$$

DNV-RP-C205, Appendix A, gives two methods of calculating the parameters, a general version and a simplified version. For the purpose of this thesis, the simplified version is chosen, as it is much less complicated. For the simplified version the exponent of the high frequency tail is $N=4$ for all sea states, and the spectral width parameter $M=4$ is used for all sea states.

For the simplified version of the Torsethaugen spectrum the calculation of the parameters is as follows

$$\Gamma_{Sj} = f_{nj}^{-4} \exp[-f_{nj}^{-4}]; j = 1, 2 \quad 3-(23)$$

$$G_0 = 3.26$$

$$\gamma_{F1} = \gamma \exp\left[-\frac{1}{2\vartheta^2}(f_{n1}-1)^2\right] \quad 3-(24)$$

$$\gamma_{F2} = 1$$

$$\vartheta = 0.07 \text{ for } f_{nj} < 1 \text{ and } \vartheta = 0.09 \text{ for } f_{nj} \geq 1$$

$$A_{\gamma 1} = \frac{1 + 1.1[\ln(\gamma)]^{1.19}}{\gamma} \quad 3-(25)$$

$$A_{\gamma 2} = 1$$

For the factor a_f fetch length of 370 km is chosen and $a_f = 6.6$

$$T_f = 6.6 H_S^{1/3}$$

1. Wind dominated sea ($T_p \leq T_f$)

1.1 Primary Peak

$$H_{S1} = H_{Sw} = r_{pw}H_S \quad 3-(26)$$

$$T_{P1} = T_{Pw} = T_P \quad 3-(27)$$

$$\gamma = 35 \left[\frac{2\pi H_{Sw}}{g T_P^2} \right]^{0.857} \quad 3-(28)$$

1.2 Secondary peak

$$H_{S2} = H_{Sw} = r_{ps}H_S \quad 3-(29)$$

$$T_{P2} = T_{Psw} = T_f + 2.0 \quad 3-(30)$$

$$\gamma = 1$$

The parameter r_{pw} is defined by:

$$r_{pw} = 0.7 + 0.3 \exp\left(-\left(2 \frac{T_f - T_P}{T_f - 2\sqrt{H_S}}\right)^2\right) \quad 3-(31)$$

2. Swell dominated sea ($T_f \leq T_p$)

2.1 Primary Peak

$$H_{S1} = H_{Sw} = r_{ps}H_S \quad 3-(32)$$

$$T_{P1} = T_{Psw} = T_P \quad 3-(33)$$

$$\gamma = 35 \left[\frac{2\pi H_S}{g T_f^2} \right]^{0.857} \left(1 + 6 \frac{T_p - T_f}{25 - T_f} \right) \quad 3-(34)$$

2.2 Secondary peak

$$H_{S2} = H_{Sw} = \left(\sqrt{1 - r_{ps}^2} \right) H_S \quad 3-(35)$$

$$T_{P2} = T_{Pw} = 6.6H_{Sw}^{1/3} \quad 3-(36)$$

$$\gamma = 1$$

Where:

$$r_{ps} = 0.6 + 0.4 \exp\left(-\left(\frac{T_p - T_f}{0.3(25 - T_f)}\right)^2\right) \quad 3-(37)$$

3.2.1 Verification that the Torsethaugen spectra is correct

To check if the Torsethaugen spectrum is done correct in the MATLAB calculations the following formula should match

$$H_S = 4\sigma \quad 3-(38)$$

$$\sigma^2 = \sum S_{TH}(f_i) \cdot \Delta f_i \quad 3-(39)$$

Where S_{TH} is the Torsethaugen spectrum.

H_S is defined as 4 times the standard deviation and therefor this check was done numerous of times to be sure that the calculations give the correct Torsethaugen spectra.

Table 12: Check of Torsethaugen spectra

H_S (m)	T_P (s)	σ^2	σ	$H_S = 4\sigma$
3	5	0.5681	0.7537	3.0149
5	8	1.5946	1.2628	5.0510
7	6	3.0795	1.7548	7.0194
9	13	5.2092	2.2824	9.1295
13	10	10.7327	3.2761	13.1043

There are minor differences in the selected H_S and the calculated H_S , which makes it safe to present data using Torsethaugen spectrum further in the thesis.

3.2.2 Lay away weather criteria

When calculating the weather criteria for the lay away part of the installation procedure using Torsethaugen spectrum, $Z_{0.95}$ was only calculated since this is the percentile used for the presentation of the weather criteria. The 95-percentile was calculated the same way as in section

3.1.1, with H_s restricted to heave motion of 0.6 m (double amplitude) for every T_p from 0 to 13 seconds with steps of 0.01 seconds. Then using the lowest H_s within groups of T_p as follows

Table 13: Weather criteria lay away using Torsethaugen

T_p (s)	H_s (m)
$0 \leq t_p < 5$	1.34
$5 \leq t_p < 7$	1.39
$7 \leq t_p < 10$	0.98
$10 \leq t_p < 13$	0.7

3.2.3 Converting criteria from JONSWAP to Torsethaugen

All weather criteria except for the lay away task are collected from the Ocean Installer Visund installation analysis report. These criteria are done by using regular wave analysis. To do a simple calculation of the weather criteria for Torsethaugen, the H_s and T_p from the weather criteria (calculated from the design wave and period) is put in as JONSWAP spectra. The JONSWAP spectra need to be converted to criteria matching Torsethaugen spectra. The conversion is done as follows:

1. Selecting the T_p that approximately represents the largest heave motions by looking at the vessel RAO for 0 and 15 degrees. One T_p is selected for each group of T_p used for the weather criteria.
2. By using the selected T_p and the matching H_s within the T_p -group for the weather criteria the 95-percentile heave motion amplitude is calculated for JONSWAP spectra.
3. Now the 95-percentile H_s is calculated for the Torsethaugen spectra using the selected T_p and setting the restriction for vessel heave motion as calculated in step 2.

This is a conservative way of calculating the weather criteria since there is no analysis backing up the criteria. The results show an approximation of which direction the value of H_s is going when using Torsethaugen instead of JONSWAP.

Table 14: Conversion of weather criteria to Torsethaugen

T_p used in weather criteria	T_p used to calculate related heave motion	Weather criteria JONSWAP (Hs)	Related heave motion (double amplitude) from JONSWAP	Weather criteria Torsethaugen (Hs)
During Operation				
$0 \leq T_p < 5$	$T_p = 5$	All	-	All
$5 \leq T_p < 10$	$T_p = 8$	3.5 m	2.17 m	3.3 m
$10 \leq T_p < 13$	$T_p = 13$	3.5 m	4.14 m	3.7 m
During Contingency Plan				
$0 \leq T_p < 5$	$T_p = 5$	All	-	All
$5 \leq T_p < 10$	$T_p = 8$	5 m	3.24 m	4.2 m
$10 \leq T_p < 13$	$T_p = 13$	5 m	6.03 m	5.1 m

*Note: Since the largest recorded data of Hs for T_p between 0s to 5s is Hs=2.4m, there is no point in giving a restriction for these periods. Also worth saying is that the typical T_p in the North Sea is around 6-10s. However, it is worth knowing that if there were restrictions, the weather criteria for Torsethaugen would have been smaller than the weather criteria for JONSWAP.

By comparing the weather criteria in Table 14 between JONSWAP and Torsethaugen, the smaller periods for Torsethaugen gives higher probability of larger heave motion than JONSWAP. While the larger periods for Torsethaugen gives lower probability of larger heave motion than JONSWAP. To get a better understanding a comparison between JONSWAP and Torsethaugen spectra is made using Hs=3.5 and $T_p=5, 8$ and 13.

Comparing the first two figures (Figure 3-18 and Figure 3-19) showing the spectra for 5s, the Torsethaugen spectrum has a lot of energy in the larger periods (see red circle Figure 3-19) as a result of taking the swell waves as well as the wind waves into count. The JONSWAP spectrum is only showing the wind waves resulting waves only around the smaller periods. Comparing the spectra to the vessel RAO (Figure 3-9), since the Torsethaugen spectrum has a portion of the energy in larger periods, the result is a higher probability of larger heave motions using the Torsethaugen spectrum. Figure 3-20 and Figure 3-21 ($T_p=8s$) has the same difference as Figure 3-18 and Figure 3-19. For both these comparisons an increase in Hs will increase the difference between the two spectra. Another noticeable difference is that the smaller the response from the RAO at T_p , the bigger the difference between heave motion in Torsethaugen and JONSWAP is, as Torsethaugen covers a wider area of periods.

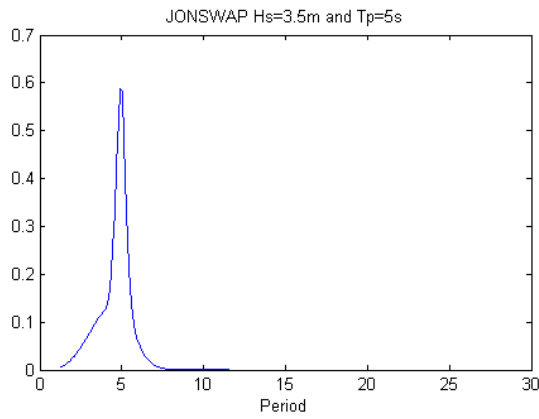


Figure 3-18: JONSWAP spectra $H_s=3.5m$ and $T_p=5s$

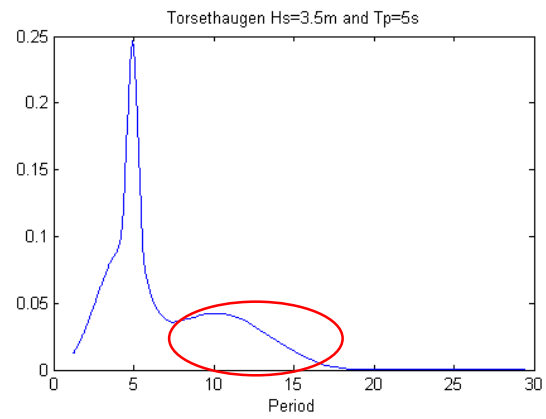


Figure 3-19: Torsethaugen spectra $H_s=3.5m$ and $T_p=5s$

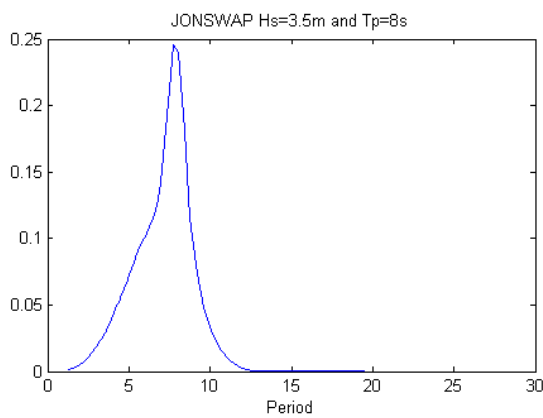


Figure 3-20: JONSWAP spectra $H_s=3.5m$ and $T_p=8s$

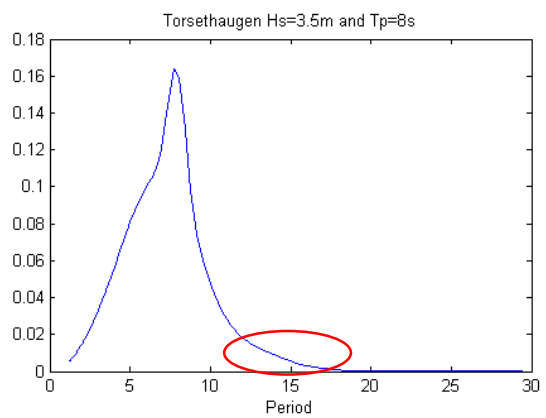


Figure 3-21: Torsethaugen spectra $H_s=3.5m$ and $T_p=8s$

Comparing Figure 3-22 and Figure 3-23 with $T_p=13s$, the reason for the higher probability of larger heave motion using JONSWAP is marked with red in the Torsethaugen spectrum. There is more energy in the smaller periods in the Torsethaugen spectrum. This results in a lower probability of being in the higher periods that would have resulted in larger heave motion. For $T_p=13$ and $H_s < 12m$, decreasing H_s will result in increasing difference of the probability of the heave motion where Torsethaugen would have the smallest. For $T_p=13$ and $H_s > 12m$, by increasing H_s the difference of the probability of the heave motion will increase where Torsethaugen will have the largest motions. An operation in a sea state where $H_s=12m$ is not realistic, therefore there is no need of taking this discussion further.

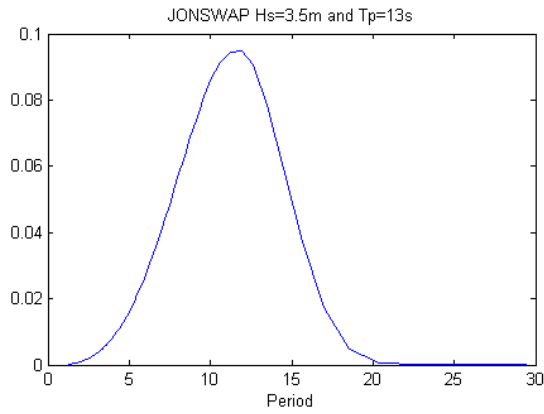


Figure 3-22: JONSWAP spectra $H_s=3.5m$ and $T_p=13s$

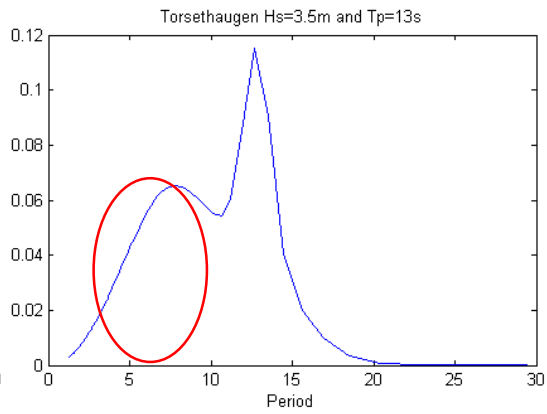


Figure 3-23: Torsethaugen spectra $H_s=3.5m$ and $T_p=13s$

3.2.4 Weather criteria and durations

The result of the calculations done in section 3.2.3 and the conversion of the weather restrictions from JONSWAP to Torsethaugen give this new table for the operation tasks and their weather criteria.

Table 15: Weather criteria and duration Torsethaugen

Operation	Weather Criteria (Hs)				Duration
	$0 \leq T_p < 5$	$5 \leq T_p < 10$	$10 \leq T_p < 13$		
Task 1 - Subsea end initiation to Visund PIW.	All	3.3 m	3.7 m		49 hrs.
	$0 \leq T_p < 5$	$5 \leq T_p < 7$	$7 \leq T_p < 10$	$10 \leq T_p < 13$	
Task 2 - Lay away. (see section 3.2.2)	1.3 m	1.3 m	0.9 m	0.7 m	3 hrs.
	$0 \leq T_p < 5$	$5 \leq T_p < 10$	$10 \leq T_p < 13$		
Task 3 - Visund temporary laydown of subsea ETH.	All	3.3 m	3.7 m		11 hrs.
	$0 \leq T_p < 5$	$5 \leq T_p < 10$	$10 \leq T_p < 13$		
Contingency laydown of dynamic section.	All	4.2 m	5.1 m		
	$0 \leq T_p < 5$	$5 \leq T_p < 10$	$10 \leq T_p < 13$		
Task 4 - Catenary flip and lay dynamic section towards platform.	All	3.3 m	3.7 m		16 hrs.
	$0 \leq T_p < 5$	$5 \leq T_p < 10$	$10 \leq T_p < 13$		
Task 5 - Topside end handshake to Visund PIW.	All	3.3 m	3.7 m		34 hrs.

3.2.4.1 Duration of the operation using hindcast data

Using the new weather criteria gives new operation durations. The simulation of the Torsethaugen duration is done the same way as for the JONSWAP simulation section 3.1.3.1. This is by using the total sea as the limiting weather criteria. Results of the simulation are shown below.

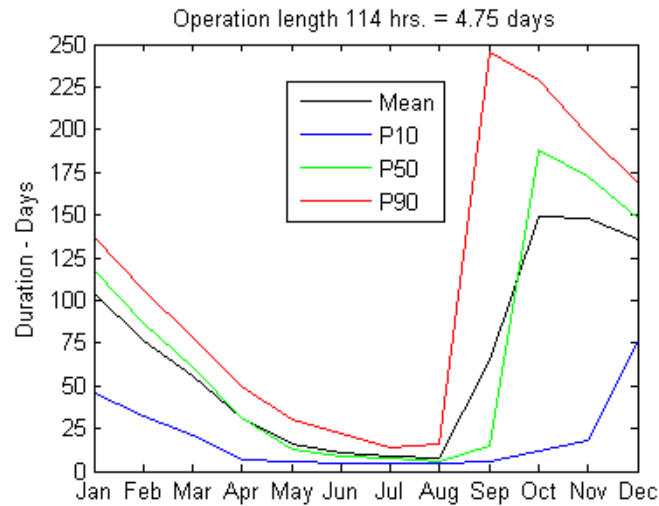


Figure 3-24: Duration of the operation using Torsethaugen, Heidrun

Table 16: Duration of the operation using Torsethaugen, Heidrun

Operation length 114 hrs. = 4,75 days				
Month	Mean Duration Torsethaugen (days)	P10 Duration Torsethaugen (days)	P50 Duration Torsethaugen (days)	P90 Duration Torsethaugen (days)
January	104.97	48.50	116.83	136.77
February	76.61	28.14	85.83	105.75
March	55.34	22.59	60.38	78.25
April	30.95	8.23	31.21	48.95
May	15.94	5.36	13.19	30.91
June	10.99	4.75	8.79	22.69
July	9.70	4.89	7.65	15.00
August	8.50	4.75	6.23	16.16
September	64.29	5.34	14.55	242.61
October	146.57	11.34	186.04	227.16
November	147.64	35.80	170.48	196.16
December	135.97	79.52	147.83	167.77

There is not much difference between the average duration of the operation using JONSWAP- and Torsethaugen weather criteria. This shows that choosing either JONSWAP or Torsethaugen does not make much of a difference in the durations.

3.3 Wind Waves and Swells Simulation using JONSWAP spectra

By separating into two sea states, one for wind waves and one for the swell waves, it is possible to look at what impact the roll motion as well as the heave motion has on the operation duration. The hindcast data gives this possibility showing significant wave height, spectral peak period and direction of both wind- and swell waves (marked in red in figure below).

WAM WIND AND WAVES																	
LATITUDE: 65.29, LONGITUDE: 7.32																	
				WIND		TOTAL SEA						WIND SEA			SWELL		
YEAR	M	D	H	WSP	DIR	HS	TP	TM	DIRP	DIRM	HS	TP	DIRP	HS	TP	DIRP	
1957	9	1	6	7.0	33.	1.1	5.2	4.3	36.	26.	0.7	5.2	36.	0.8	5.2	351.	
1957	9	1	9	7.9	21.	1.1	5.2	4.2	21.	27.	0.9	5.2	21.	0.6	6.3	66.	
1957	9	1	12	8.4	26.	1.2	5.7	4.3	21.	26.	1.1	5.2	21.	0.6	6.9	351.	
1957	9	1	15	8.1	27.	1.3	5.7	4.5	21.	25.	1.1	5.7	21.	0.7	6.9	6.	
1957	9	1	18	7.0	36.	1.3	6.3	4.8	21.	24.	0.7	5.2	36.	1.1	6.3	6.	
1957	9	1	21	5.3	25.	1.3	6.3	5.1	6.	22.	0.4	3.9	36.	1.2	6.3	6.	
1957	9	2	0	4.6	54.	1.3	6.9	5.3	6.	19.	0.3	3.2	51.	1.2	6.9	6.	
1957	9	2	3	3.2	92.	1.2	6.9	5.6	21.	18.	0.1	0.0	223.	1.2	6.9	21.	
1957	9	2	6	4.2	129.	1.2	6.9	5.8	21.	16.	0.1	2.4	111.	1.2	6.9	21.	
1957	9	2	9	4.1	135.	1.1	6.9	5.8	21.	16.	0.1	2.4	111.	1.1	6.9	21.	

Figure 3-25: Hindcast data showing wind- and swell waves

The simulation is done conservatively with wind waves passing through the vessel at 0 degrees (head seas) creating no roll. The swells pass through the boat at the angular difference between the wind- and the swell waves creating the only contribution to the vessel roll motion.

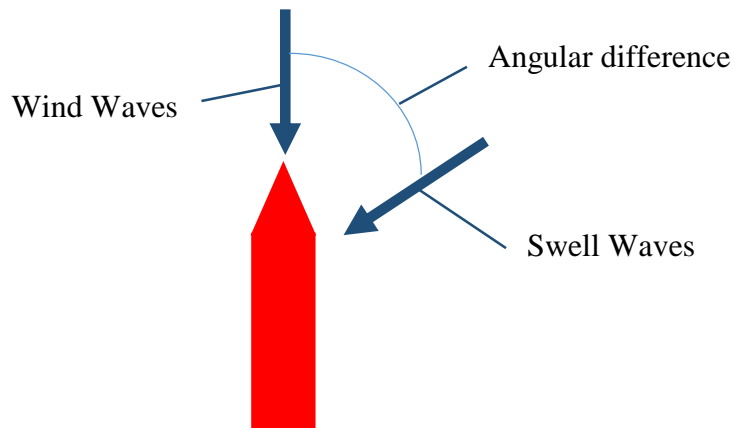


Figure 3-26: Vessel with wind- and swell waves

For the purpose of this simulation, the calculation of the wave spectrum is done by using JONSWAP for both wind- and swell waves. The simulation is separated into three parts:

1. Using restrictive resultant heave motion of wind- and swell waves.
2. Restrictive roll angle as a consequence of the swell direction. The roll angle is calculated using the closest RAO for roll (steps of 15 degrees from 0 degrees to 180 degrees).
3. Combined criteria for both roll and heave motion

3.3.1 Resultant heave motion simulation

First check for the simulation is how the swells will affect the vessel heave motion. The relative response from the RAO is bigger the closer the direction of the sea is to 90 degrees for smaller periods (Figure 3-27). This means that the swells might cause bigger heave motions compared to using total sea, where all the sea in this thesis was done head seas.

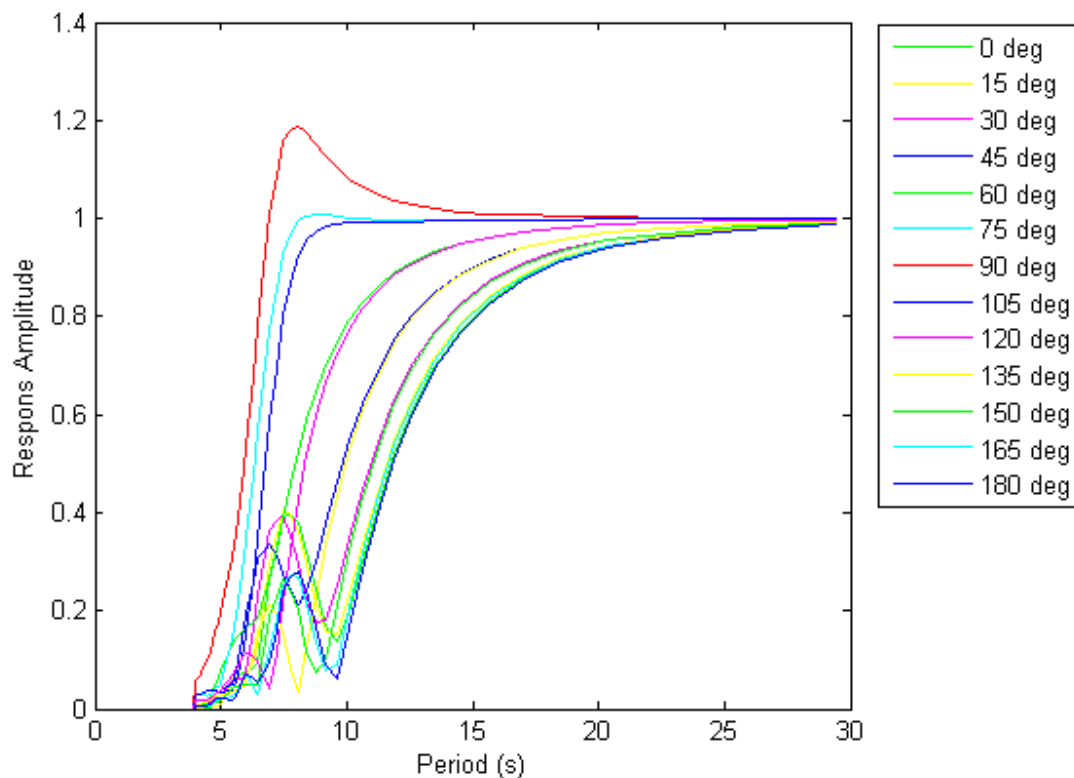


Figure 3-27: Normand Vision RAO for heave motion

After calculating the two JONSWAP spectrum (swell and wind waves), the response spectrum for both cases is developed and then summarized to one resultant response spectrum.

$$S_{Ztot}(f_i) = (|RAO_{heave}(f_i)|^2 \cdot S_{Jswell}(f_i)) + (|RAO_{heave}(f_i)|^2 \cdot S_{Jwind}(f_i)) \quad 3-(40)$$

The calculation of the response spectrum and the JONSWAP spectrum for both swell and wind waves is done the same way as in section 3.1.1 using formula 3-(1) to 3-(5). But instead of calculating γ for the swell spectrum,

$$\gamma_{swell} = 1$$

this is to create a wider spectrum that will be more realistic than using the calculated γ formula 3-(4).

The figures below show the calculation of S_{Ztot} figurative. The sea state is taken from the hindcast data, and is chosen because it is a good picture of the how the two different heave response spectra (wind and swell waves) combined gives a new total heave response spectrum.

Table 17: Sea state from hindcast data

Wave type	T_P	H_S
Swells	16.41 s	1.3 m
Wind waves	7.82 s	3.1 m

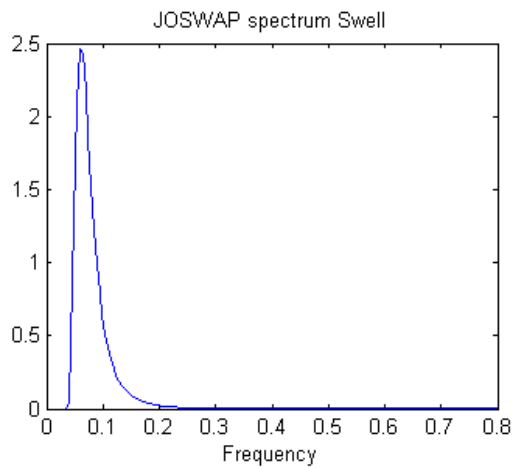


Figure 3-28: JONSWAP Swell spectrum

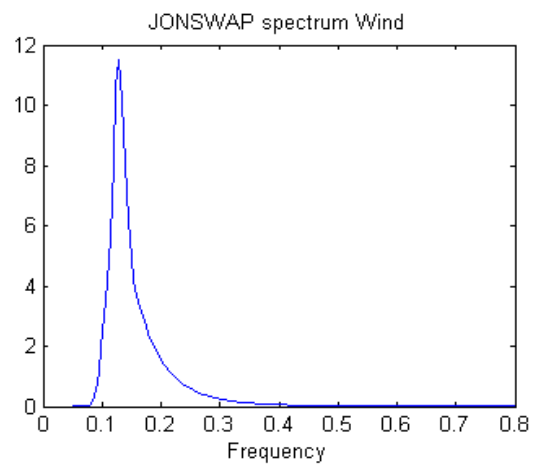


Figure 3-29: JONSWAP Wind Wave spectrum

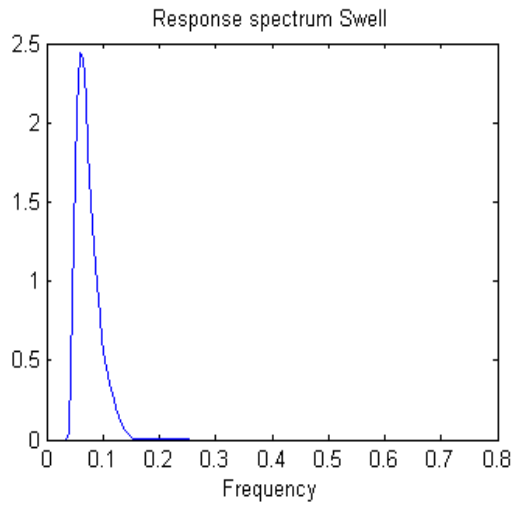


Figure 3-30: Heave response Swell spectrum

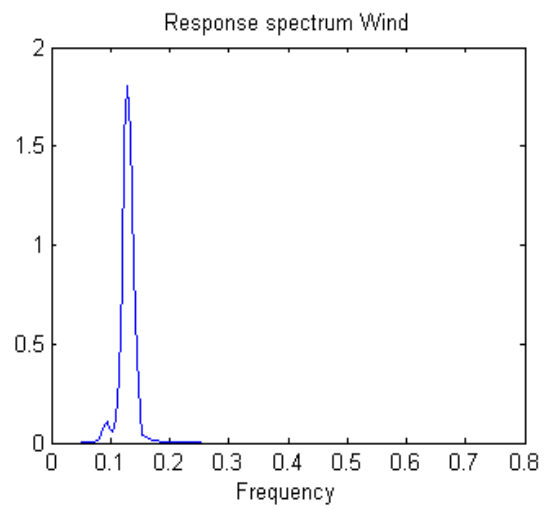


Figure 3-31: Heave response Wind Wave spectrum

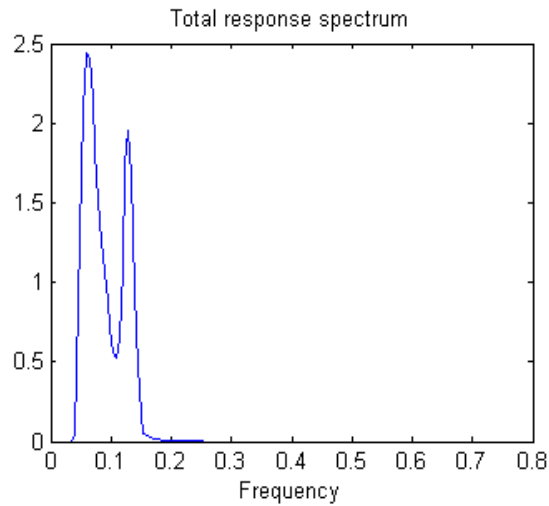


Figure 3-32: Total Heave Response Spectrum

The new total heave response spectrum is then used as the response spectrum when calculating 95-percentile for total heave motion for all sea states in the hindcast data (formula 3-(6) to 3-(9), 3-(12) and 3-(14) section 3.1.1).

$$Z_{0.95} = \sigma \sqrt{-2 \ln \left(1 - 0.95^{\frac{1}{n_{3h}}} \right)} \quad 3-(41)$$

3.3.1.1 Weather Criteria

For the simulation of the operation using resultant heave motion, the criteria will not be as for the earlier simulations with sea states of T_P and H_S . Instead, the 95-percentile for total heave motion in each sea state will be used to see whether the sea state is operable or not.

To develop a weather criteria plan for the operation Table 14 was used for all task except the lay away task. Table 14 holds heave motion criteria calculated from the weather criteria identified by Ocean Installer. Since the criteria is separated into different groups of spectral peak periods (T_P) there is different criteria for heave motion in each task of the operation ($0 \leq T_P < 5$, $5 \leq T_P < 10$ and $10 \leq T_P < 13$). When separating into groups of T_P and separating the sea state into swell and wind waves, there are two different sea states at the same time with different T_P . To solve the problem with T_P groups, a conservative approach by using the largest of the heave criteria for each task is used. For the lay away task the heave motion criteria, as explained in section 3.1.1, is set to be 0.6m (double amplitude).

Table 18: Weather Criteria Heave Motion Simulation

Operation	Heave motion criteria	Duration
Task 1 - Subsea end initiation to Visund PIW.	4 m	49 hrs.
Task 2 - Lay away.	0.6 m	3 hrs.
Task 3 - Visund temporary laydown of subsea ETH.	4 m	11 hrs.
Contingency laydown of dynamic section.	6 m	
Task 4 - Catenary flip and lay dynamic section towards platform.	4 m	16 hrs.
Task 5 - Topside end handshake to Visund PIW.	4 m	34 hrs.

3.3.1.2 Simulation

By using the weather criteria Table 18 an operational simulation is done. The criteria are compared to the resultant heave motion from the swell and wind waves in the hindcast data chronologically. The MATLAB simulation has the same output as described in section 3.1.3.1. By using only the highest heave motion calculated from the criteria when using total sea from head seas (Table 14), the simulation should allow more sea to pass through. This is because of

the smaller periods where the criteria for heave motion originally are lower. If the simulation shows worse operation duration it will mean that the swell waves has such an impact on the heave motion (because of the angular difference from the wind waves), that it is an important parameter to discuss when analyzing and planning the operation.

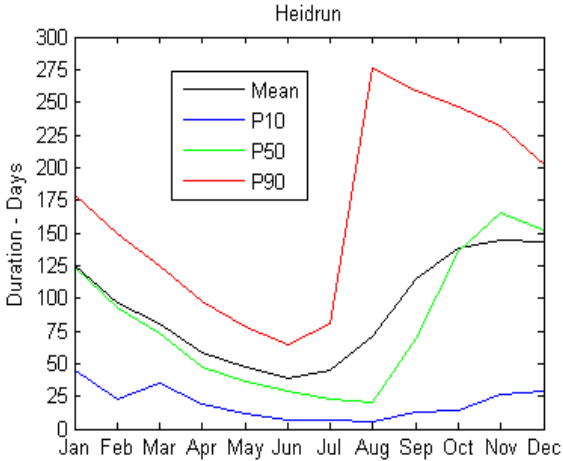


Figure 3-33: Duration of the Operation Resultant Heave Motion

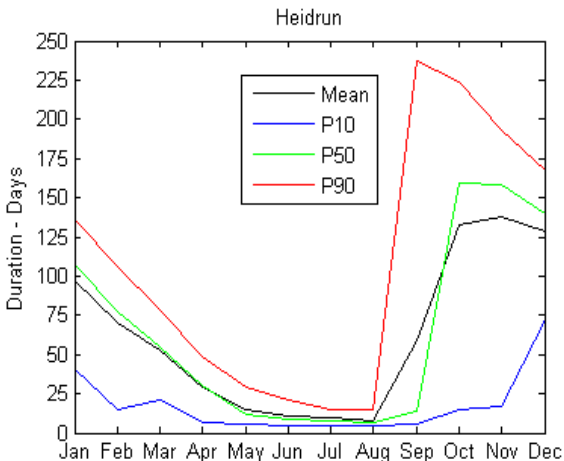


Figure 3-34: Duration of the Operation Total Sea JONSWAP

Table 19: Duration of the Operation Resultant Heave Motion

Resultant Heave Motion, Operation length 114 hrs. = 4.75 days				
Month	Mean Duration	P10 Duration	P50 Duration	P90 Duration
January	124.68	45.88	124.00	180.00
February	96.73	23.13	93.00	149.00
March	80.71	34.63	72.63	125.38
April	58.79	18.75	47.00	97.88
May	47.15	11.63	36.25	78.38
June	38.41	7.13	29.00	64.63
July	43.97	6.63	22.00	81.13
August	70.00	5.00	20.50	275.63
September	115.01	12.38	69.88	258.38
October	138.25	13.63	135.63	247.13
November	144.98	25.88	165.25	232.25
December	143.04	28.88	150.63	202.25

Comparing Figure 3-33 and Table 19 with Figure 3-34 and Table 11, the best comparable data is looking at the moths that were considered the best and operable, May to August. Here the

durations for the operations is significantly longer for the simulations done by separating the sea state into swell and wind waves from two different directions.

Table 20: Comparing Total Sea and Resultant Heave Motion Durations

Month	Mean Duration	P10 Duration	P50 Duration	P90 Duration
Total sea JONSWAP one direction, Operation length 114 hrs. = 4.75 days				
May	14.92	5.25	12.13	29.63
June	10.78	4.75	9.00	21.00
July	9.10	4.75	7.13	14.63
August	7.75	4.75	6.13	14.88
Resultant Heave Motion, Operation length 114 hrs. = 4.75 days				
May	47.15	11.63	36.25	78.38
June	38.41	7.13	29.00	64.63
July	43.97	6.63	22.00	81.13
August	70.00	5.00	20.50	275.63

For the specific operation described in this thesis the overall operation except the lay away task, is not that much restricted to the heave motion. Since the pipe is hanging free underneath the vessel and is allowed to move as long as it does not over bend. Therefor these numbers might be somewhat confusing, and should not be regarded that relevant for the operational part. As for the wave statistics, the durations are relevant as they show how swell and wind waves from different directions, compared to total sea from one direction, decrease the operable conditions related to heave motion.

3.3.2 Roll angle simulation

For the operation described in section 2.4, the roll angle can also contribute to damage of the product. As the pipe is hanging through the moonpool, the roll angle might damage the pipe if it collides with the moonpool edge.

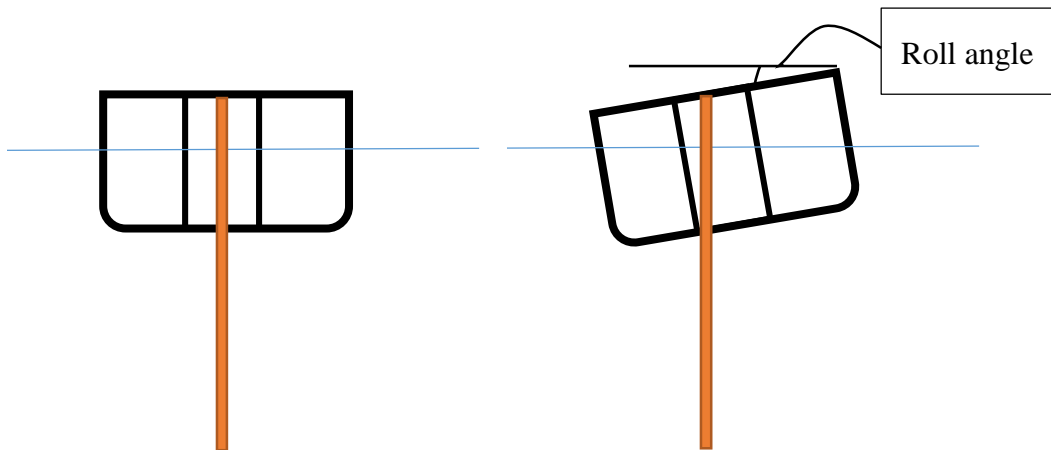


Figure 3-35: Roll angle with horizontal pipe colliding with moonpool

Another factor regarding allowable vessel roll angle is that the pipe is not hanging directly horizontal while laying the pipe. This decreases the roll angle before the pipe collides with the moonpool.

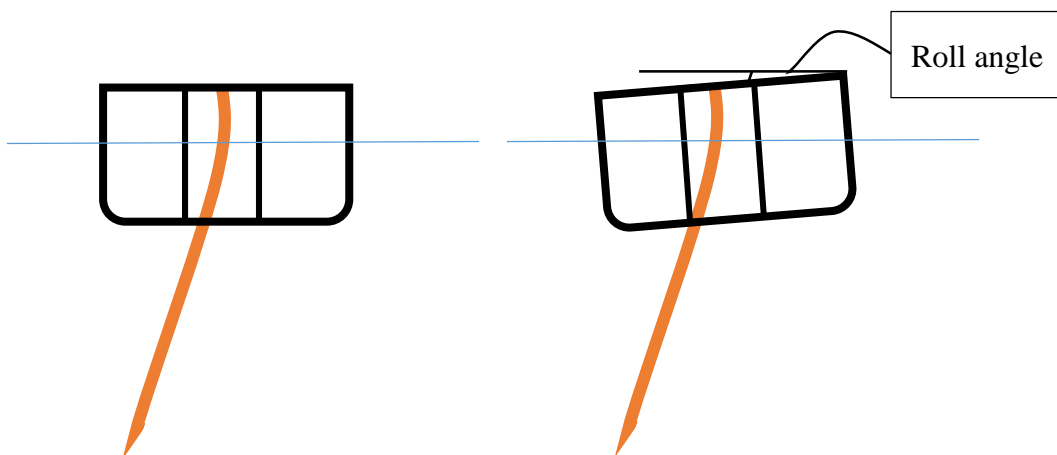


Figure 3-36: Roll angle with bending pipe colliding with moonpool

The operation has several limits to roll angle depending on the pipe configuration of the operation. To avoid a complicated simulation of the operation durations, the simulations regarding roll angle is done with 3 different limitations of roll angles for the whole operation:

1. 2 degree roll angle for the operation and 5 degree roll angle in the safe condition
2. 3 degree roll angle for the operation and 5 degree roll angle in the safe condition
3. 4 degree roll angle for the operation and 5 degree roll angle in the safe condition

The Normand Vision RAOs for roll is provided by Ocean Installer. The RAOs for roll is without the anti-roll compensation. Further work can be done doing the same simulations with anti-roll compensation.

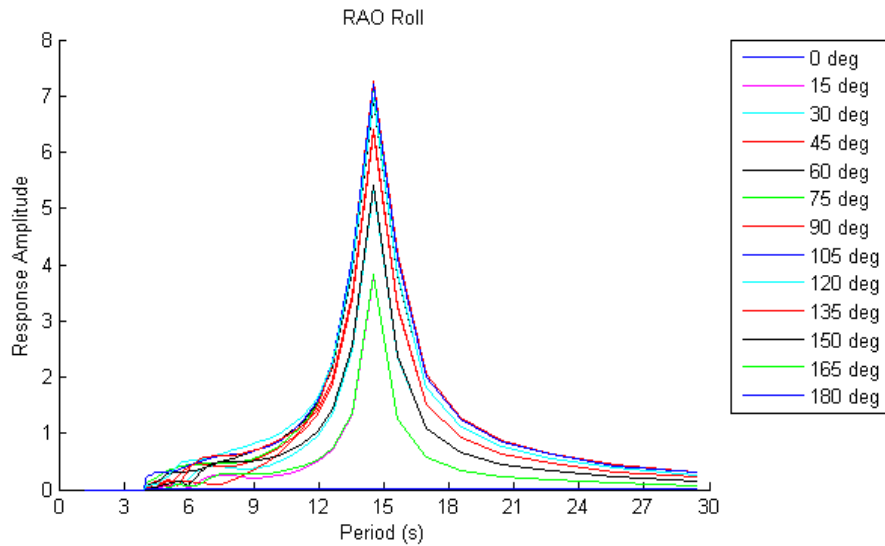


Figure 3-37: RAOs for roll Normand Vision

The RAOs for roll of the vessel Normand Vision has the natural period for roll at 14.5s (Figure 3-37). 0° is head seas and 180° is following sea. The response amplitude varies with the direction of the waves having the largest top at 90° and the other higher tops at the natural period of wave directions close to 90°. The smallest tops are for wave directions of 0° and 180° which do not make any roll (0 response amplitude for all periods), and the other smaller tops at the natural period for wave directions close to 0° and 180°.

3.3.2.1 Pitch Motion Contribution to Damage Pipe

One should notice that the pitch motion from the wind waves could also cause damage to the pipe. The possibility of pitch motion damaging the pipe is not calculated. Comparing the RAO for roll and pitch at 0° (Figure 3-38), the response amplitude for roll is much larger than pitch.

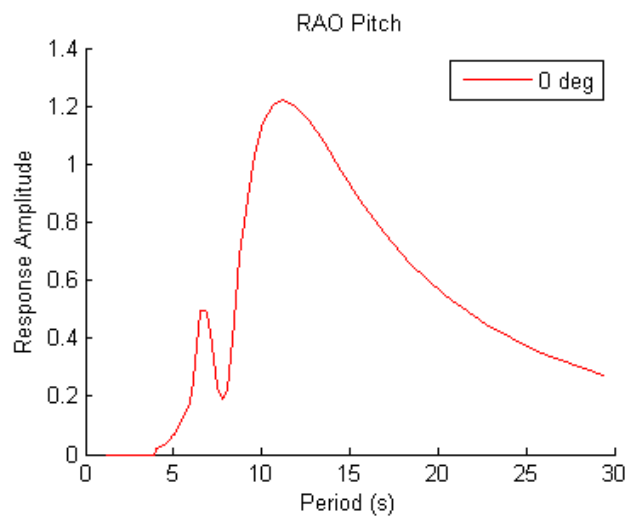


Figure 3-38: RAO pitch 0°

Table 21 shows H_s and T_p to create pitch motion of 3°, 4° and 5° with wind waves at head seas. What is seen is that the H_s needs to be larger than the largest recorded H_s for T_p less than 8s for all angles. For the larger T_p (almost like swell waves) the H_s needs to be relatively high. This means that not taking the pitch motion into the calculations will be conservative, but the results will not vary to much from calculations done with both heave and pitch motion. It should also be said that the pitch motion might need larger angles to damage the pipe.

Table 21: H_s limiting Pitch Motion with Wind Waves head seas (0°)

T_p (s)	H_s (m)			Max recorded H_s (m) for wind waves
	3° Pitch	4° Pitch	5° Pitch	
6.5	7.7	10.3	12.8	3.3
7.0	7.0	9.3	11.6	3.8
7.5	6.9	9.3	11.6	4.2
8.0	5.9	8.0	10.1	4.4
8.5	4.7	6.2	7.8	5.1
9.0	3.9	5.2	6.4	5.8
9.5	3.5	4.6	5.6	6
10.0	3.2	4.2	5.2	7.4
10.5	3.1	4.0	4.9	7.6
11.0	3.0	3.9	4.8	7.9
11.5	2.9	3.8	4.7	8.3
12.0	2.9	3.8	4.7	9.4
12.5	2.9	3.8	4.7	9.4
13.0	2.8	3.8	4.7	11.1

3.3.2.2 Linear Roll Angle Calculations

The calculation of roll angles is throughout this thesis done linearly, which is conservative. By linear roll calculation the roll angle only depend on the wave amplitude, and roll damping is not considered. For small roll angles this is close to real life, but as the roll angle increases the roll damping also increases. Increasing roll damping increases the differences in the linear and nonlinear roll calculations. Linear roll angles are larger than nonlinear roll angles.

“Roll motions are by far the most difficult motions of a ship to predict. It is therefore appropriate to discuss this motion separately, even though it is strongly coupled with sway and yaw. It is an accepted fact of ship hydrodynamics that the damping arising from the creation of

the waves (the principal source of damping for heave, pitch, sway and yaw) is almost vanishingly small for the rolling of typical ship forms. Other mechanisms for damping, such as viscous effects, occur naturally. However, these mechanisms lead to roll dampings which are no larger than the wave damping, and thus the total damping from all sources is still small. It is typical for roll motions to have an effective nondimensional damping ratio of considerably less than 5 percent for barehulled ship. Waves that have an encounter frequency near roll resonance can, and do, cause typical ships to roll severely. These large roll angles can give rise to strong nonlinearities in the hydrodynamic damping and sometimes in the static roll restoring moment. These conditions further complicate any analysis of the roll motions.”
(Lewis, 1989)

3.3.2.3 Roll criteria and operation simulation

The simulations are based on the criteria in Table 22. For this specific simulation the heave motion criteria of 0.6m for the lay away task is not considered, meaning that the only parameter preventing the possibility of finishing the operation is the roll angle criteria.

Table 22: Roll angle simulation criteria

Operation	Roll angle			Duration
	Simulation number 1	Simulation number 2	Simulation number 3	
Task 1 - Subsea end initiation to Visund PIW.	2°	3°	4°	49 hrs.
Task 2 - Lay away.	2°	3°	4°	3 hrs.
Task 3 - Visund temporary laydown of subsea ETH.	2°	3°	4°	11 hrs.
Contingency laydown of dynamic section.	5°	5°	5°	
Task 4 - Catenary flip and lay dynamic section towards platform.	2°	3°	4°	16 hrs.
Task 5 - Topside end handshake to Visund PIW.	2°	3°	4°	34 hrs.

To simulate the operation for these criteria, the H_s giving the 95-percentile roll angle corresponding to the simulation number (both operational and contingency tasks) is calculated from 0 to 30 seconds with steps of 0.5 seconds. The 95-percentile roll angle is based on a swell spectrum meaning that $\gamma = 1$. Since the wind waves are set to be head seas (0°) the only contribution to roll are the swells. This is a conservative approach as it is almost impossible to maneuver the vessel with wind waves at only head seas. If the wind waves are slightly out of head seas, the wind waves will contribute to roll as well. This is not taking into count when doing the roll calculation. The criteria were set by using groups with steps of 1 second for T_p , and then using the lowest criteria for H_s within that group as the weather criteria for the simulation. This is to create a little uncertainty factor to the T_p . A quick figurative explanation of this procedure is shown below for the limitation of 4° roll angle for the operational tasks. H_s is the limiting H_s for roll angle of 4° and wave direction of 90° .

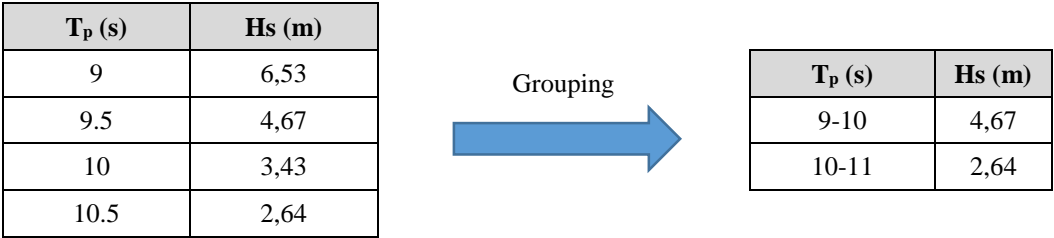


Figure 3-39: Grouping of limiting H_s to roll of 4° and wave direction of 90°

The simulated operation duration for the different roll angles and the original JONSWAP total sea duration are shown in the figures and table below.

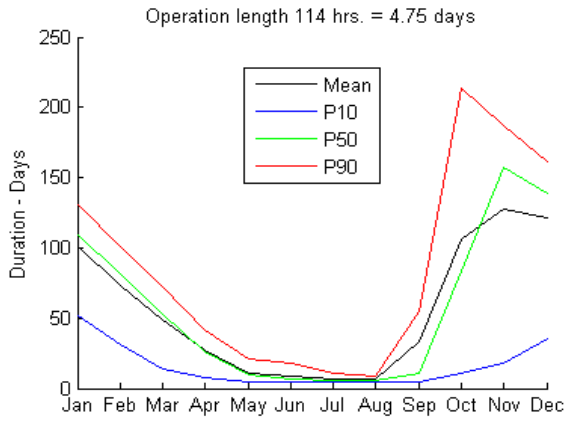


Figure 3-40: Operation Duration 2° roll

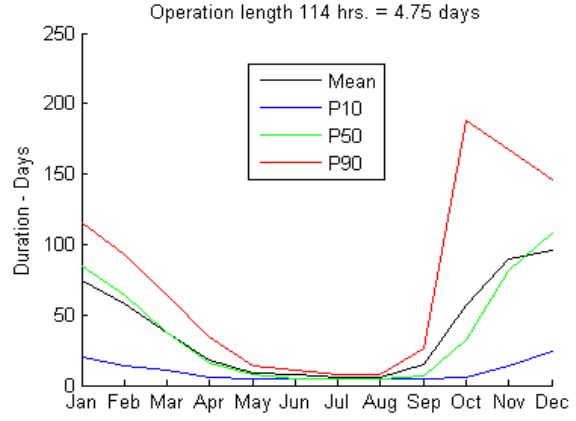


Figure 3-41: Operation Duration 3° roll

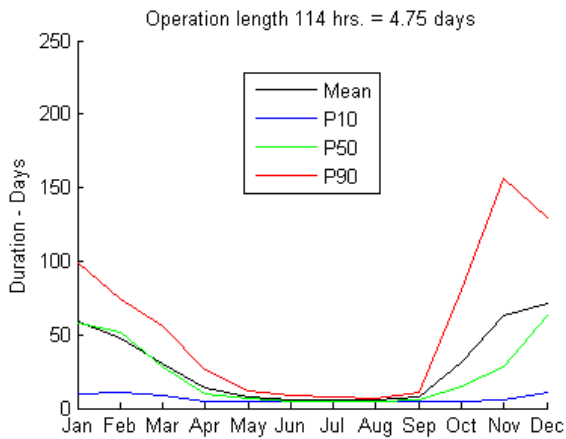


Figure 3-42: Operation Duration 4° roll

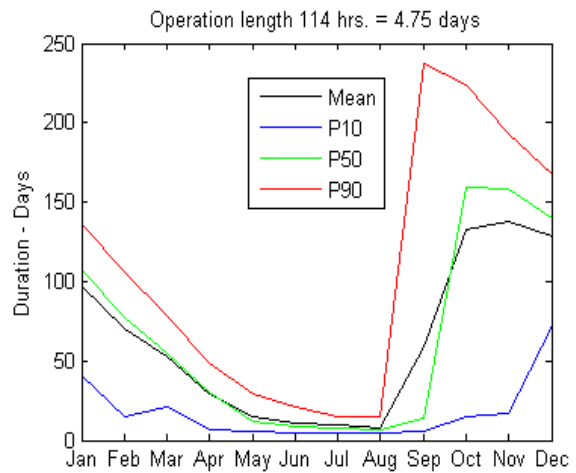


Figure 3-43: Duration of the Operation Total Sea JONSWAP

Operation length 114 hrs. = 4.75 days				
Month	Mean Duration (days)	P10 Duration (days)	P50 Duration (days)	P90 Duration (days)
2° Roll				
May	10.90	4.75	9.50	20.50
June	9.12	4.75	6.38	18.25
July	6.98	4.75	5.88	11.25
August	6.54	4.75	5.25	8.88
September	33.28	4.75	10.75	54.75
3° Roll				
May	9.00	4.75	8.13	13.88
June	7.20	4.75	4.75	11.25
July	6.01	4.75	4.75	8.13
August	5.69	4.75	4.75	7.75
September	15.27	4.75	6.75	25.63
4° Roll				
May	7.95	4.75	6.63	12.13
June	6.07	4.75	4.75	8.38
July	5.62	4.75	4.75	7.38
August	5.33	4.75	4.75	6.50
September	7.83	4.75	5.88	10.63
Total sea JONSWAP one direction				
May	14.92	5.36	12.02	28.46
June	10.78	4.75	8.68	21.71
July	9.94	4.93	7.25	16.95
August	8.07	4.75	6.15	14.84
September	59.39	5.27	13.79	234.48

Looking at Figure 3-40, Figure 3-41 and Figure 3-42 and comparing to Figure 3-43. The figures show that the operation is more based on roll motion than heave motion. The durations for 2° roll are closest to the original weather criteria developed by Ocean Installer. To verify that the operational weather criteria are based on roll angle, the H_s that gives a 95-percentile roll angle equal to 3° for different T_p is calculated. 3° roll is chosen instead of 2° roll because adding the heave limitation to the lay away task will probably increase the operation duration. The calculations are based on a JONSWAP spectrum using a calculated γ as in section 3.1.1.

Originally the weather criteria was $H_S=3.5\text{m}$. Max H_S in the table below is the maximum total sea H_S found in the hindcast data within the corresponding group of T_p . N/A means that the H_S giving a roll angle of 3° is so much higher than the max H_S that it is not applicable. All H_S for the groups of T_p below 6.5s is not applicable and is therefore not considered relevant to the table. Marked with red are where H_S is below the originally weather criteria of $H_S=3.5\text{m}$.

Table 23: H_S giving roll angle of 3° to corresponding groups of T_p

Hs (m) giving roll angle of 3° for different wave directions (degrees). 0° is head seas														
T_p (s)	0	15	30	45	60	75	90	105	120	135	150	165	180	Max Hs (m)
6.5	N/A	N/A	N/A	N/A	N/A	N/A	N/A	N/A	N/A	N/A	N/A	N/A	N/A	3.6
7.0	N/A	N/A	N/A	N/A	N/A	N/A	N/A	5.3	5.0	5.4	N/A	N/A	N/A	4.4
7.5	N/A	N/A	N/A	6.5	5.8	5.9	N/A	4.9	4.5	5.0	6.5	N/A	N/A	5.3
8.0	N/A	N/A	N/A	6.1	5.1	5.5	N/A	4.6	4.1	4.7	6.0	N/A	N/A	5.0
8.5	N/A	N/A	7.0	5.4	4.5	4.9	N/A	4.2	3.7	4.3	5.7	N/A	N/A	5.7
9.0	N/A	N/A	6.1	4.5	3.8	4.1	5.3	3.6	3.3	3.8	5.1	N/A	N/A	6.3
9.5	N/A	N/A	4.9	3.6	3.1	3.2	3.7	2.9	2.8	3.2	4.3	7.9	N/A	6.5
10.0	N/A	6.8	3.8	2.8	2.4	2.4	2.6	2.3	2.3	2.6	3.4	6.2	N/A	8.2
10.5	N/A	5.0	2.9	2.2	1.9	1.9	2.0	1.8	1.8	2.1	2.7	4.7	N/A	8.0
11.0	N/A	3.9	2.3	1.8	1.6	1.5	1.5	1.5	1.5	1.7	2.2	3.7	N/A	8.1
11.5	N/A	3.1	1.9	1.5	1.3	1.3	1.3	1.3	1.3	1.4	1.9	3.0	N/A	8.1
12.0	N/A	2.6	1.7	1.3	1.2	1.1	1.1	1.1	1.1	1.3	1.6	2.6	N/A	9.6
12.5	N/A	2.4	1.5	1.2	1.1	1.1	1.1	1.1	1.1	1.2	1.5	2.3	N/A	9.5
13.0	N/A	2.3	1.5	1.2	1.1	1.1	1.1	1.0	1.1	1.2	1.5	2.2	N/A	11.4

The weather criteria which was provided by Ocean Installer and was used for the simulation of the operation section 3.1.3.1 had a criteria of $H_S=3.5\text{m}$ for all tasks except the lay away task (the weather criteria for the lay away task in section 3.1.3.1 was calculated based on limiting the heave motion to 0.6m). By looking at the values for H_S which limits the vessel roll angle to 3° in Table 23, $H_S=3.5\text{m}$ could easily be set as an weather criteria but now allowing the waves from all directions, as long as the operation is only based on roll limitations. Only requirement would be a decrease in the weather criteria for some directions with T_p longer than 9s.

Table 23 might look a bit strange for periods less than 10s. The limiting H_S to roll of 3° for wind direction of 90° is a bit higher than the wave direction of 60° , 75° , 105° , 120° and 135° .

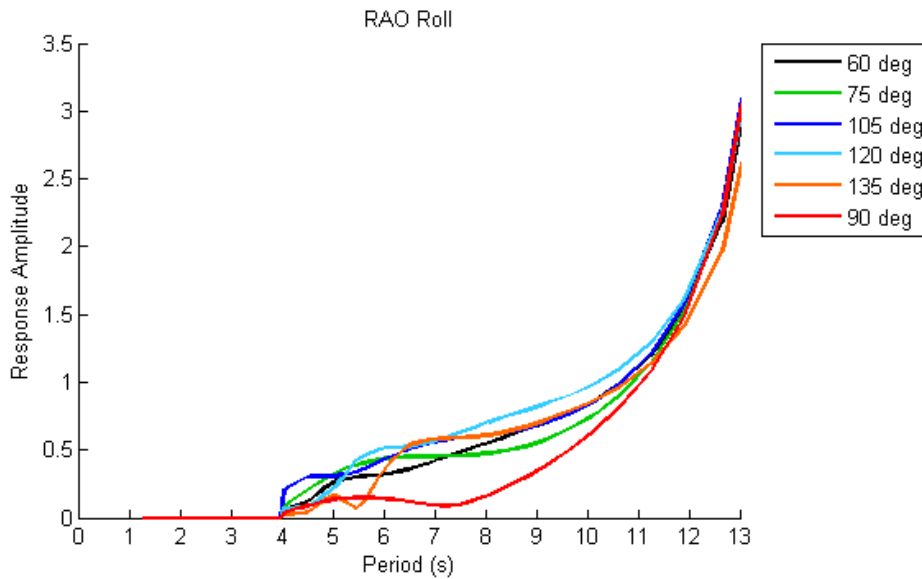


Figure 3-44: Section of RAOs for roll for selected wave directions

As Figure 3-44 is showing, the response amplitude for roll for wave direction of 90° is small for T_p less the 10s. Basically this says the same as Table 23, that to reach a roll angle of 3° the value for H_s needs to be higher for 90° than for rest of the directions shown in Figure 3-44.

3.3.3 Roll Angle and Heave Combined in one Simulation

The roll angle simulation is done with all tasks set to a specific roll angle limitation. The roll angle created by the swells, and wind waves from head seas only creating heave motion. For the roll angle simulation lay away task has a limitation regarding the roll angle instead of heave motion limited to 0.6m which was specified in section 2.4.2. To handle this a new simulation is done using roll angle of 3° for all tasks except the lay away task and the contingency task. An operation with limiting roll angle of 3° for all tasks and 5° for the contingency plan had durations which are assumed to be closest to the original weather criteria given by Ocean Installer (section 3.3.2.3) adding 0.6 heave restriction to the lay away task. The contingency plan will continue to be limited by a roll angle of 5° for this simulation. A summary of the weather criteria will look like this.

Table 24: Operation Criteria combining resultant heave motion and roll angle

Operation	Limiting criteria	Duration
Task 1 - Subsea end initiation to Visund PIW.	3° roll angle	49 hrs.
Task 2 - Lay away.	0.6m resultant heave motion	3 hrs.
Task 3 - Visund temporary laydown of subsea ETH.	3° roll angle	11 hrs.
Contingency laydown of dynamic section.	5° roll angle	
Task 4 - Catenary flip and lay dynamic section towards platform.	3° roll angle	16 hrs.
Task 5 - Topside end handshake to Visund PIW.	3° roll angle	34 hrs.

This simulation should give operation durations longer than the 3° roll angle simulation in section 3.3.2. Now that the lay away task is limited to a resultant heave motion of 0.6m, which is calculated from both wind waves and swells, the probability of finishing the lay away task is less. This is shown and explained by using a typical sea state for swell, and then find the H_s for wind wave that will generate a resultant heave motion of 0.6m together with the swell. Some of this calculation is shown in the table below. A JONSWAP spectrum is used for both waves where $\gamma = 1$ for the swell and γ is calculated for the wind waves.

Table 25: Wind Wave giving 0.6m Heave Motion

Swell			Gives limiting wind wave head seas of →	Wind Wave which will give 0.6m Heave Motion	
H _s (m)	T _p (s)	Direction		H _s (m)	T _p (s)
0.8	7.6	45°		4.17	5
				0.81	8
				0.37	13

As Table 25 shows, having wave from the side limits the criteria for wind waves head significantly compared to the weather criteria from section 3.1.3. This limitation should show

longer simulated operation duration than the original 3° roll operation, even though the lay away task only has a duration of 3 hours.

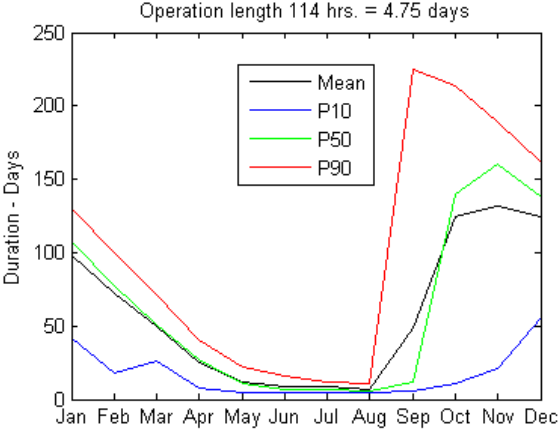


Figure 3-45: Operation Duration 3° Roll and 0.6m Heave

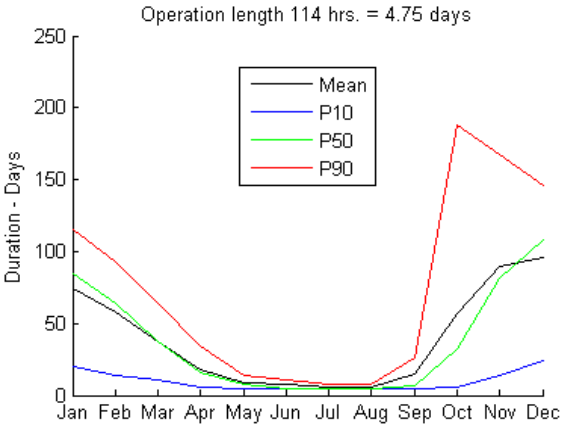


Figure 3-46: Operation Duration 3° Roll

Table 26: Durations for 3° Roll Simulation and Combined Heave and Roll Simulation

Operation length 114 hrs. = 4.75 days				
Month	Mean Duration (days)	P10 Duration (days)	P50 Duration (days)	P90 Duration (days)
3° roll and 0.6m heave motion for the lay away task				
May	11.82	4.75	10.38	22.25
June	9.07	4.75	6.75	15.63
July	7.54	4.75	6.50	11.25
August	6.66	4.75	5.88	10.75
3° roll				
May	9.00	4.75	8.13	13.88
June	7.20	4.75	4.75	11.25
July	6.90	4.75	4.75	8.88
August	6.05	4.75	4.75	7.75

As seen from Figure 3-45, Figure 3-46 and Table 26 the durations of combined roll and heave motion simulation for the actual operational months does not have high impact. Still the 3-hour task, with restriction of 0.6m heave motion, increases the mean duration in the best month (August) by 0.61 days = 14.64 hours. Longer durations, lower heave restrictions and operating in other months will increase the duration even more.

4 COMPARING SIMULATIONS FOR DIFFERENT FIELDS

The same simulations as in section 3.1, 3.3.1, 3.3.2 and 3.3.3 are compared for the different locations (Ekofisk, Statfjord, Heidrun and Snøhvit) in this section. The results should show differences between the locations as described in section 2.1.2.4 and 2.1.2.5. The operation durations are the sum of waiting on weather and operation length.

4.1 Total Sea using JONSWAP spectrum

The first comparing is based on the simulation done in section 3.1.3. For this simulation the weather criteria were provided by Ocean Installer, except the lay away task. The weather criteria for the lay away task was calculated by limiting the vessel heave motion to 0.6m using JONSWAP spectra and a 95-percentile heave motion. The heave motion is the double amplitude, which is a conservative approach as the waves do not have the same distance from the crests and trough to the waterline. The same simulation is done converting the criteria to Torsethaugen spectra for Heidrun. This simulation showed minor differences and therefor only the simulation using JONSWAP spectra is calculated for the rest of the fields. These simulations are based on the total sea in the hindcast data, which is a combination between wind waves and swells. Figure 4-1 shows the simulated operation durations for the different fields. The different fields and their locations compared to the hindcast data point are shown in Figure 2-5. Appendix A: Simulated Operation Duration Tables, shows detailed simulated duration tables.

Table 27: Main Findings, Total Sea using JONSWAP spectrum

Field	Main Findings
Heidrun	Operable: May-August Best months: July-August Worst Spreading: September
Ekofisk	Operable: All year depending on risk Best months: June-August Worst Spreading: November-February
Statfjord	Operable: May-August Best months: June-August Worst Spreading: September
Snøhvit	Operable: May-August Best months: June-August Worst Spreading: November

Total Sea using JONSWAP spectra

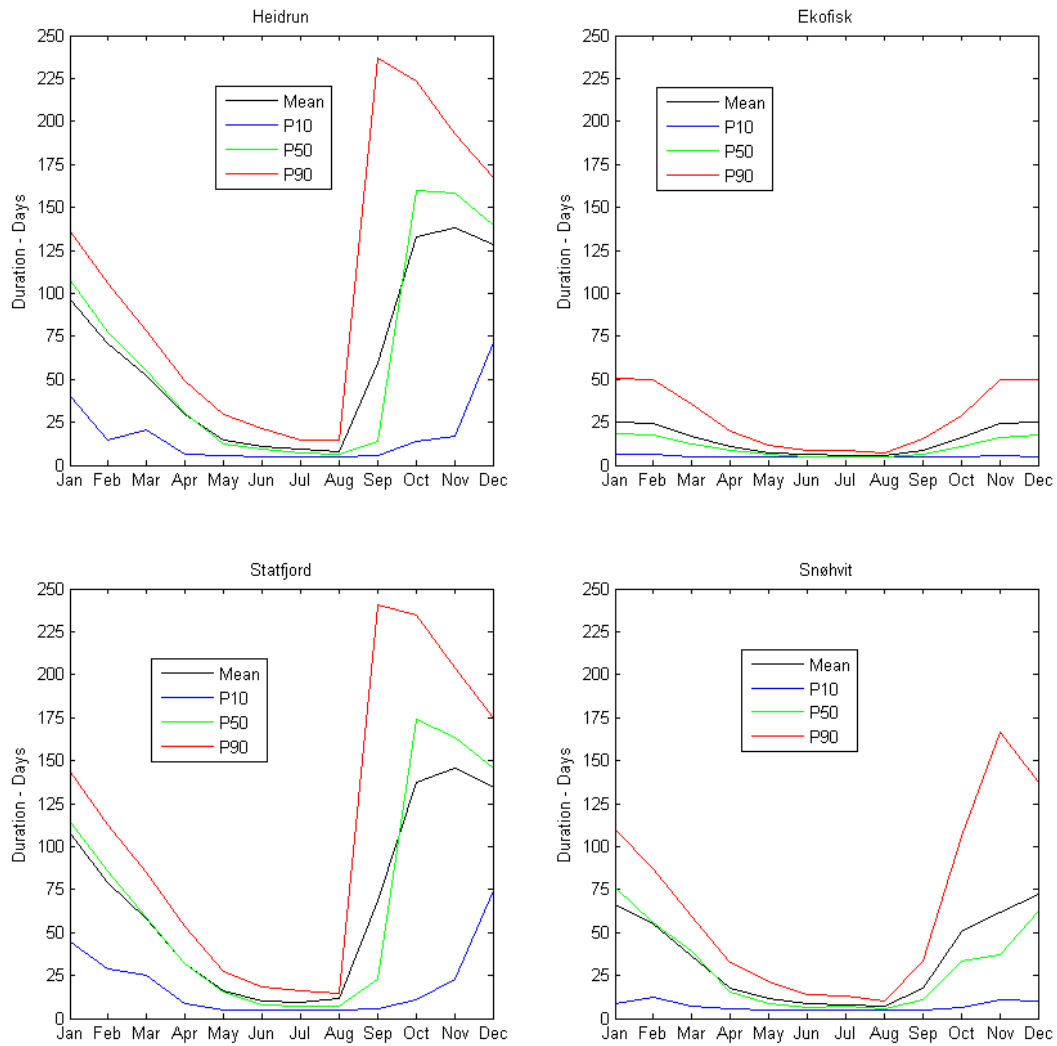


Figure 4-1: Simulated Durations for Total Sea using JONSWAP spectra, Different Fields

4.2 4m Resultant Heave Motion for the Operation Tasks

The second comparison is based on the simulation done in section 3.3.1. For this simulation the weather criteria is limited by a resultant heave motion (double amplitude) of swells and wind waves to 4m for the operation tasks, except the lay away task which is restricted to 0.6m heave. The contingency plan is limited to 6m heave motion. The resultant heave motion is calculated for each hindcast data using JONSWAP spectra and a 95-percentile for resultant heave motion. The heave motion is calculated by having the wind waves at head seas (0°) and the swells at the angular difference from the wind waves (Figure 3-26). Only the heave motion is used for this simulation and the swells contribution to roll is neglected, which is conservative and not a realistic operation. Having wind waves at only head seas (0°) is also conservative, as it is almost an impossible way of maneuvering the vessel. Figure 4-2 shows the simulated operation durations for the different fields. The different fields and their locations compared to the hindcast data point are shown in Figure 2-5. Appendix A: Simulated Operation Duration Tables, shows detailed simulated duration tables.

Table 28: Main Findings, 4m Resultant Heave Motion for the Operation Tasks

Field	Main Findings
Heidrun	Operable: None Best month: August Worst Spreading: August
Ekofisk	Operable: All year depending on risk Best month: June Worst Spreading: November
Statfjord	Operable: None Best month: July Worst Spreading: September
Snøhvit	Operable: None Best months: May-August Worst Spreading: September

4m Heave for Operation Task and 6m Heave for Contingency Position

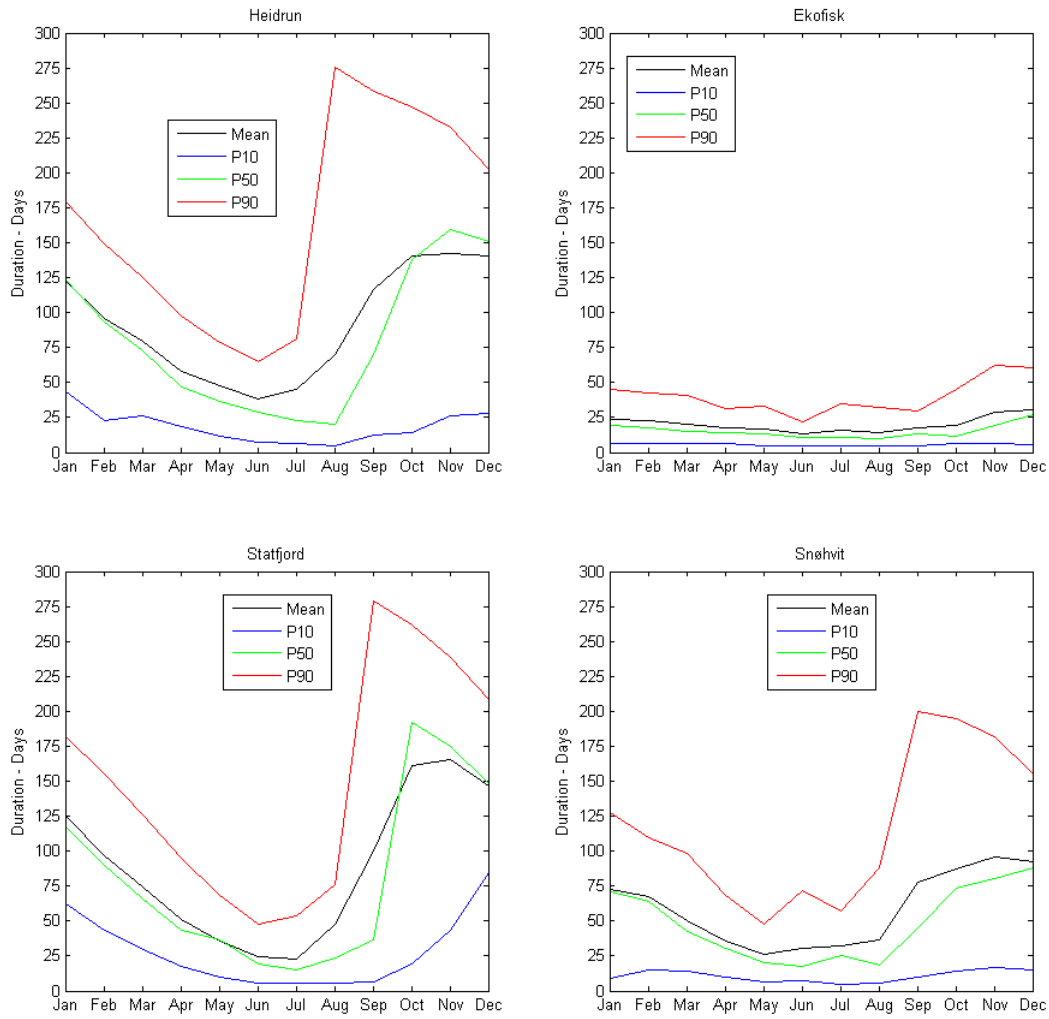


Figure 4-2: Simulated Durations for Resultant Heave Motion

4.3 3° Roll Limitation for the Operation Tasks

The third comparison is based on the simulation done in section 3.3.2. For this simulation the weather criteria is limited by 3° roll motion created by the swells for the operation tasks and 5° roll created by the swells for the contingency plan. The limiting roll motion is set by a limitation of H_s and calculated for groups T_p using JONSWAP spectra and a 95-percentile for roll motion. The calculations are done conservatively with wind waves at head seas (0°) and swells at the angular difference from the wind waves (Figure 3-26). This gives the wind waves no contribution to roll which is only possible at 0° and 180°. For a better simulation this can be done by wind waves at $0 \pm 15^\circ$ that will contribute to roll motion and give a more realistic operation simulation. This is not done in this thesis but can be done in further work. For Heidrun the roll simulation is done for 2°, 3° and 4° (Figure 3-40 to Figure 3-42). For the rest of the simulation only 3° roll is simulated. These durations are a bit shorter than the original criteria. Knowing that the duration will increase by adding heave limitation to the lay away task this seems to be the most relevant roll angle for the operation simulation. Figure 4-3 shows the simulated operation durations for the different fields. The different fields and their locations compared to the hindcast data point are shown in Figure 2-5. Appendix A: Simulated Operation Duration Tables, shows detailed simulated duration tables.

Table 29: Main Findings, 3° Roll Limitation for the Operation Tasks

Field	Main Findings
Heidrun	Operable: May-August Best months: June-August Worst Spreading: October
Ekofisk	Operable: All year depending on risk Best months: June-September Worst Spreading: January
Statfjord	Operable: May-August Best months: June-August Worst Spreading: November
Snøhvit	Operable: May-September Best months: June-August Worst Spreading: December

3° Roll for Operation Task 5° Roll for Contingency Position

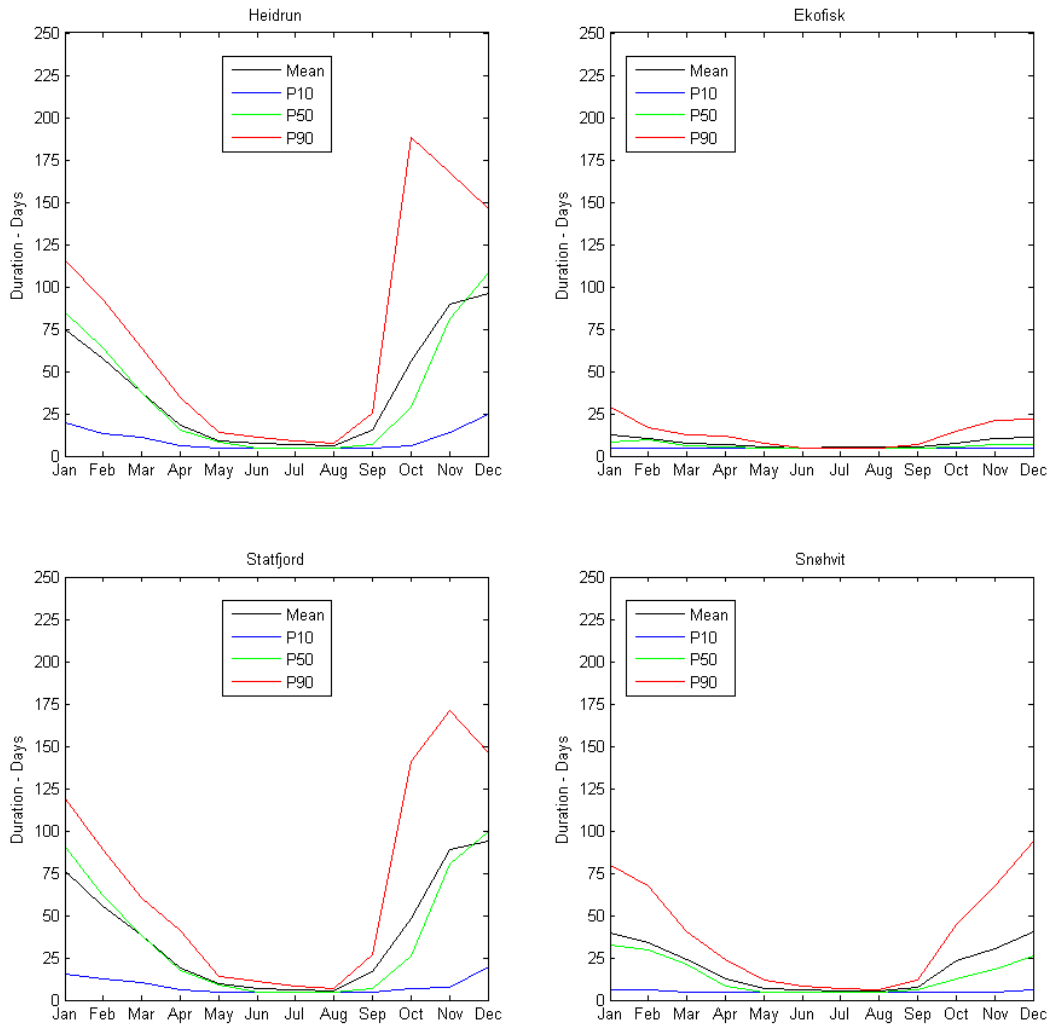


Figure 4-3: Simulated Durations for 3° Roll Motion

4.4 3° Roll with 0.6m Heave Limitation for the Lay Away Task

The last comparison is based on the simulation done in section 3.3.3. For this simulation the weather criteria is limited by 3° roll motion created by the swells for the operation tasks, except the lay away task which is restricted to 0.6m resultant heave motion. The contingency plan is limited to 5° roll motion created by the swells. The limiting roll motion is set by a limitation of H_s and calculated for groups of T_p using JONSWAP spectra and a 95-percentile for roll motion as in section 4.3. The resultant heave motion is calculated for each hindcast data using JONSWAP spectra and a 95-percentile for resultant heave motion as in section 4.2. Figure 4-4 shows the simulated operation durations for the different fields. The different fields and their locations compared to the hindcast data point are shown in Figure 2-5. Appendix A: Simulated Operation Duration Tables, shows detailed simulated duration tables.

Table 30: Main Findings, 3° Roll with 0.6m Heave Limitation for the Lay Away Task

Field	Main Findings
Heidrun	Operable: May-August Best month: August Worst Spreading: September
Ekofisk	Operable: All year depending on risk Best months: June-August Worst Spreading: November-February
Statfjord	Operable: May-August Best month: August Worst Spreading: October
Snøhvit	Operable: May-August Best months: June-August Worst Spreading: November

3° Roll for Operation Task 5° Roll for Contingency Position 0.6m Heave Lay Away Task

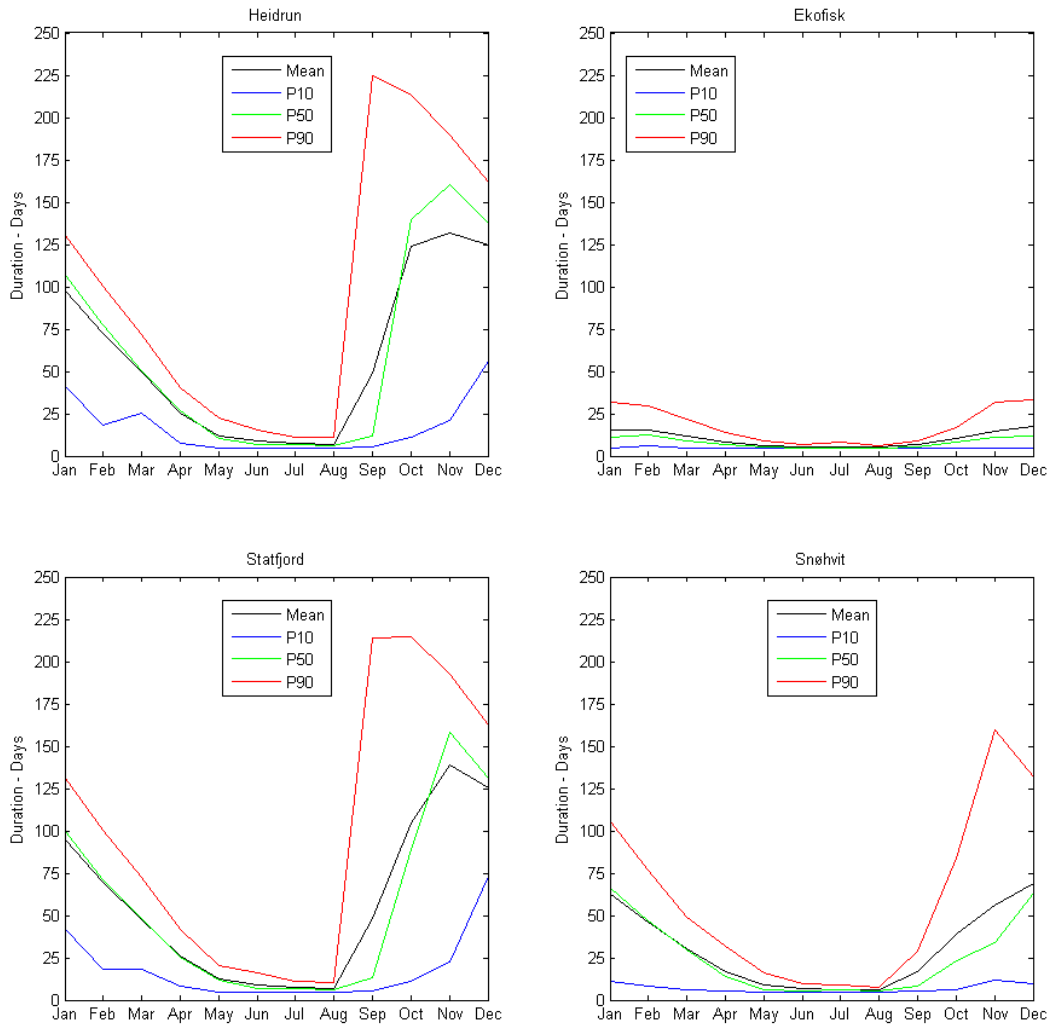


Figure 4-4: Simulated Durations for 3° Roll Motion and 0.6m Heave Motion

5 DISCUSSING SIMULATED OPERATION DURATION RESULTS

This section discusses the results of the different fields in section 4. To get a better understanding section 4 also covers a quick summary of the calculations done in the analysis (section 3). For more detailed simulated operation duration see tables Appendix A.

5.1 Ekofisk

Ekofisk is well sheltered from swells in all direction except north. The fetch length, where the wind waves are generated, is short. Since the fetch length is short in all directions, except north, the wind waves are not allowed to develop into waves containing a lot of potential energy (Figure 2-21 to Figure 2-14 to see the distribution of wind wave and swell direction, and wave energy). A result of this is that Ekofisk field in general has waves with much less energy than the rest, resulting in shorter operation durations, especially in the winter months.

5.2 Statfjord and Heidrun

Statfjord and Heidrun are very much alike. Both fields are relatively close to each other, and have open sea to the west where most of the swells are generated (North Atlantic Ocean). Looking at it theoretically, Statfjord should have waves containing less energy than Heidrun since Statfjord is more sheltered by the United Kingdom. This can be seen in the duration of the heave restricted operation simulation (Figure 4-2), but this is not enough to make a conclusion. The reason for the simulated operation durations being very much alike might be a combination between the dispersion length, the fetch length and the sheltering. What is meant by this is that the dispersion length is longer for Heidrun than Statfjord, resulting in less energy for swells generated in the North Atlantis Ocean. However, since Statfjord more sheltered than Heidrun, Heidrun allows for longer fetch lengths generating bigger local wind waves, resulting in more energy. This combination might weighing up for each other and be the reason why the durations is very much alike. See Figure 2-18 to Figure 2-23 for swell and wind wave directional spreading and energy for both fields.

5.3 Snøhvit

Snøhvit has relatively shorter durations, especially in the winter months, compared to Statfjord and Heidrun. Looking at Figure 2-20 to Figure 2-23, it does not look like the main reason is the wind wave energy. The wind wave energy is very much alike for Snøhvit as for Statfjord and

Heidrun. By comparing the swell energy there is a difference. The swell energy is less for Snøhvit, and the reason is believed to be the dispersion length to the swells generated in the North Atlantic Ocean, where most of the swells come from (can be seen in the directional spreading Figure 2-27 and Figure 2-28). The dispersion length of swells generated in the North Atlantic Ocean is a lot longer for Snøhvit than for Statfjord and Heidrun, resulting in less energy.

6 CONCLUSION

The first key observation is that the operation durations varies with the different fields. The Ekofisk field has the possibility of performing the operation all year with not much risk of waiting on weather. This is the case for all simulations except the simulation with limiting heave motions. With limiting heave motions, for the whole operation, the operation would be difficult to perform without any problems regarding waiting on weather.

The operation duration at Statfjord and Heidrun are quite similar which is reasonable since the fields are not too much apart and not sheltered by the United Kingdom. Comparing all simulation for these two fields, the best operation months would be June, July and August. Having the operation done in these months would make the risk of waiting for weather much less than the other months. One should also notice the sudden increase of risk of waiting for weather in some of the simulations for the month of September. A delay in start of the operation in August can therefore have huge consequences.

For the Snøhvit field the operational months are similar to Heidrun and Statfjord. The months that are most efficient and giving less risk of waiting on weather is June, July and August. The main difference at Snøhvit compared to Statfjord and Heidrun is that the winter months has relatively less operation duration. Still the risk of waiting on weather is too high to plan for an operation in these months.

The second conclusion is regarding using total sea or swells and wind waves when simulating the operation durations. Total sea are of good use if the weather criteria for H_S and T_p are defined before the simulation. The total sea H_S is normally higher than both swell and wind waves, and gives good estimation of the operation duration. To simulate an operation with limitations regarding vessel motion, separating the total sea into swells and wind waves, with different directions, gives the best estimation. This makes it possible to estimates both wave's contribution to e.g. heave and roll. Wind waves head seas will contribute to heave while the angular difference between swell and wind waves will cause roll and heave from the swell. Using total sea at head seas will only contribute to heave, and have no contribution to roll motion. Limiting heave motion with contribution from two directional waves shows much longer simulated duration than using one direction total sea. Limiting the whole operation to heave is only illustrative as the operation is originally limited to roll. Roll limitations shows similar simulated duration as one direction total sea.

The third key observation is the influence from swells created in the North Atlantic Ocean. This area has large wind speeds and huge open seas which gives long fetch lengths. Long fetch lengths create high-energy waves which travel all the way to the Norwegian continental shelf. For Snøhvit, Heidrun and Statfjord most swells come from west looking at the wave direction rose diagrams, which is the direction to the North Atlantic Ocean. These swells contain a lot of energy and should be considered when planning the operation. For Ekofisk most swells come from north since the field is well sheltered in all other directions. What is observed is that 50 % of the time when Statfjord has swells coming from west (the North Atlantic Ocean), Ekofisk will have waves coming from north to west within the first 12 hours. This might be since the swells are bent around the United Kingdom's east coast, and thereby the swells from the North Atlantic Ocean also influence the Ekofisk field. The North Atlantic Ocean's influence on Ekofisk is not a conclusive observation and gives a possibility of further work.

6.1 Further Work

Calculations of vessel motion using two directional spectra is done by having wind waves at head seas (0°) to vessel. This is a conservative approach, if the vessel is slightly out of head seas the contribution of roll and heave motion will change. For further work it is possible to add a safety margin of $\pm 15^\circ$ for the wind wave direction. Comparing the worst- and best-case vessel motion in an operation simulation will give another factor to the risk picture, when planning the marine operation.

Another interesting result would be to see the difference in the operation simulation having the vessel against the swells instead of the wind waves.

The roll calculations in the thesis is done using RAO without anti-roll tanks. Using anti-roll tanks will change the simulated operation durations, and the impact would also be an interesting result.

Limiting vessel pitch motion is not calculated and analyzed in the thesis. Pitch motion could also damage the pipe, and therefore a simulation with pitch, roll and heave limitations would be of interest.

Investigation of the impact on Ekofisk from the swells generated in the North Atlantic Ocean is also interesting. A quick calculation in section 2.1.2.6 shows that 50% of the time when swells at Statfjord come from west (the North Atlantic Ocean), Ekofisk will have swells coming from west to north within the first 12 hours.

REFERENCES

- Andersen, O. J., 2009. *The peak period in the WAM10 hindcast archive*, s.l.: Statoil.
- Det Norske Veritas, 2010. *DNV-RP-C205 Environmental Conditions and Environmental Loads*, s.l.: DNV.
- Eik, K. J., 2012. *Norne Field Metocean Design Basis*, s.l.: Statoil.
- Haver, S. K., 2013. *Prediction of Characteristic Response for Design Purposes*, s.l.: Statoil.
- Lewis, E. V., 1989. *Principles of Naval Architecture - Volume III, Motions in Waves and Controllability*. 2nd ed. s.l.:The Society of Naval Architects and Marine Engineers.
- Norwegian Petroleum Directorate, 2015. *Fact Pages - Norwegian Petroleum Directorate*. [Online]
Available at: <http://factpages.npd.no/factpages/>
[Accessed 2 June 2015].
- Ocean Installer, 2015. *Normand Vision*. [Online]
Available at: <http://www.oceaninstaller.com/portfolio/normandvision/>
[Accessed 7 June 2015].
- Ocean Installer, 2015. *NORMAND VISION -Offshore Construction Vessel*. [Online]
Available at: <http://www.oceaninstaller.com/wp-content/uploads/2012/03/Normand-Vision-Brochure-02-2015.pdf>
[Accessed 16 March 2015].
- Ocean Installer, 2015. *Riser Installation Analysis Report - Visund (A21, A05, A20) Risers*, Stavanger: Ocean Installer.
- Pinet, P. R., 2003. *Invitation to Oceanography*. 3rd ed. s.l.:Jones and Bartlett Publishers.
- Reistad, M. et al., 2009. *A high-resolution hindcast of wind and waves for The North Sea The Norwegian Sea and The Barents Sea*, s.l.: Norwegian Meteorological Institute.
- Remote Sensing Systems (RSS), 2009. <http://www.remss.com/>. [Online]
Available at: http://images.remss.com/qscat/scatterometer_data_monthly.html
[Accessed 10 May 2015].

Statoil, 2015. *Ekofisk*. [Online]

Available at:

<http://www.statoil.com/no/OurOperations/ExplorationProd/partneroperatedfields/Ekofisk/Pages/default.aspx>

[Accessed 2 June 2015].

Statoil, 2015. *Heidrun*. [Online]

Available at:

<http://www.statoil.com/no/OurOperations/ExplorationProd/ncs/heidrun/Pages/default.aspx>

[Accessed 2 June 2015].

Statoil, 2015. *Snøhvit*. [Online]

Available at:

<http://www.statoil.com/no/ouoperations/explorationprod/ncs/snoehvit/pages/default.aspx>

[Accessed 2 June 2015].

Statoil, 2015. *Statfjord-Området*. [Online]

Available at:

<http://www.statoil.com/no/ouoperations/explorationprod/ncs/statfjord/pages/default.aspx>

[Accessed 2 June 2015].

Thomson, R. E., 1981. *Oceanography of the British Columbia Coast*. Ottawa: Department of Fisheries and Oceans.

Torsethaugen, K., 1996. *Model for Double Peaked Wave Spectrum, Rep. No. STF22 A96204*, Trondheim: SINTEF Civil and Envir. Engineering.

Torsethaugen, K. & Haver, S., 2004. *Simplified Double Peak Spectral Model of Ocean Waves*, Toulon: Proceedings of the Fourteenth Offshore and Polar Engineering Conference.

Ward, D. J., 2015. <http://www.darrinward.com/lat-long/>. [Online]

Available at: <http://www.darrinward.com/lat-long/>

[Accessed 1 May 2015].

APPENDIX A: SIMULATED OPERATION DURATION TABLES

Table A - 1: Total Sea using JONSWAP spectrum, Heidrun

Operation length 114 hrs. = 4,75 days - Heidrun				
Month	Mean Duration Original Criteria (days)	P10 Duration Original Criteria (days)	P50 Duration Original Criteria (days)	P90 Duration Original Criteria (days)
January	96.94	40.75	108.13	136.63
February	70.42	14.75	77.13	105.63
March	52.38	20.63	55.13	78.25
April	29.46	6.25	30.63	49.00
May	14.92	5.25	12.13	29.63
June	10.78	4.75	9.00	21.00
July	9.10	4.75	7.13	14.63
August	7.75	4.75	6.13	14.88
September	60.29	5.25	14.13	237.13
October	134.96	15.63	160.75	223.63
November	137.97	17.13	158.38	193.00
December	128.23	71.75	139.63	167.63

Table A - 2: Total Sea using JONSWAP spectrum, Ekofisk

Operation length 114 hrs. = 4,75 days - Ekofisk				
Month	Mean Duration Original Criteria (days)	P10 Duration Original Criteria (days)	P50 Duration Original Criteria (days)	P90 Duration Original Criteria (days)
January	24.95	6.50	18.50	50.88
February	24.01	6.13	17.63	49.75
March	16.94	4.75	12.25	35.63
April	11.02	4.75	8.38	20.13
May	7.08	4.75	6.13	11.38
June	6.19	4.75	4.88	8.25
July	5.87	4.75	4.75	7.88
August	5.69	4.75	4.75	7.13
September	8.42	4.75	6.00	15.25
October	16.20	4.75	10.88	29.13
November	24.24	5.38	16.25	49.75
December	25.33	4.75	17.63	49.63

Table A - 3: Total Sea using JONSWAP spectrum, Staffjord

Operation length 114 hrs. = 4,75 days - Staffjord				
Month	Mean Duration Original Criteria (days)	P10 Duration Original Criteria (days)	P50 Duration Original Criteria (days)	P90 Duration Original Criteria (days)
January	107.84	44.75	115.00	143.63
February	79.20	28.88	85.88	112.63
March	57.69	25.25	59.00	84.63
April	31.97	8.38	31.50	53.50
May	15.82	4.88	15.38	27.25
June	10.13	4.75	7.63	18.38
July	9.14	4.75	6.88	16.38
August	11.40	4.75	7.13	14.63
September	68.17	5.75	23.00	241.00
October	137.61	10.75	174.25	234.75
November	145.47	22.75	163.88	203.75
December	134.11	74.13	145.75	174.63

Table A - 4: Total Sea using JONSWAP spectrum, Snøhvit

Operation length 114 hrs. = 4,75 days - Snøhvit				
Month	Mean Duration Original Criteria (days)	P10 Duration Original Criteria (days)	P50 Duration Original Criteria (days)	P90 Duration Original Criteria (days)
January	66.67	8.63	76.25	110.13
February	54.89	12.50	56.13	87.38
March	36.58	6.75	39.38	59.38
April	17.49	5.88	15.00	32.88
May	11.30	4.75	8.50	21.00
June	8.57	4.75	6.63	13.75
July	8.14	4.75	7.25	13.38
August	6.86	4.75	5.63	10.38
September	17.33	4.88	11.13	33.38
October	50.46	6.63	33.63	106.13
November	61.84	10.50	36.75	166.63
December	72.43	10.13	62.50	137.63

Table A - 5: 2m Resultant Heave Motion for the Operation Tasks, Heidrun

Operation length 114 hrs. = 4,75 days - Heidrun				
Month	Mean Duration Resultant Heave (days)	P10 Duration Resultant Heave (days)	P50 Duration Resultant Heave (days)	P90 Duration Resultant Heave (days)
January	124.68	45.88	124.00	180.00
February	96.73	23.13	93.00	149.00
March	80.71	34.63	72.63	125.38
April	58.79	18.75	47.00	97.88
May	47.15	11.63	36.25	78.38
June	38.41	7.13	29.00	64.63
July	43.97	6.63	22.00	81.13
August	70.00	5.00	20.50	275.63
September	115.01	12.38	69.88	258.38
October	138.25	13.63	135.63	247.13
November	144.98	25.88	165.25	232.25
December	143.04	28.88	150.63	202.25

Table A - 6: 2m Resultant Heave Motion for the Operation Tasks, Ekofisk

Operation length 114 hrs. = 4,75 days - Ekofisk				
Month	Mean Duration Resultant Heave (days)	P10 Duration Resultant Heave (days)	P50 Duration Resultant Heave (days)	P90 Duration Resultant Heave (days)
January	23.45	6.50	19.13	45.00
February	22.78	6.75	17.25	42.63
March	19.92	6.13	14.63	40.75
April	17.78	6.88	14.25	31.50
May	16.75	5.00	13.00	33.38
June	13.17	4.75	10.75	22.13
July	14.82	4.75	10.63	32.13
August	14.06	4.75	9.88	32.00
September	17.11	5.00	12.63	29.38
October	18.92	6.13	11.38	44.75
November	28.70	6.25	19.00	62.00
December	30.20	5.38	26.75	61.00

Table A - 7: 2m Resultant Heave Motion for the Operation Tasks, Staffjord

Operation length 114 hrs. = 4,75 days - Staffjord				
Month	Mean Duration Resultant Heave (days)	P10 Duration Resultant Heave (days)	P50 Duration Resultant Heave (days)	P90 Duration Resultant Heave (days)
January	125.11	62.75	118.00	182.25
February	96.88	43.00	90.13	155.13
March	73.98	30.00	66.00	126.13
April	51.48	17.38	43.38	95.13
May	35.61	9.50	36.38	68.50
June	24.92	5.50	19.00	47.38
July	22.56	5.25	15.00	53.75
August	47.31	5.63	23.75	76.13
September	98.49	6.75	33.50	278.63
October	158.66	15.25	192.25	261.50
November	165.41	43.00	174.63	238.25
December	146.17	84.75	148.13	208.25

Table A - 8: 2m Resultant Heave Motion for the Operation Tasks, Snøhvit

Operation length 114 hrs. = 4,75 days - Snøhvit				
Month	Mean Duration Resultant Heave (days)	P10 Duration Resultant Heave (days)	P50 Duration Resultant Heave (days)	P90 Duration Resultant Heave (days)
January	72.68	9.13	70.88	128.13
February	67.33	15.00	63.63	110.00
March	50.19	14.00	42.63	98.50
April	35.55	9.88	30.63	68.75
May	25.92	6.13	20.38	47.75
June	30.48	7.13	17.38	72.13
July	31.97	5.00	25.13	56.88
August	36.79	6.00	18.63	87.75
September	76.22	9.75	43.50	199.50
October	86.01	13.63	69.00	194.50
November	95.91	17.00	80.00	181.75
December	92.60	15.00	88.00	155.25

Table A - 9: 3° Roll Limitation for the Operation Tasks, Heidrun

Operation length 114 hrs. = 4,75 days - Heidrun				
Month	Mean Duration 3° Roll (days)	P10 Duration 3° Roll (days)	P50 Duration 3° Roll (days)	P90 Duration 3° Roll (days)
January	74.74	20.00	84.88	115.50
February	57.43	13.50	64.00	92.25
March	37.28	11.25	37.38	64.25
April	18.10	5.75	15.63	34.38
May	9.00	4.75	8.13	13.88
June	7.20	4.75	4.75	11.25
July	6.90	4.75	4.75	8.88
August	6.05	4.75	4.75	7.75
September	15.15	4.75	6.75	25.63
October	56.24	6.13	29.13	188.50
November	89.62	13.63	81.13	167.63
December	95.90	24.50	108.13	146.25

Table A - 10: 3° Roll Limitation for the Operation Tasks, Ekofisk

Operation length 114 hrs. = 4,75 days - Ekofisk				
Month	Mean Duration 3° Roll (days)	P10 Duration 3° Roll (days)	P50 Duration 3° Roll (days)	P90 Duration 3° Roll (days)
January	12.54	4.75	8.25	29.00
February	10.37	4.75	9.38	17.00
March	7.77	4.75	5.75	12.25
April	7.00	4.75	5.38	11.75
May	5.59	4.75	4.75	7.50
June	4.94	4.75	4.75	4.75
July	5.71	4.75	4.75	4.75
August	5.14	4.75	4.75	4.75
September	5.32	4.75	4.75	6.75
October	7.44	4.75	5.25	14.63
November	10.50	4.75	7.13	21.25
December	11.26	4.75	7.00	21.75

Table A - 11: 3° Roll Limitation for the Operation Tasks, Statfjord

Operation length 114 hrs. = 4,75 days - Statfjord				
Month	Mean Duration 3° Roll (days)	P10 Duration 3° Roll (days)	P50 Duration 3° Roll (days)	P90 Duration 3° Roll (days)
January	76.49	15.63	90.88	119.25
February	55.18	12.25	61.63	88.75
March	37.98	10.50	38.25	60.25
April	19.11	6.38	17.63	40.88
May	9.35	4.75	8.75	13.75
June	6.52	4.75	4.75	10.75
July	6.00	4.75	4.75	8.13
August	5.47	4.75	4.75	6.88
September	17.07	4.75	6.75	27.13
October	48.05	6.88	25.88	141.38
November	89.25	7.25	80.38	171.13
December	94.01	19.88	99.38	146.38

Table A - 12: 3° Roll Limitation for the Operation Tasks, Snøhvit

Operation length 114 hrs. = 4,75 days - Snøhvit				
Month	Mean Duration 3° Roll (days)	P10 Duration 3° Roll (days)	P50 Duration 3° Roll (days)	P90 Duration 3° Roll (days)
January	39.58	6.38	32.25	80.13
February	33.93	5.88	29.88	67.50
March	24.07	5.00	21.25	40.50
April	12.20	4.75	8.50	24.13
May	6.74	4.75	4.75	11.63
June	5.80	4.75	4.75	8.13
July	5.45	4.75	4.75	7.00
August	5.11	4.75	4.75	5.75
September	7.59	4.75	5.75	12.13
October	23.02	4.75	12.25	45.00
November	30.49	5.00	18.38	67.50
December	40.01	5.88	26.00	93.63

Table A - 13: 3° Roll with 0.6m Heave Limitation for the Lay Away Task, Heidrun

Operation length 114 hrs. = 4,75 days - Heidrun				
Month	Mean Duration 3° Roll and 0.6m Heave (days)	P10 Duration 3° Roll and 0.6m Heave (days)	P50 Duration 3° Roll and 0.6m Heave (days)	P90 Duration 3° Roll and 0.6m Heave (days)
January	98.20	41.50	107.25	130.63
February	72.63	18.00	77.25	100.13
March	49.62	25.63	50.63	71.63
April	25.38	7.50	27.00	40.63
May	11.82	4.75	10.38	22.25
June	9.07	4.75	6.75	15.63
July	7.54	4.75	6.50	11.25
August	6.66	4.75	5.88	10.75
September	48.97	5.50	12.00	224.75
October	124.02	11.00	139.50	213.38
November	132.05	21.13	160.00	189.38
December	124.80	55.88	137.63	161.50

Table A - 14: 3° Roll with 0.6m Heave Limitation for the Lay Away Task, Ekofisk

Operation length 114 hrs. = 4,75 days - Ekofisk				
Month	Mean Duration 3° Roll and 0.6m Heave (days)	P10 Duration 3° Roll and 0.6m Heave (days)	P50 Duration 3° Roll and 0.6m Heave (days)	P90 Duration 3° Roll and 0.6m Heave (days)
January	15.67	4.88	11.25	31.88
February	15.23	5.88	12.25	30.00
March	11.46	4.75	8.75	21.75
April	8.46	4.75	6.50	14.25
May	6.39	4.75	5.13	8.88
June	5.33	4.75	4.75	6.63
July	5.65	4.75	4.88	8.38
August	5.07	4.75	4.75	5.75
September	6.61	4.75	5.25	9.25
October	10.08	4.75	7.88	16.50
November	14.54	4.88	11.13	31.88
December	17.33	4.75	12.00	32.88

Table A - 15: 3° Roll with 0.6m Heave Limitation for the Lay Away Task, Staffjord

Operation length 114 hrs. = 4,75 days - Staffjord				
Month	Mean Duration 3° Roll and 0.6m Heave (days)	P10 Duration 3° Roll and 0.6m Heave (days)	P50 Duration 3° Roll and 0.6m Heave (days)	P90 Duration 3° Roll and 0.6m Heave (days)
January	94.90	42.25	100.13	131.63
February	69.31	18.38	71.00	100.63
March	47.85	18.25	48.50	72.63
April	25.90	8.25	25.63	41.63
May	12.70	4.88	11.50	20.38
June	8.77	4.75	6.88	15.75
July	7.21	4.75	6.50	10.88
August	6.81	4.75	6.00	10.25
September	48.26	5.13	13.13	214.25
October	104.83	11.25	89.25	214.63
November	138.80	22.75	158.25	192.63
December	125.69	73.25	131.13	162.63

Table A - 16: 3° Roll with 0.6m Heave Limitation for the Lay Away Task, Snøhvit

Operation length 114 hrs. = 4,75 days - Snøhvit				
Month	Mean Duration 3° Roll and 0.6m Heave (days)	P10 Duration 3° Roll and 0.6m Heave (days)	P50 Duration 3° Roll and 0.6m Heave (days)	P90 Duration 3° Roll and 0.6m Heave (days)
January	62.76	11.13	66.25	105.88
February	46.28	8.50	47.13	76.75
March	30.57	6.13	29.50	49.00
April	16.67	5.63	14.00	32.00
May	9.09	4.75	6.38	16.25
June	6.70	4.75	5.63	10.00
July	6.35	4.75	5.88	8.75
August	6.04	4.75	5.25	7.38
September	16.54	5.38	8.50	28.75
October	38.86	6.00	23.00	84.25
November	55.89	11.63	34.13	159.50
December	68.68	9.38	63.38	132.13

APPENDIX B: MASTER THESIS OBJECTIVES

MSc theses 2015

Title: **Planning of a marine operation with focus on discussing limiting wave conditions**

Student: Magnus Håland

Background

Marine operations do generally require rather good weather for a certain period of time in order to be executed by a reasonable safety margin. If operation is done using a certain vessel, the vessel motions are the parameters that determine whether or not an operation can be performed. The critical vessel motion will vary from operation to operation, but often the heave or roll motion will be the important motions. Slowly varying motions like surge and yaw is often limited by applying dynamic positioning devices. Thus emphasis is in most often given to the wave frequent motions.

In this theses the focus is on the planning of an actual or a generic marine operation. It is assumed that it is the heave and roll of the vessel that limits the possibility of perming the planned duration. An important parameter is also the required duration of good weather windows. The vessel motions can be assumed to be linear functions of the wave process. This will be inaccurate for rolling, but it can be assumed that rolling is controlled by anti-rolling devices.

The purpose is to investigate the feasibility of the planned operation in various seasons. Variability in number of available weather windows for each month and the variability from year to year shall be investigated. As a base case, the sea state is characterized by the significant wave height and spectral peak period in combination with a JONSWAP spectrum. But shall also consider the effect of double peaked spectra in two ways; i) Using the Torsethaugen spectrum, ii) Using the wind induced sea and swell as given be the hindcast model is independent and simultaneously occurring wave systems. In this connection one shall also use

the respective directions of propagation for the two wave systems. If time permits results regarding feasibility can be compared for another offshore area, e.g. southern North Sea.

The necessary weather information will be given by the Norwegian hindcast data base, NORA10, giving weather characteristics every 3 hours from September 1st 1957 – June 30th 2014.

Below a possible division into sub-tasks is given.

1. Describe the characteristics of the marine operations that is planned to study. The critical response parameter shall be defined. A possibility is to adopt heave at center of gravity as the critical response. The accept criteria for this parameter, e.g. the b-percentile of the 3-hour extreme value distribution, shall be suggested. The base case duration of the operation shall also be given.
2. Prepare the hindcast data file by:
 - * Randomize the spectral peak period.A reference describing how this can be done will be provided.
Present monthly and annual scatter diagrams for Hs and Tp.
3. Determine the values of significant wave height and spectral peak period for which the sea state is acceptable for the marine operation assuming vessel to head against long crested waves. Determine the percentage of time sea states are below the accept level for all year and month by month. This can be done by screening the hindcast data file. A window referring to a given month should start in the month, but it may in in the following month.
4. For the weather limit and the required window length for the operation, establish the number of possible operation windows for the whole period 1957 – 2014. Determine the no. of windows for the various months show variability from year to year. What is the expected duration including waiting time for completing the operation for the various months. Assume operation is ready for being the 1st of each month.
5. Repeat 4) for the cases where Torsethaugen spectrum is used. Vessel is still assumed to head against the waves.

6. A short sea state is characterized by the JONSWAP spectra with, generally, direction of propagation. Vessel is expected to head against the wind sea waves and the swell from the direction given. For this purpose RAOs must be determined from all heading angles of ship.
Calculate the b – percentile of the 3-hour extreme value distribution of resulting heave and roll. Calculate the expected total duration including waiting time for each month assuming operation is ready to start the 1st of each month.
7. For an operation requiring a rather long execution time, the variability of the actual duration shall be investigated by simulating the operation in the weather history provided by the hindcast data.
8. If time permits repeat 4) for a position in Southern North Sea.

The candidate may of course select another scheme as the preferred approach for solving the requested problem.

The work may show to be more extensive than anticipated. Some topics may therefore be left out or reduced after discussion with the supervisor without any negative influence on the grading.

The candidate should in the report give a personal contribution to the solution of the problem formulated in this text. All assumptions and conclusions must as far as possible calculations or be supported references. The candidate should apply all available sources to find relevant literature and information on the actual problem.

The report shall be well organized and give a clear presentation and discussion of the work and all conclusions. It is important that the text is well written and that the tables and figures are used to support the verbal presentation. The report should be complete, but still as short as possible.

The final report must contain this text, an acknowledgement, summary, main body, conclusions, suggestions for further work, symbol list, references and appendices. All figures, tables and equations shall be identified by numbers. References should be given by author and year in the text, and presented alphabetically in the reference list. The report must be submitted in two copies unless otherwise has been agreed with the supervisor.

The supervisor may require that the candidate should give a written plan that describes the progress of the work after having received this text. The plan may contain a table of content for the report and also assumed use of computer resources. As an indication such a plan should be available by mid March.

From the report it should be possible to identify the work carried out by the candidate and what has been found in the available literature. It is important to give references to the original source for theories and experimental results.

The report must be signed by the candidate, include this text, appear as a paperback, and - if needed - have a separate enclosure (binder, diskette or CD-ROM) with additional material.

Supervisor: Sverre Haver, University of Stavanger.